Reprints of published artices

NLRX1 acts as tumor suppressor by regulating TNF-α induced apoptosis and metabolism in cancer cells

Kritarth Singh [a,b], Anastasia Poteryakhina [c], Andrei Zheltukhin [c], Khyati Bhatelia [a,b], Paresh Prajapati [a,b], Lakshmi Sripada [a,b], Dhanendra Tomar [a], Rochika Singh [a], Arun K. Singh [a], Peter M. Chumakov [c,*], Rajesh Singh [a,**]

[a] Department of Biochemistry, Faculty of Science, The Maharaja Sayajirao University of Baroda, Vadodara, Gujarat, India
[b] Department of Cell Biology, School of Biological Sciences and Biotechnology, Indian Institute of Advanced Research, Gandhinagar, India
[c] Engelhardt Institute of Molecular Biology, Russian Academy of Sciences, Moscow, Russia

ABSTRACT

Chronic inflammation in tumor microenvironment plays an important role at different stages of tumor development. The specific mechanisms of the association and its role in providing a survival advantage to the tumor cells are not well understood. Mitochondria are emerging as a central platform for the assembly of signaling complexes regulating inflammatory pathways, including the activation of type-I IFN and NF-κB. These complexes in turn may affect metabolic functions of mitochondria and promote tumorigenesis. NLRX1, a mitochondrial NOD-like receptor protein, regulate inflammatory pathways, however its role in regulation of cross talk of cell death and metabolism and its implication in tumorigenesis is not well understood. Here we demonstrate that NLRX1 sensitizes cells to TNF-α induced cell death by activating Caspase-8. In the presence of TNF-α, NLRX1 and active subunits of Caspase-8 are preferentially localized to mitochondria and regulate the mitochondrial ROS generation. NLRX1 regulates mitochondrial Complex I and Complex III activities to maintain ATP levels in the presence of TNF-α. The expression of NLRX1 compromises clonogenicity, anchorage-independent growth, migration of cancer cells in vitro and suppresses tumorigenicity in vivo in nude mice. We conclude that NLRX1 acts as a potential tumor suppressor by regulating the TNF-α induced cell death and metabolism.

© 2015 Elsevier B.V. All rights reserved.

1. Introduction

Clinical and experimental studies suggest that inflammation is intricately linked with tumorigenesis. In colorectal, hepatic, breast and several other cancer types, an inflammatory condition may precede the development of malignancy [1–3]. For example, inflammatory bowel disease (IBD) is associated with colon cancer and an infection by *Helicobacter pylori* progressively leads to gastric carcinoma [3,4]. However, despite the numerous examples of the apparent association of chronic inflammatory conditions with higher incidences of cancer, the molecular mechanisms linking these pathologies are still not well understood.

Inflammation, irrespective of its origin, promotes cell survival, proliferation of malignant cells and conditions the tumor microenvironment for further metastasis. Emerging clinical reports suggest that the levels of specific cytokines are altered in patients with different cancer types including breast, gastric, colorectal and hepatocellular carcinomas [5]. Increased levels of pro-inflammatory cytokines such as tumor necrosis factor alpha (TNF-α), macrophage migration inhibitory factor (MIF), transforming growth factor beta (TGF-β), interleukins-6, -8, -10 and -18 (IL-6, IL-8, IL-10 and IL-18) were reported in patients with advanced-stage pancreatic, colorectal and breast cancers [6–15]. Serum levels of TNF-α were elevated in eight independent types of cancer including breast, colorectal and gastric carcinomas [5,9,13]. In tumor microenvironment, TNF-α secreted by tumor cells or by inflammatory cells, promotes tumor cell survival through the stimulation of NF-κB pathway [16]. The activation of NF-κB up-regulates the expression of genes stimulating cell cycle progression and promotes epithelial–mesenchymal transition [17]. The binding of TNF-α to Type I TNF receptor (TNFR1) results in a pro-survival stimulation of NF-κB, through the formation of proximal plasma membrane bound complex I consisting of TNF receptor-associated protein with death domain (TRADD), receptor-interacting protein 1 (RIP1) and TNF receptor-associated factor 2 (TRAF2). During the TNF-α induced apoptosis, the complex-I dissociates from TNFR1 and recruits the Fas-associated death domain (FADD) and Caspase-8, forming cytosolic complex-II, where Caspase-8 is activated, which further initiates the downstream proteolytic cascade

[18,19]. The emerging evidences suggest that Caspase-8 may translocate to different subcellular sites including mitochondria in response to different stimuli [20–22]. TRADD, TRAF2 and RIP1 subunits of complex-II together with Pro-caspase-8 have been reported to translocate to mitochondria during the TNF-α induced apoptosis [23]. The functional relevance of Caspase-8 and other subunits of complex-II translocation to mitochondria is not clear.

Stimulation of the cells with TNF-α induces reactive oxygen species (ROS) generation however the regulatory mechanisms in different pathological conditions are still not clear. The mitochondrial Complex I and Complex III are the major sites of ROS generation [24]. Impaired Complex I and Complex III activities alter mitochondrial integrity by decreasing membrane potential, ATP synthesis and oxygen consumption [25]. The alteration of mitochondrial functions in response to TNF-α shifts the cancer cell metabolism toward glycolysis [26] however the mechanisms are not well understood. Upregulated glycolysis is a characteristic metabolic hallmark of cancer cells that is required to meet the bioenergetic demands. Thus, TNF-α signaling may confer a selective advantage to cancer cells for survival and proliferation through constitutive activation of NF-κB and reprogramming of metabolism. However, molecular mechanisms for the TNF-α-mediated regulation of mitochondrial bioenergetic function remains elusive.

Mitochondria are emerging as a critical signaling platform for the assembly of signallosomes regulating the inflammatory pathways [27]. Mitochondrial antiviral signaling protein (MAVS) localizes on the outer membrane of mitochondria and serves as an adaptor protein for RIG1, recognizing dsRNA during viral infections. MAVS is essential for the type-I IFN and NF-κB activation during viral infections [28]. Recent studies have suggested that COX5B, a subunit of Cytochrome c Oxidase (CcO) complex negatively regulates antiviral innate immunity by inhibiting MAVS signallosomes at the mitochondria [29]. Similarly, mediator of IRF3 activation (MITA) is a mitochondria-associated ER membrane (MAM) protein located in the area of close juxtaposition between mitochondria and ER. MITA is a crucial regulator of IFN and NF-κB signaling during infection by DNA viruses [30]. The study from our lab suggests that MITA is also an important regulator of inflammation acting as a potential tumor suppressor in breast cancer [31]. Similarly, a highly conserved NOD-like receptor with a mitochondria localization signal, the nucleotide-binding domain (NBD) and leucine-rich repeat (LRR)-containing family member X1 (NLRX1) [32] is an important component of TLR mediated inflammatory pathways [33]. The role of the NLRX1 in regulating the cross talk of inflammation and mitochondrial function and its involvement in carcinogenesis is not well understood.

In the present work, we identify NLRX1 as a crucial regulator of TNF-α induced cell death and reveal its potential role as a tumor suppressor. We report here that NLRX1 sensitizes cells to the TNF-α induced apoptosis by potentiating Caspase-8 at the level of complex-II. NLRX1 contributes to the TNF-α induced generation of ROS by regulating the activities of mitochondrial respiratory Complex I and Complex III. NLRX1 negatively regulates clonogenic survival of tumor cells in vitro and tumor growth in vivo by modulating oxidative phosphorylation and metabolism.

2. Materials and methods

2.1. Cell culture and reagents

HEK293, HeLa, and MCF-7 cells were cultured in Dulbecco's modified Eagle's media (DMEM, Life Technologies, Carlsbad, CA, USA). T47D and MDA-MB-231 cells were cultured in RPMI 1640 (Life Technologies, USA) and Leibovitz's L-15 media (HI-MEDIA, India) respectively. Media were supplemented with 10% (v/v) heat-inactivated fetal bovine serum (Life Technologies), 1% penicillin, streptomycin and neomycin (PSN) antibiotic mixture (Life Technologies). Full

length NLRX1 (isoform 1) cloned into pcDNA3.1 vector was provided by Dr. S E Girardin (University of Toronto, Ontario, Canada). Full length TRIM13 and HA-TRAF2 were kind gifts from Dr. Olle Sangfelt (Department of Oncology/Pathology, Cancer Centrum Karolinska, Stockholm, Sweden) and Dr. S M Srinivasula (IISER, Thiruvananthapuram, Kerala, India), respectively. The primary antibodies used were NLRX1, β-actin and c-MYC (Abcam, Cambridge, UK), PARP, Caspase-8 (Cell Signaling Technology, Inc., USA) and anti-HA peroxidase (Roche Applied Science, IN, USA). HRP-conjugated anti-mouse and anti-rabbit antibodies (Thermo Scientific, Inc., IL, USA) were used. TNF-α (Tumor Necrosis Factor-alpha) and Mito-TEMPO were procured from Enzo Life Sciences, Inc. USA. Cyclohexamide, antimycin, rotenone, H_2O_2, oligomycin and N-Acetyl Cysteine (NAC) were purchased from Sigma-Aldrich, USA. z-VAD-fmk (N-Benzyloxycarbonyl-Val-Ala-Asp(O-Me) fluoromethyl ketone) (BioVision, Inc., CA, USA), IETD-fmk (Ile-Glu(OMe)-Thr-Asp(OMe)-fluoromethyl ketone) (Clontech Laboratories, Inc., USA) were used. CM-H$_2$DCFDA and MitoSOX™ Red were purchased from Molecular Probes Inc., USA.

2.2. Cell death and proliferation assay

Cell death and proliferation was quantified by Trypan blue exclusion assay and MTT assay respectively as previously described [31].

2.3. Generation of stable cell lines

MT-RFP stable cell line in MCF-7 was generated as previously described to study mitochondrial localization of NLRX1 [34]. Similarly, stable knockdown of NLRX1 were generated in HEK293 and HeLa cells. Cells were transfected with NLRX1 shRNA and control shRNA and stable clones were selected and maintained in puromycin (3 μg/ml) containing DMEM.

2.4. Immunoprecipitation and Western blotting

For immunoprecipitation, HEK293 cells were plated at a density of 2×10^6 cells/90 mm^2 dish and transfected with indicated constructs using a calcium phosphate transfection method. After 24 h of transfection, the cells were treated with TNF-α/CHX for an indicated time interval, thereafter the cells were washed with cold DPBS (Life Technologies) and harvested. Cells were lysed in NP40 IP lysis buffer (100 mM NaCl, 50 mM Tris–HCl, 10% Glycerol, 0.1% Nonidet P-40) containing complete protease inhibitor cocktail (Roche Applied Science, IN, USA) and incubated on ice for 1 h and centrifuged at 13,000 rpm for 15 min at 4 °C. Supernatant was collected and incubated overnight with Anti-HA Affinity Matrix on a roller shaker at 4 °C. The beads were washed three times with NP40 IP lysis buffer, resuspended in 5 × SDS-PAGE sample buffer, resolved on 12% SDS-PAGE and analyzed by Western blotting using specific antibodies.

For Caspase-8 and Caspase-3 immunoblotting, HEK293 cells were plated at a density of 5×10^5 cells/well in a 6-well plate and transfected with indicated constructs using calcium phosphate transfection method. After 24 h of transfection, the cells were treated with indicated reagents for specific time. The cells were harvested in cold PBS and lysed in RIPA lysis buffer (150 mM NaCl, 50 mM Tris–HCl, 1% Triton X-100, and complete protease inhibitor cocktail (Roche, Germany), and analyzed by Western blotting as indicated above. Western blot quantification was performed by densitometry using Image J 1.45 software (NIH, MD, USA).

2.5. Caspase-8 luciferase assay

Caspase-8 activation assay was performed using Caspase-Glo® 8 Assay Systems (Promega, USA) according to manufacturer instructions as described previously [35].

2.6. Confocal microscopy

Mitochondrial localization of NLRX1 was monitored by confocal microscopy. Briefly, MT-RFP-MCF-7 stable cell line were plated on cover slip at the density of 1.5×10^5 cells/well in a 24-well plate followed by transfection with indicated expression vector. After 24 h of transfection, the cells were treated with TNF-α for four hours and fixed with 4% paraformaldehyde. The cells were monitored by Zeiss LSM 710 confocal microscope (Carl Zeiss, Inc., Germany). Images were captured, pseudo-colored and analyzed by Zen Black software. Colocalization was quantified by correlation using Image J 1.45 software (NIH, MD, USA).

2.7. Subcellular fractionation and Western blotting

Mitochondrial localization of NLRX1 and Caspase-8 were analyzed by Western blotting using isolated mitochondria. HEK293 cells were plated at the density of 2×10^6 cells/90 mm² dish and transfected with indicated constructs using calcium phosphate transfection method. Cells were treated with TNF-α/CHX for 8 h and washed with cold PBS, harvested by centrifugation at 600 ×g for 10 min. Cell pellets were resuspended in mitochondria isolation buffer (200 mM mannitol, 70 mM sucrose, 1 mM EGTA, 10 mM HEPES; pH 7.4, 1× protease inhibitor cocktail (Sigma-Aldrich, USA) and incubated on ice for 5 min. The cells were disrupted by passing through a 24G sterile syringe needle and centrifuged at 600 ×g for 10 min to separate nuclei and cell debris. The supernatant (cytosolic fraction) was collected and centrifuged again at 10,000 ×g for 10 min. The pellet (mitochondrial fraction) were washed twice with isolation buffer and lysed with mitochondria lysis buffer (50 mM Tris–HCl, pH 7.5, 150 mM NaCl, 2 mM EDTA, 2 mM EGTA, 0.2% Triton X-100, 0.3% NP40 and 1× Protease Inhibitor Cocktail. The mitochondrial and cytosolic protein concentrations were assessed using Bradford protein estimation assay. Equal proteins were loaded and resolved on 12% SDS-PAGE and analyzed by Western blotting using indicated antibodies.

2.8. ROS measurements

Intracellular and mitochondrial ROS production was measured by CM-H$_2$DCFDA (10 μM) and MitoSOX Red (5 μM) staining respectively. Briefly, HEK293 and HeLa cells were plated in 24-well plates at the density of 1.5×10^5 cells/well. After overnight incubation, the cells were transfected with NLRX1 and NLRX1 shRNA1 using calcium phosphate transfection protocol. Twenty-four hours post transfection, the cells were treated with indicated reagents for 4 h and stained with indicated reagent and monitored under fluorescence microscope (Olympus IX81 microscope; Olympus, Tokyo, Japan). Minimum of 5 images and 80–100 cells were used for analysis.

Similarly, ROS levels were quantified by fluorometry. Briefly, MCF-7 and HEK293 cells were transfected with indicated constructs. The cells were treated with indicated reagents for 4 h and stained with CM-H$_2$DCFDA (12.5 μM) in DPBS for intracellular ROS quantification and MitoSOX Red (2.5 μM) in DMEM for mitochondrial superoxide quantification. The cells were washed with DPBS and normalized to 1×10^6 cells/ml. Fluorescence intensity was quantified by fluorometer (Hitachi High-Technologies Corp., Japan) with excitation/emission at 495/520–540 nm and 510/570–600 nm, respectively.

2.9. Mitochondrial Complex I and Complex III assays

The activities of mitochondrial Complex I and Complex III was analyzed spectrophotometrically. Briefly, HEK293 cells were seeded at the density of 5×10^5 cells/well in the 6-well plate. After overnight incubation, the cells were transfected with indicated construct using calcium phosphate transfection protocol and treated as indicated. The NLRX1 knockdown stable cell line and the NLRX1 expressing cells were harvested and washed with cold DPBS. The cells were subjected to 2–3 freeze–thaw cycles in a freeze–thaw complete solution (0.25 M sucrose, 20 mM Tris–HCl (pH 7.4), 40 mM KCl, 2 mM EDTA supplemented with 1 mg/ml fatty acid-free BSA, 0.01% Digitonin and 10% Percoll). The cells were washed again with the freeze–thaw solution devoid of digitonin and resuspended in Complex I assay buffer (35 mM potassium phosphate (pH 7.4), 1 mM EDTA. 2.5 mM NaN$_3$, 1 mg/ml BSA, 2 μg/ml antimycin A, 5 mM NADH). The reaction was started by adding 80 μg of cell lysate to 500 μl of assay buffer in 1 ml quartz cuvette. Complex I activity was measured for 3 min by monitoring the decrease in absorbance at 340 nm after the addition of 2.5 mM acceptor decylubiquinone indicating the oxidation of NADH.

Similarly, for Complex III activity, NLRX1 knockdown stable cells were seeded at a density of 2.5×10^6 cells/90 mm² dish. The cells were harvested and washed with cold DPBS. All the subsequent steps were performed at 4 °C. The cells were suspended in 0.5 ml of 20 mM hypotonic potassium phosphate buffer (pH 7.5) and lysed using a 24G sterile syringe and subjected to freeze–thaw cycle. The cell lysate (80 μg) was added to the 500 μl of Complex III assay buffer (25 mM potassium phosphate (pH 7.5), 0.025% Tween-20, and 300 μM NaN$_3$, 75 μM Cytochrome c) in cuvette and the baseline observance was monitored at 550 nm for 2 min. The reaction was started by the addition of 100 μM decylubiquinol (freshly prepared 2.5 mM stock) monitoring the increase in absorbance at 550 nm for 2 min.

2.10. ATP measurements

The levels of ATP were measured in NLRX1 expressing and NLRX1 KD cells under different conditions by an ATP dependent luciferase assay using ATP determination kit (Molecular Probes/Life Technologies, ON, Canada).

2.11. Soft agar assay, colony formation assay and scratch assay

Anchorage-independent potential was assessed by soft agar assay, clonogenic activity and migration ability of cancer cells were determined as described previously [31,36].

2.12. Animal experiments

Animal studies were performed according to the rules and protocols approved by the Bioethical committee of the Engelhardt Institute of Molecular Biology, Moscow, Russia. A total of 48 nude mice (5 week old Balb/c *nu/nu*) were used in the current expeiment. RKO colon carcinoma cells carrying empty lentiviral vector pLSLP, NLRX1 shRNA1 (Sigma TRCN0000129459) and over expressing NLRX1 (lentiviral construct pLCMV-NLRX1-puro) were used. Cells were trypsinized, washed three times in ice-cold PBS and inoculated subcutaneously in four locations (left and right hind and shoulders) at a density of 1×10^6 cells in 0.1 ml per inoculum. Fifteen micrograms of purified human recombinant TNF-α (gift of Dr. Alexey Sazykin, Moscow State University) was inoculated intraperitoneally 24 h later, and control mice were inoculated with PBS. The mice were inspected every two days and tumor size was measured. Tumor volume was calculated according to the following formula: ellipsoid volume: 1/6 ∗ pi ∗ a ∗ b ∗ c, where a, b, and c are linear sizes of the tumor in three dimensions.

Expression levels of NLRX1 transcripts in the cell lines were monitored by real time PCR with EVA-green dye.

The following primers were used:

NLRX1-For: AACGGTGCTGGTGACACA;
NLRX1-Rev: GCTCAGCTCATTGAAGTAGA.

The level of NLRX1 inhibition was 85% in RKO cells. Levels of NLRX1 transcripts in the hyperexpressor cell lines were 8-fold compared to

controls for RKO cells. Basal levels of NLRX1 transcripts (compared to β-actin control transcripts) were roughly similar for RKO cells.

2.13. Statistical analysis

Data are expressed as mean ± SEM of at least two or three independent experiments. Unpaired two-tailed Student's t tests were performed unless otherwise noted and *P < 0.05, **P < 0.01 and ***P < 0.001 were considered to denote significance. GraphPad Prism® was used to perform all the statistical analyses.

3. Results

3.1. NLRX1 sensitizes TNF-α induced cell death

To study the role of NLRX1 in regulation of cell death and survival in response to different physiological stress, we transfected HEK293 cells with NLRX1, exposed the cells to different stimuli and monitored cell death by trypan blue exclusion assay (Fig. 1A). The expression of NLRX1 had no significant effect on cell survival in the untreated conditions. The expression of NLRX1 showed no effect on cell death in response to oxidative stress induced by Rotenone and H_2O_2. The co-treatment of NLRX1-expressing cells with TNF-α and the translation inhibitor cyclohexamide (CHX) showed significantly increased cell death (Fig. 1A). Similarly, transfection of HeLa cells with NLRX1 significantly increased the number of trypan blue positive cells following the TNF-α/CHX treatment (Fig. S1A). These results suggest that NLRX1 specifically sensitizes the cells to TNF-α induced death. This conclusion was further confirmed by downregulating NLRX1 using specific shRNA in HEK293 cells. Three different shRNAs were checked for the efficient knockdown of NLRX1. The shRNA1 of NLRX1 showed maximum downregulation hence it was further used in the study (Fig. 1B). The constructs expressing NLRX1-specific shRNAs were transfected to HEK293 cells and cell death was monitored by trypan blue exclusion staining. Knockdown of NLRX1 by all of the shRNAs increased the cell survival following TNF-α/CHX treatment, although significant increase was achieved with shRNA1 (Fig. 1C). Similarly, the transfection of NLRX1 shRNA1 in HEK293 showed maximum cell survival (Fig. S1B). To further
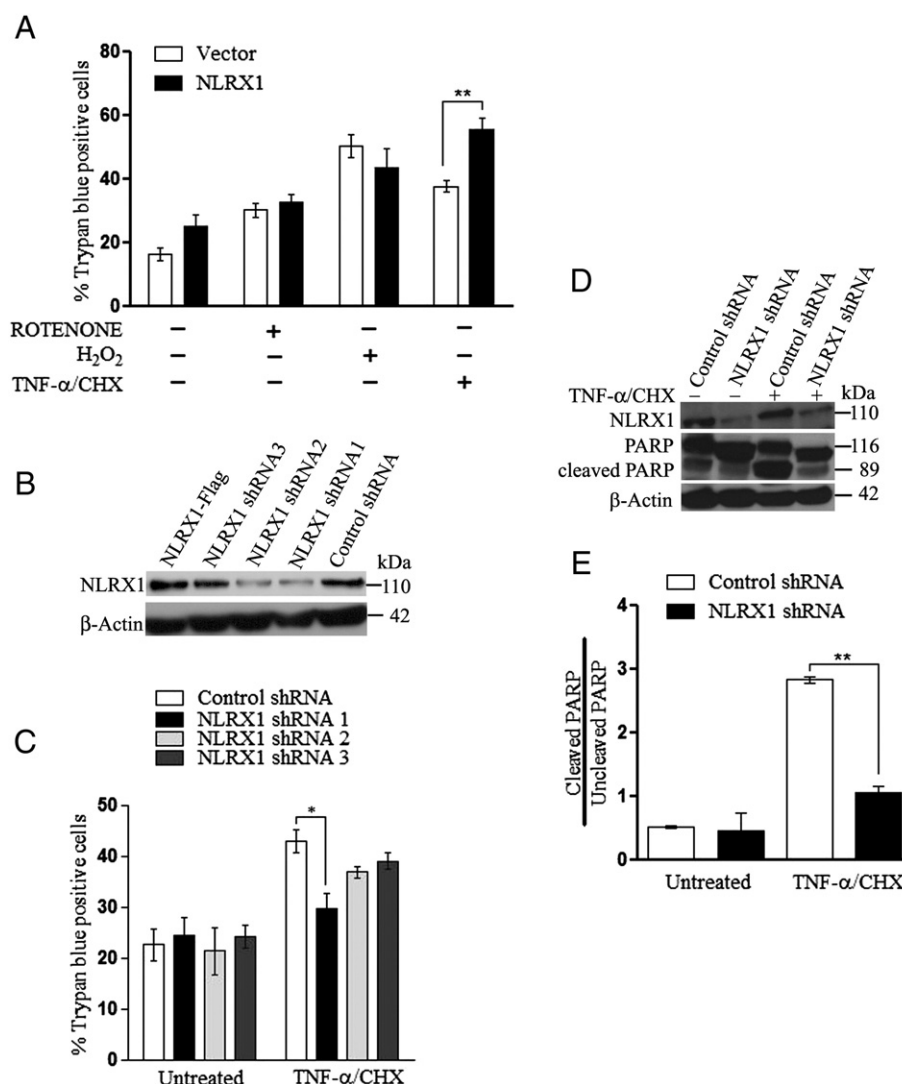

Fig. 1. NLRX1 regulates TNF-α induced cell death. (A) HEK293 cells were transfected with NLRX1 and vector control followed by treatment with Rotenone (50 μM), H_2O_2 (100 μM) and TNF-α/CHX (10 ng/25 μM). The cell death was monitored by Trypan blue exclusion assay. (B) HEK293 cells were transfected with control shRNA, NLRX1-Flag and three different shRNAs targeting NLRX1, namely NLRX1 shRNA 1, 2 and 3. Cell lysates were analyzed for NLRX1 expression by Western blotting. (C) HEK293 cells were transfected with control shRNA and three shRNA targeting NLRX1. Cells were subjected to TNF-α/CHX treatment for 24 h and analyzed cell death by Trypan blue staining. (D) NLRX1 shRNA and control shRNA stable HEK293 cells were treated with TNF-α/CHX for 6 h. Cell lysates were subjected to Western blotting with PARP specific antibody. (E) Quantification of PARP cleavage detected by Western blotting was performed using densitometry and ratios of cleaved to uncleaved PARP are indicated (results are representative of two independent experiments). Data in (A) and (C) depict mean ± SEM values (n = 3). Asterisk (*) indicates that p value < 0.05, for SEM.

investigate the mechanism of TNF-α induced cell death, PARP immuno-blotting was performed after NLRX1 knockdown. PARP is cleaved by executioner caspases during TNF-α induced apoptosis [37]. NLRX1 knockdown HEK293 cells were treated with TNF-α/CHX for 6 h and PARP cleavage was monitored. Western blotting showed 110 kDa and 89 kDa band corresponding to native and cleaved form of PARP in control shRNA transfected cells. The knockdown of NLRX1 showed decreased levels of 89 kDa bands corresponding to cleaved subunit of PARP as compared to the control (Fig. 1D, E). To rule out the possibility of a cell line-specific phenomenon, the expression of NLRX1 in MCF-7 cells also showed increased levels of cleaved PARP subunit as compared to vector transfected cells (Fig. S1C). Collectively, the results indicate that NLRX1 is an important regulator of TNF-α induced cell death. The similar study from Soares et al. [38] also reported a key role of NLRX1 in cell death and cancer susceptibility during the preparation of the manuscript. Several findings from our study is in consonance with this study, however, the two studies differ in respect to the response to TNF-α/CHX treatment. It is highly probable that transformed cell lines with a variable expression level of NLRX1 may differ in sensitivity to TNF-α/CHX. The cell death data reported in the current study showed different levels of cell death in HEK293, MCF-7 breast and HeLa which had a different expression level of NLRX1.

3.2. Caspase activation is essential for the NLRX1 mediated sensitization of TNF-α induced cell death

The cleavage of PARP suggests the activation of caspases in the presence of NLRX1. The activation of caspases plays a major role in TNF-α induced cell death [18] hence we planned to confirm the role of caspases in the NLRX1 mediated sensitization to TNF-α induced cell death. Firstly, we analyzed Caspase-8 and Caspase-3 activations at different time points by Western blotting (Fig. 2A). High levels of 41 kDa and 18 kDa bands corresponding to cleaved subunits p43 and p18 of Caspase-8 were detected as early as 4 h in the presence of TNF-α/CHX in NLRX1 transfected HEK293 cells, as compared to vector transfected cells (Fig. 2A). Similarly, a 17 kDa band corresponding to the cleaved subunit of Caspase-3 was detected 4 h after the TNF-α/CHX treatment (Fig. 2A). Quantification of Caspase-8 activity was also monitored at different time points in HEK293 cells transfected with vector control and NLRX1 in the presence of TNF-α/CHX. The enzymatic activity of Caspase-8 was high at 4 h and remained elevated till 8 h in NLRX1 transfected cells as compared to vector control (Fig. 2B). Similarly, the expression of NLRX1 in MCF-7 cells showed increased levels of cleaved Caspase-8 subunits as compared to vector transfected cells in the presence of TNF-α/CHX. (Fig. S1C). Conversely, knockdown of NLRX1 in HEK293 cells showed a significant decrease in the levels of cleaved subunits of Caspase-8 (p43 and p18) as compared to control (Fig. 2C).

To confirm the role of NLRX1 in TNF-α induced Caspase-8 activation and cell death, Caspase-8 activity was monitored upon co-treatment of the cells with the pan-caspase inhibitor, z-VAD-fmk and TNF-α/CHX at the 4 h time point. A decrease in Caspase-8 enzymatic activity was observed following inhibition of caspases in NLRX1 transfected cells (Fig. 2D). This result was confirmed by Western blotting showing reduced levels of cleaved Caspase-8 subunits in the presence of z-VAD-fmk (Fig. 2E). Similarly, HEK293 cells were transfected with NLRX1, treated with TNF-α or with TNF-α/CHX in the absence or presence of the pan-caspase inhibitor z-VAD-fmk and monitored cell death. We observed no significant difference in cell death between NLRX1-transfected and vector-transfected cells, both in untreated conditions and in the presence of TNF-α. Treatment with TNF-α/CHX sensitized NLRX1 expressing cells to TNF-α induced cell death as observed earlier. The co-treatment of the NLRX1 expressing cells with TNF-α/CHX and z-VAD-fmk attenuated cell death (Fig. 2F). Interestingly, the co-treatment of cells with the Caspase-8 specific inhibitor z-IETD-fmk significantly increased cell survival as assessed by trypan blue staining. All the above

evidences strongly suggest the role of NLRX1 in regulation of TNF-α-mediated Caspase-8 activation.

3.3. NLRX1 associates with the TNF-α induced complex-II to promote Caspase-8 activity

The binding of TNF-α to its cell surface receptor and formation of complex-II initiates cell death program by recruiting Caspase-8 and other adaptor proteins. The observed stimulation of Caspase-8 activity by NLRX1 as early as 4 h after TNF-α/CHX treatment suggests that NLRX1 may act at the level of complex-II formation. Recent studies implicate an essential role of ubiquitin ligases in the assembly and activation of Caspase-8 [35,39,40]. RING family E3 ligase TRAF2 interacts with Caspase-8 at complex-II and sets a threshold for Caspase-8 activation [39]. Similarly, our recent observation has demonstrated the role of the RING E3 ligase, TRIM13 in regulation of Caspase-8 activation downstream of complex-II [35]. We planned to test the association of NLRX1 with TNF-α induced signaling complexes and the role of the E3 ligases in regulation of NLRX1 mediated activation of Caspase-8. HEK293 cells were co-transfected NLRX1 with TRAF2 and TRIM13 and were treated with TNF-α/CHX. In agreement with our earlier report [35], the expression of TRIM13 increased the levels of 41 kDa and 18 kDa bands corresponding to processed Caspase-8 in the absence/presence of TNF-α/CHX (Fig. 3A). However, the co-expressions of TRIM13 and NLRX1 decreased the activation of Caspase-8 in the presence of TNF-α/CHX. Similarly, in agreement with earlier report the expression of TRAF2 attenuated the processing and activation of Caspase-8 to that of control level. Co-expression of TRAF2 significantly reversed the NLRX1-mediated increase in levels of processed Caspase-8 in presence of TNF-α. Taken together, the data supported our hypothesis that NLRX1 affects the activity of Caspase-8 at the level of complex-II formed after TNF-α stimulation. To test whether NLRX1 may interact with components of complex-II, we performed co-immunoprecipitation (IP) analysis. We co-expressed NLRX1 along with HA-TRAF2 and Myc-RIP1 in HEK293 cells, treated the cells with TNF-α/CHX for 5 min and 8 h to analyze Complexes I and -II, respectively. We immunoprecipitated TRAF2, a subunit of both complexes with HA-antibodies and analyzed the interactions. By Western blotting we identified a 110 kDa band corresponding to NLRX1, a 78 kDa band of RIP1 and Casaspe-8, after eight hours of TNF-α/CHX treatment. There was no pull down of NLRX1, RIP1 and Caspase-8, after five minutes of TNF-α/CHX treatment (Fig. 3B). The result indicates that NLRX1 associates with TNF-α induced signaling complex-II to promote the activation of Caspase-8.

3.4. NLRX1 localizes to mitochondria and augments the TNF-α induced ROS production

NLRX1 localizes to mitochondria, although its functional significance is still not well understood. Similarly, Caspase-8 is also known to be localized to mitochondria hence, we hypothesized that the crosstalk between NLRX1 and Caspase-8 may regulate mitochondrial function in response to TNF-α. We analyzed the cellular localization of NLRX1 in the absence/presence of TNF-α. We transfected MCF-7-MT-RFP stable cell line with NLRX1-GFP and monitored the cellular localization of proteins by confocal microscopy. We observed that a significant fraction of NLRX1 co-localizes with mitochondria (Fig. 4A, B) in the presence of TNF-α. This observation was further confirmed by subcellular fractionation. The mitochondrial and cytoplasmic fractions from the TNF-α/CHX treated NLRX1-HEK293 cells were analyzed by Western blotting. The high level of pro-caspase-8 was detected (the 55 kDa band) in the mitochondrial fraction of untreated cells. The increased levels 43 kDa and 18 kDa corresponding to the cleaved subunits of Caspase-8 (p43 and p18) were higher in NLRX1 transfected mitochondrial fraction as compared to vector control in the presence of TNF-α/CHX. NLRX1 was specifically enriched in the mitochondrial fraction of both untreated and treated cells (Fig. 4C). The quality of mitochondrial and cytosolic
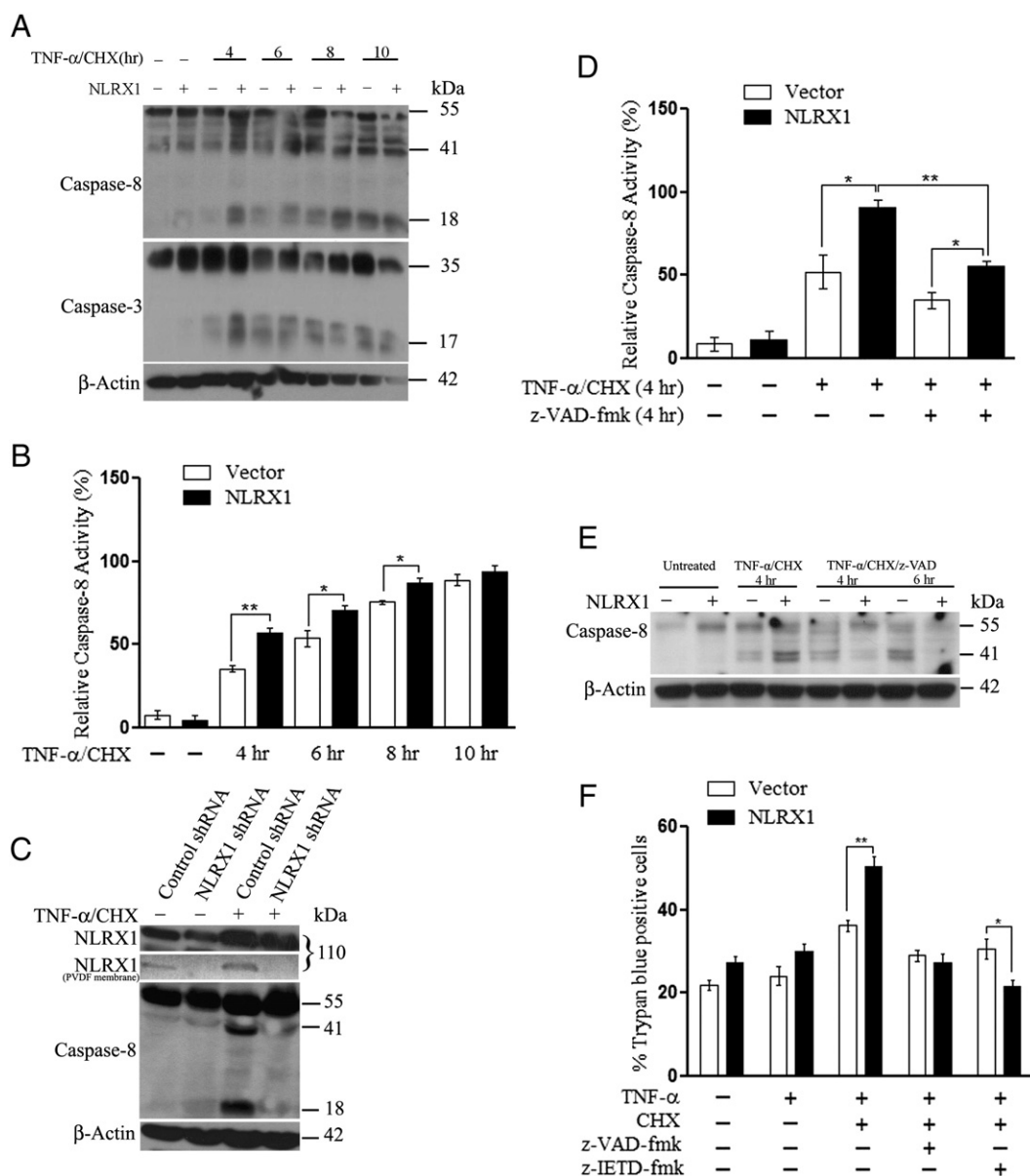
Fig. 2. NLRX1 regulates Caspase-8 activity during TNF-α induced cell death. (A) HEK293 cells were transfected with NLRX1 and treated with TNF-α/CHX for indicated time. The cell lysates were analyzed by Western blotting using Caspase-8 and Caspase-3 specific antibodies. (B) HEK293 cells were transfected and treated as indicated in (A) and Caspase-8 activity was analyzed at different time points by Caspase-8 Glo luciferase assay system (n = 2).(C) NLRX1 shRNA and control shRNA stable HEK293 cells were treated with TNF-α/CHX for 4 h and Caspase-8 activation was analyzed by Western blotting. (D and E) HEK293 cells were transfected with NLRX1 and vector and treated with TNF-α/CHX or TNF-α/CHX and z-VAD-fmk (20 μM) for indicated time. The Caspase-8 activation was analyzed by Caspase-8 Glo luciferase assay system (n = 2) (D) and Western blotting (E). (F) HEK293 cells were transfected with NLRX1 and vector control followed by treatment with TNF-α/CHX, z-VAD-fmk (20 μM) and z-IETD-fmk (10 μM). After 24 h of treatment, cell death was measured by trypan blue exclusion assay (n = 3). Asterisk (*) indicates that p value < 0.05, for SEM.

fractions was also analyzed using antibodies to NDUFS2, a subunit of mitochondrial Complex I, and to RPS9, a component of 40S ribosomal subunit. The NDUFS2 was found exclusively in the mitochondrial fraction whereas RPS9 was detected only in the cytosol. Together, these results demonstrate that NLRX1 localizes to mitochondria in the presence of TNF-α/CHX.

Emerging evidences suggest that caspases may cleave subunits of the ETC and regulate ROS during different stress conditions [41]. The role of the crosstalk between NLRX1 and Caspase-8 in regulation of ROS and activity of mitochondrial complexes of ETC is not well understood. To test whether NLRX1 may regulate TNF-α induced ROS generation, the NLRX1 knockdown HeLa cells were treated with TNF-α/CHX and stained with the oxidant-sensitive dye, CM-H₂DCFDA. As expected, the TNF-α/CHX treatment increased ROS levels in control cells. Interestingly, the knockdown of NLRX1 substantially attenuated the TNF-α/

CHX stimulated generation of ROS (Fig. 5A). To confirm this, intracellular ROS formation in HEK293 cells was quantified in the presence of TNF-α/CHX alone or in combination with N-Acetyl Cysteine (NAC), an antioxidant. ROS generation was significantly decreased in NLRX1 knockdown (KD) HEK293 cells while co-treatment with NAC further suppressed ROS level in NLRX1 KD HEK293 cells in the presence of TNF-α/CHX (Fig. 5B). Based on these results, we concluded that NLRX1 localizes to mitochondria and participates in the TNF-α induced ROS generation.

Mitochondria is one of the major sites of ROS under different stress conditions. We hypothesized that a cross talk between NLRX1 and Caspase-8 may regulate mitochondrial function, including the generation of ROS. To test this possibility, mitochondrial superoxide generation in NLRX1 and vector transfected MCF-7 cells was quantified in the presence of TNF-α/CHX alone or in combination with Mito-TEMPO, a
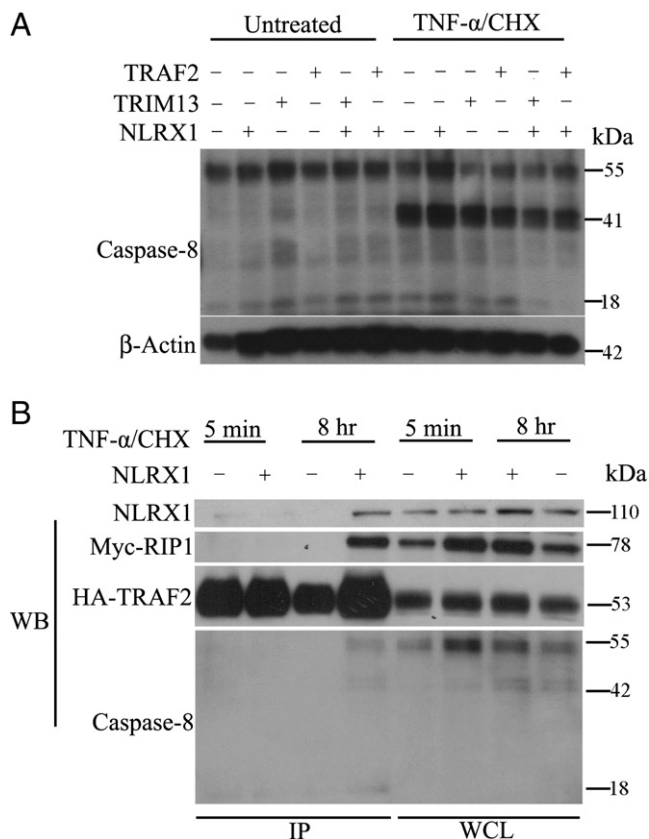
Fig. 3. NLRX1 interacts with complex-II during TNF-α induced cell death. (A) HEK293 cells were cotransfected with NLRX1 in combination with TRAF2 and TRIM13. The cells were treated with TNF-α/CHX for 4 h. Cell lysates were analyzed by Western blotting with Caspase-8 antibody. (B) HEK293 cells were transfected with NLRX1-Flag, HA-TRAF2, Myc-RIP1 followed by co-treatment with TNF-α/CHX for 5 min and 8 h. Immunoprecipitation with anti-HA antibody was performed and interacting proteins were analyzed by Western blotting with indicated antibodies.

mitochondrial superoxide scavenger. The expression of NLRX1 significantly induced mitochondrial ROS in the presence of TNF-α/CHX while co-treatment with Mito-TEMPO suppressed superoxide formation as compared to vector control (Fig. 5C). Similarly, we treated NLRX1 transfected HEK293 cells with TNF-α/CHX and mitochondrial ROS level was analyzed by staining cells with MitoSOX Red and visualized under fluorescence microscope. NLRX1 expression alone stimulated mitochondrial superoxide formation in untreated condition which further increased significantly in the presence of TNF-α/CHX as compared to vector control (Fig. S2A).

To determine the role of Caspase-8 in amplification of TNF-α induced ROS generation, HeLa cells expressing NLRX1 were pretreated with z-IETD-fmk, then treated with TNF-α/CHX and the intracellular ROS was assessed by CM-H$_2$DCFDA staining. ROS levels were significantly increased in NLRX1 transfected cells as compared to vector transfected cells in the presence of TNF-α/CHX. The inhibition of Caspase-8 with z-IETD-fmk decreased the level of ROS in NLRX1 transfected cells treated with TNF-α/CHX (Fig. 5D). ROS quantification in MCF-7 cells transfected with NLRX1 and vector control yielded similar results both in the presence of TNF-α/CHX and co-treatment with z-IETD-fmk (Fig. 5E). We also tested whether blocking ROS generation may rescue TNF-α/CHX induced death of NLRX1 expressing MCF-7 and HEK293 cells. As observed earlier, expression of NLRX1 had no significant effect on cell survival in the untreated conditions and in the presence of Rotenone and H$_2$O$_2$. Treatment with TNF-α/CHX sensitized NLRX1 expressing cells to TNF-α induced cell death, in contrast, co-treatment with NAC significantly increased cell survival of NLRX1 transfected cells as compared to vector transfected cells (Fig. S2B).

Similar results were obtained in HEK293 cells transfected with NLRX1 and treated with TNF-α/CHX along with Mito-TEMPO (Fig. S2C). All together, these data suggested that NLRX1 regulates Caspase-8 activity to modulate mitochondrial ROS and cell death during TNF-α induced apoptosis.

3.5. NLRX1 regulates mitochondrial respiratory Complex I and Complex III to maintain ATP levels in the presence of TNF-α

As Complex I and Complex III of the mitochondrial electron transport chain are the major sites for ROS generation [42], hence we tested if NLRX1 expression may regulate their activity. The expression of NLRX1 in HEK293 cells decreased Complex I activity in the presence of TNF-α, but not after co-treatment with TNF-α and CHX. Interestingly, inhibition of Caspase-8 by z-IETD-fmk significantly increased Complex-I activity in the presence of TNF-α/CHX (Fig. 6A). Similarly, the treatment of cells with pan-caspase inhibitor z-VAD-fmk enhanced Complex I activity to the same level in both NLRX1 expressing and control cells. Conversely, the activity of respiratory Complex I increased, both in the absence/presence of TNF-α in shNLRX1 transfected cells (Fig. 6B). Similarly, the knockdown of NLRX1 in HEK293 cells increased Complex III activity, as compared to control cells, both in the absence and presence of TNF-α (Fig. 6C).

The above experiments suggest that NLRX1 regulates the activity of mitochondrial complexes which is the major source of ATP generation in the cell. Therefore, we investigated whether the expression of NLRX1 might regulate total cellular and mitochondrial ATP levels in the presence of TNF-α. The expression of NLRX1 in HEK293 cells decreased total cellular steady-state ATP level in the presence of TNF-α whereas the decrease was less evident when the cells were co-treated with TNF-α and CHX (Fig. 6D). The ATP levels were measured after 16 h of treatment with TNF-α/CHX, hence, the activated caspases may have cleaved the subunits of ETC complexes as observed earlier [23] and the decrease may not be evident. Importantly, the inhibition of Caspase-8 by z-IETD-fmk during TNF-α/CHX induced apoptosis significantly enhanced the ATP levels in NLRX1 expressing cells, while addition of z-VAD-fmk showed no significant effect on the levels of ATP. The inhibition may not be observed as z-VAD-fmk is not a potent inhibitor of the initiator caspases [43] further suggesting that activated caspase-8 may directly act on complexes of ETC in the presence of NLRX1. Total ATP levels in the NLRX1 KD HEK293 cells were significantly higher in both TNF-α and TNF-α/CHX treated cells (Fig. 6E). The mitochondrial ATP levels in NLRX1 KD HEK293 cells increased both in the absence/presence of TNF-α (Fig. S2D). Similar results were observed in MCF-7 breast carcinoma cells where NLRX1 expression showed a significant decrease in total ATP level both in the absence/presence of TNF-α (Fig. S2E). These results strongly suggest that NLRX1 regulates activity of mitochondrial complexes and maintenance of intracellular levels of ATP.

3.6. NLRX1 expression suppresses clonogenic ability, anchorage-independent growth and migration of cancer cells in vitro

The NLRX1 mediated decrease in mitochondrial respiratory complex activity suggests its important role in cancer cell metabolism. Extracellular acidification of tumor microenvironment is a common feature of tumor tissue. The acidic pH is attributed to a switch from mitochondrial respiration to aerobic glycolysis, which is a characteristic hallmark of cancer cells [30]. Interestingly, we observed that knockdown of NLRX1 in HeLa cells reversed the acidification of the culture medium (Fig. S2F), suggesting that NLRX1 may contribute to the metabolic switch toward glycolysis in tumor cells.

As we observed above that NLRX1 can modify mitochondrial metabolism and promote aerobic glycolysis, it may have an implication in regulating the clonogenic and tumorigenic potentials of tumor cells. We analyzed the NLRX1 expression in different cancer types available in
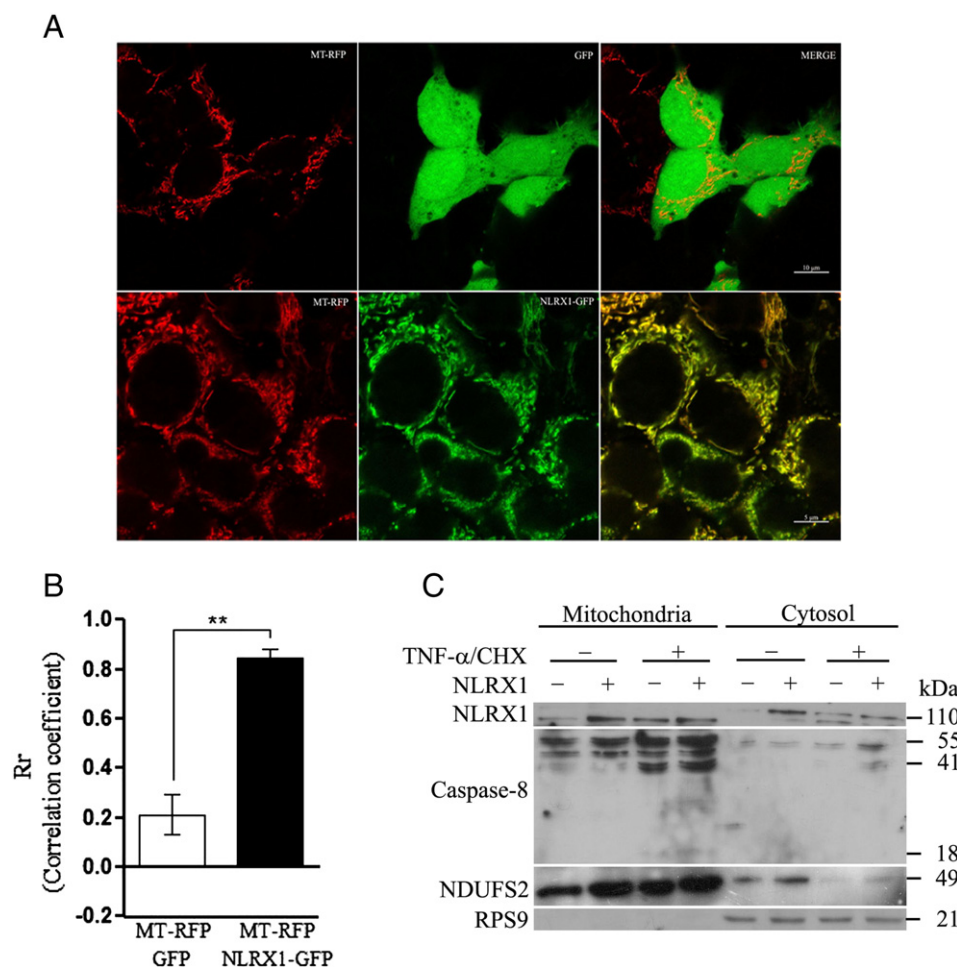
Fig. 4. NLRX1 translocates to mitochondria and regulates Caspase-8 activity at the mitochondria in the presence of TNF-α. (A) MCF-7-MT-RFP stable cell line was transfected with NLRX1-GFP and GFP control. After 24 h of transfection, cells were treated with TNF-α, fixed with 4% paraformaldehyde and visualized by confocal microscopy. Scale bar in the upper and lower panel represents 10 μm and 5 μm, respectively. (B) Colocalization quantification of confocal images by Pearson's correlation coefficient (Rr) was performed using Image J 1.45 software (NIH, MD, USA). (C) HEK293 cells were transfected with NLRX1 and control vector followed by treatment with TNF-α/CHX for 4 h. Cells were subjected to subcellular fractionation. Mitochondrial and cytoplasmic fractions from untreated and treated cells were analyzed by Western blotting with indicated antibodies. Asterisk (*) indicates that p value < 0.05, for SEM.

gene expression databases. NLRX1 mRNA levels were downregulated in breast and cervical cancers (Gene Expression across Normal and Tumor tissues (GENT), Fig. S3A, (http://medicalgenome.kribb.re.kr/GENT)). Similarly, protein expression levels of NLRX1 were lower in breast tissues as compared to normal breast tissues (Fig. S3B) (http://www.proteinatlas.org/). Therefore, we examined NLRX1 expression pattern in different breast cancer cell lines using Western blotting. NLRX1 protein levels were low in MCF-7 and T47D (ER positive) cells as compared to MDA-MB-231 and HBL-100 (ER negative) cells that demonstrated elevated levels of NLRX1 (Fig. 7A). We investigated whether NLRX1 expression in MCF-7 affected cancer phenotype using clonogenic assay and soft agar tumorigenesis assay. The clonogenic ability of NLRX1 expressing MCF-7 cells was monitored in the presence and absence of TNF-α. The expression of NLRX1 significantly decreased the clonogenic ability of MCF-7 cells in the presence of TNF-α (Fig. 7B) also shown as plating efficiency (Fig. 7B′). The soft agar assay was performed to study the role of NLRX1 in anchorage-independent cell growth. Control MCF-7 cells were able to grow in soft agar and formed large colonies in the presence of TNF-α. The NLRX1 expressing MCF-7 cells were not able to grow in soft agar and formed small colonies in the presence of TNF-α, as compared to untreated cells (Fig. 7C) plotted as colony area (Fig. C′). We further checked whether NLRX1 expression may inhibit cell migration. MCF-7 cells were transfected with NLRX1, treated with TNF-α treatment and the migration ability was analyzed by scratch assay. The NLRX1 expressing MCF-7 cells displayed a significant increase in

open wound area in the presence of TNF-α, as compared to vector transfected cells (Fig. 7D). The low level of expression of NLRX1 in MCF-7 may still regulate the cellular functions hence we further downregulated the expression by shRNA transfection. The NLRX1 knockdown in MCF-7 cells displayed an increased ability to form colonies (tumorispheres) in soft agar, as compared to control cells. The size of colonies was also increased significantly in the presence of TNF-α (Fig. S4A and S4B). Collectively, these results suggest that NLRX1 negatively regulates tumorigenic potential and migration ability in untreated condition as well as in the presence of TNF-α.

3.7. NLRX1 suppresses tumorigenicity in nude mice

To extend the cellular finding to in vivo models, we used RKO colon carcinoma cells to perform xenograft tumor formation assays in nude mice. RKO cells expressing NLRX1 shRNA1 or ectopic full length NLRX1 mRNA were injected into nude mice and the growths of subcutaneous tumors were examined every two days. In agreement with our in vitro studies, NLRX1 hyper expression negatively affected the tumorigenic potential of RKO in nude mice. In contrast, NLRX1 knockdown substantially increased the tumorigenic potential of RKO cells in the nude mice xenograft assay (Fig. 8A). Downregulation of NLRX1 significantly increased tumor volume, as well as the increased efficiency of tumor initiation. Similarly, hyper expression of NLRX1 resulted in smaller tumor volume. The effects were
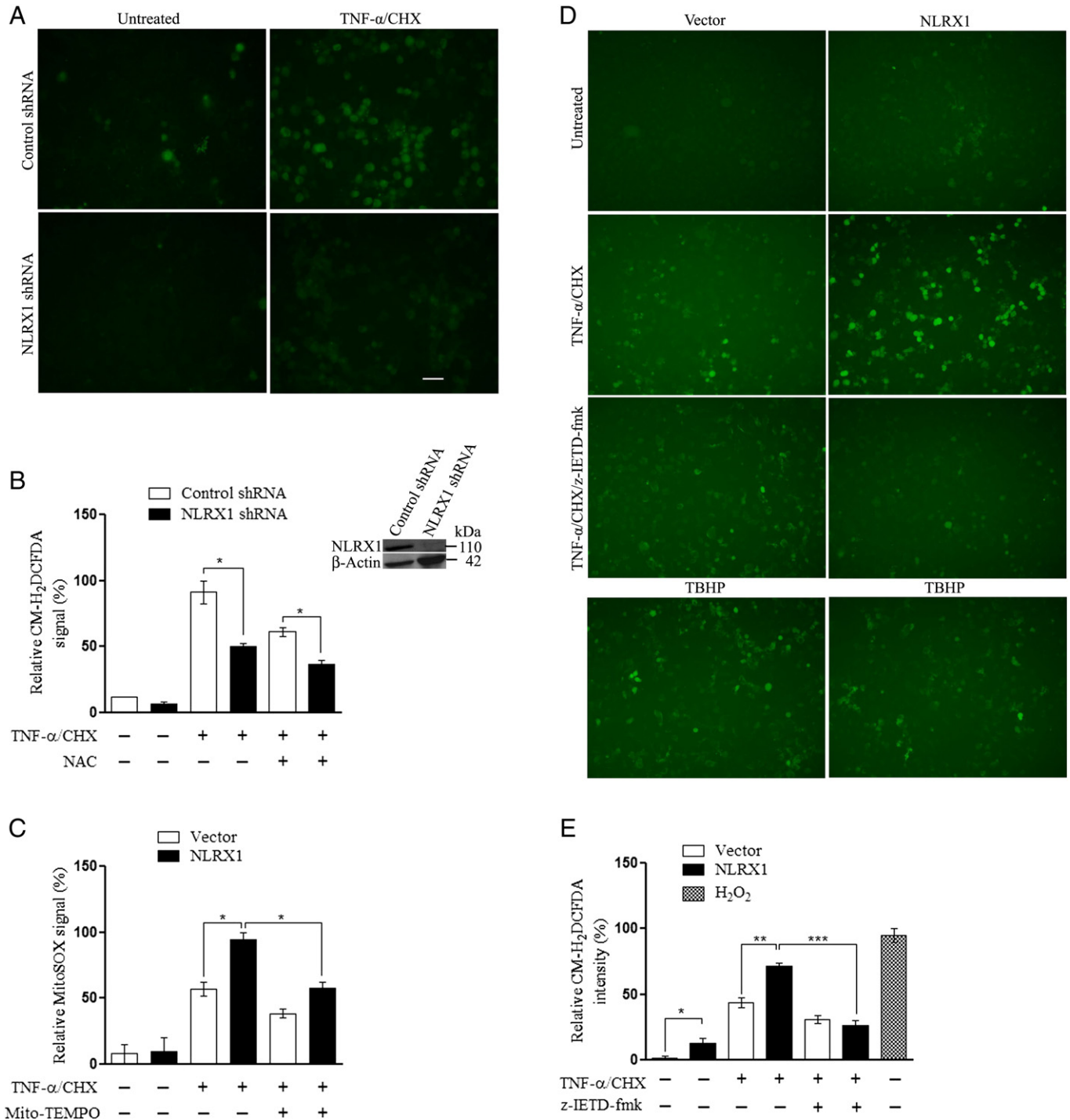
Fig. 5. NLRX1 regulated Caspase-8 activity modulates the TNF-α induced mitochondrial ROS. (A) NLRX1 shRNA and control shRNA stable HeLa cells were treated with TNF-α/CHX for 4 h. ROS production was monitored by staining the cells with CM-H$_2$DCFDA fluorescent probe and visualized under fluorescence microscope. Scale bar represents 10 μm (n = 2). NLRX1 knockdown was confirmed by Western blotting using anti-NLRX1 antibody. (B) ROS levels were analyzed in control shRNA and NLRX1 shRNA stable HEK293 cells treated with TNF-α/CHX in the absence/presence of NAC (5 mM) using CM-H$_2$DCFDA (n = 3). (C) Mitochondrial superoxide levels were quantified in NLRX1 and vector transfected MCF-7 cells treated with TNF-α/CHX in the absence/presence of Mito-TEMPO (10 μM) as described in the Materials and methods section (n = 3). (D) HeLa cells were transfected with NLRX1 and control vector followed by treatment with TNF-α/CHX alone or in combination with z-IETD-fmk for 4 h. The cells were stained with CM-H$_2$DCFDA and observed ROS production under fluorescence microscope (n = 2). (E) Intracellular ROS levels were quantified in NLRX1 and vector transfected MCF-7 cells following treatment with TNF-α/CHX and z-IETD-fmk either alone or in combination. H$_2$O$_2$ treatment (50 μM) was used as a positive control (n = 3). Data in (A)–(E) depict mean ± SEM values. Asterisk (*) indicates that p value < 0.05, for SEM.

significantly altered if mice received intraperitoneal injections of TNF-α, after a subcutaneous inoculation of RKO cells. The TNF-α treatment decreased the tumorigenic potential in all three RKO sublines producing the smallest average tumor volume in NLRX1 expressing cancer cells (Fig. 8B, C). In vivo data from nude mice with NLRX1 hyper expression and NLRX1 knockdown in RKO cells

correlate with in vitro data from MCF-7 cell line both in untreated and TNF-α treated condition. However, data with control mice in TNF-α treated condition does not comply with the in vitro study. This could be due to the difference in cell lines used for the in vivo study as both the cells differ in origin and have different tumorigenic capability [44]. Similar results were observed in other transformed
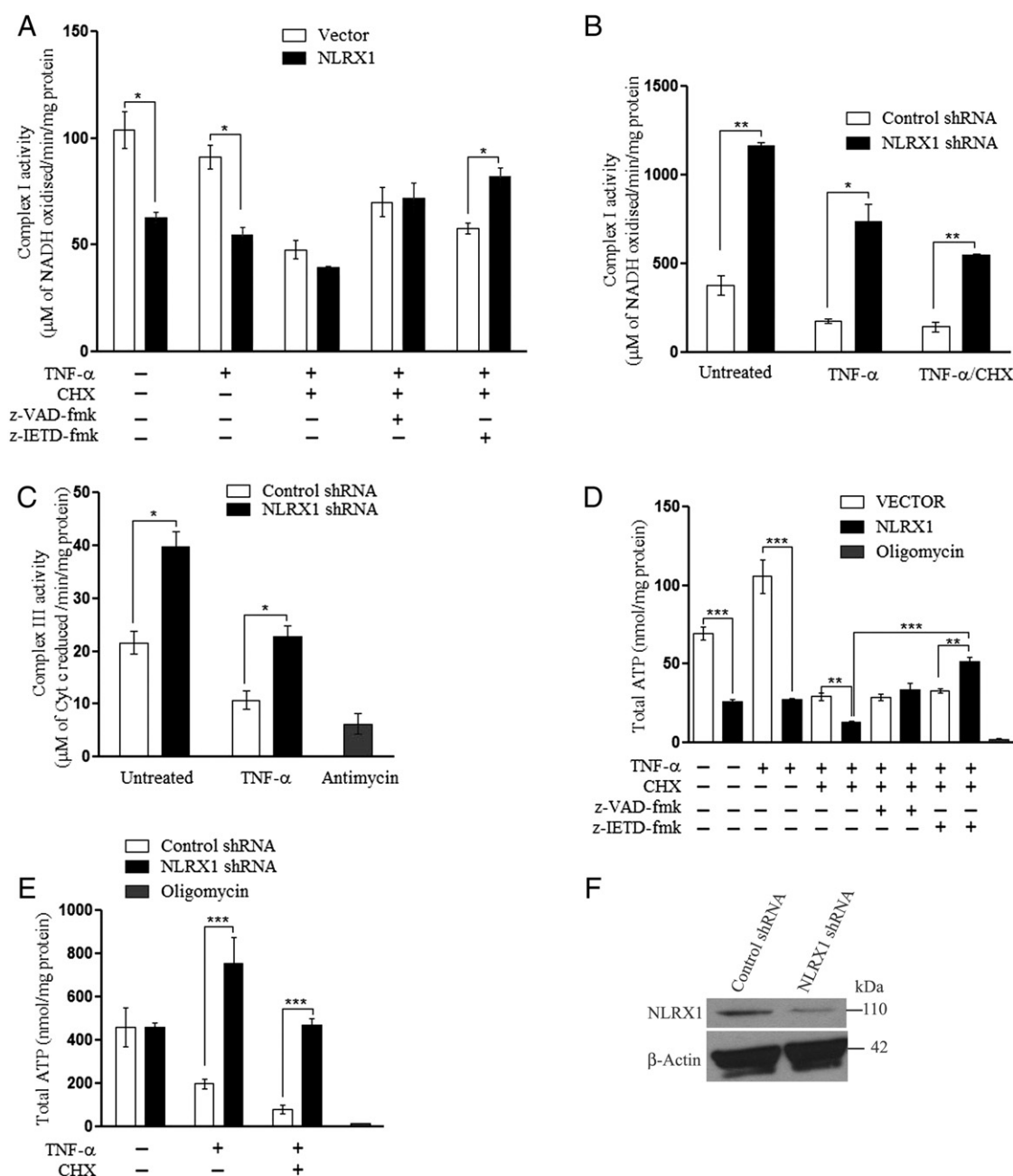
Fig. 6. NLRX1 regulates Complex I and Complex III activity to maintain ATP levels in the presence of TNF-α. (A) HEK293 cells were transfected with NLRX1 and vector control followed by treatment with TNF-α, TNF-α/CHX, z-VAD-fmk and z-IETD-fmk either alone or in combination. (B) and (C) NLRX1 shRNA and control shRNA stable HEK293 cells were treated with TNF-α and TNF-α/CHX. Complex I (B) (n = 3) and Complex III (C) (n = 2) activity were measured spectrophotometrically. (D) HEK293 cells were transfected with NLRX1 and vector control followed by treatment with TNF-α, TNF-α/CHX, z-VAD-fmk and z-IETD-fmk either alone or in combination (n = 3). (E) NLRX1 shRNA and control shRNA stable HEK293 cells were treated with TNF-α and CHX either alone or in combination. ATP levels were measured by ATP-dependent luciferase activity (n = 3). (F) Cell lysates of NLRX1 shRNA stable HeLa cells were analyzed by Western blotting to check NLRX1 expression levels. Data in (A)–(E) depict mean ± SEM values. Asterisk (*) indicates that p value < 0.05, for SEM.

cells expressing NLRX1 and NLRX1 shRNA1 both in the presence and absence of TNF-α (data not shown). These observations suggest that NLRX1 may act as a potential tumor suppressor that abrogates the tumorigenic capability of cancer cells.

4. Discussion

Chronic inflammation is intricately associated with promotion of tumor initiation and progression. The high levels of pro-inflammatory cytokines reprogram metabolic pathways and provide survival advantage to tumor cells [45]. Increased levels of TNF-α have been consistently observed in different tumor types including breast, colorectal and

gastric cancers [5]. The role of mitochondria in regulation of inflammatory pathways is emerging. The mitochondria localized NLRX1 has been reported to regulate both IFN and NF-κB pathways [32,33,46]. The role of NLRX1 in controlling inflammation, cell death and metabolism, as well as its participation in cancer initiation and progression is not well understood. In the current study, we demonstrate that NLRX1 sensitizes cells to TNF-α induced death by activating Caspase-8. The crosstalk between NLRX1 and Caspase-8 is important for regulation of mitochondrial ROS and metabolism in tumor cells.

The results obtained in the current study demonstrate that NLRX1 specifically sensitizes the cells to TNF-α induced death but does not affect responses to other stress conditions. TNF-α binds to its cognate
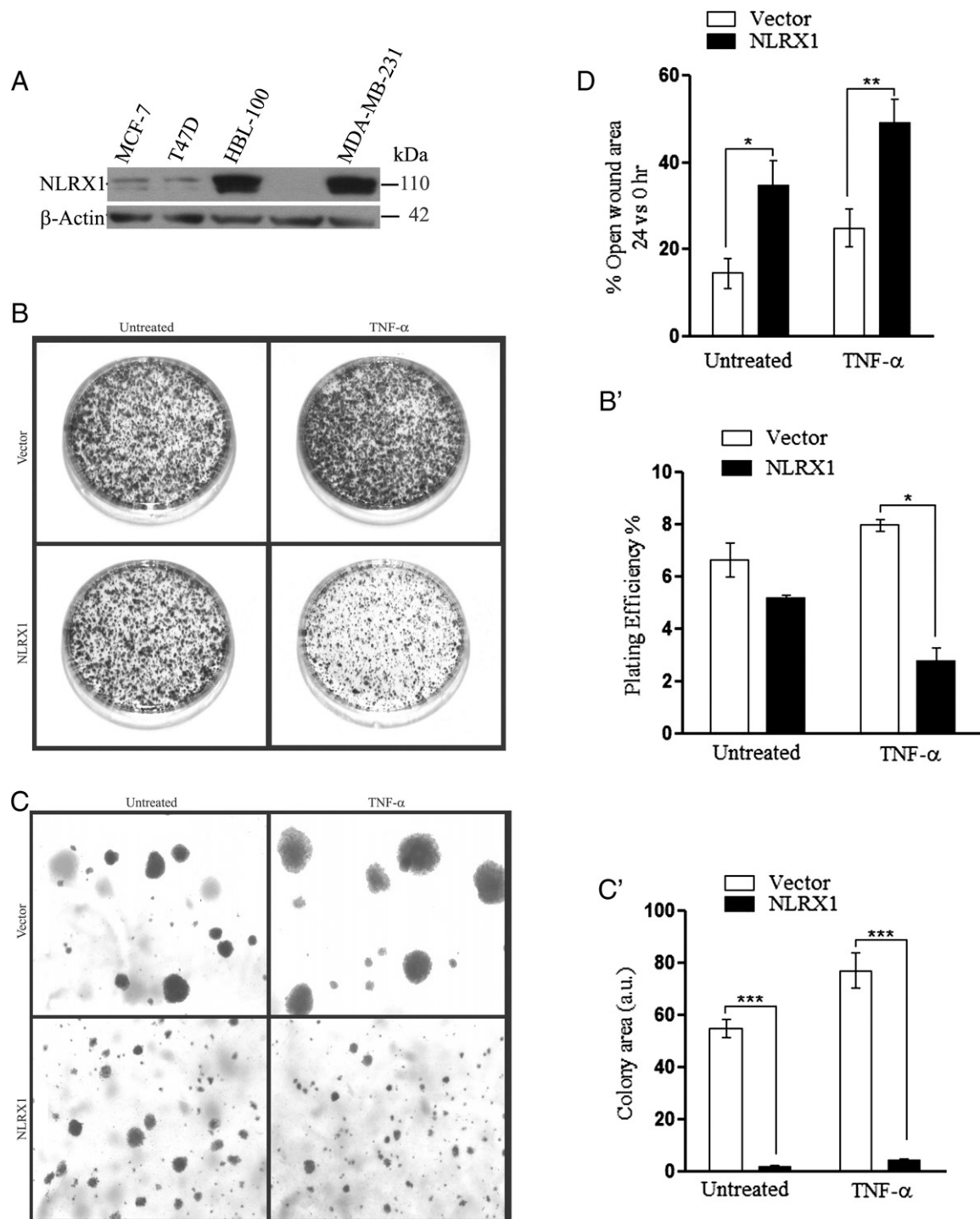
Fig. 7. NLRX1 expression in MCF-7 cells decreases tumorigenic and cell migration property. (A) The expression of NLRX1 was analyzed by Western blotting in MCF-7, T47D, HBL-100 and MDA-MB-231. (B and B') MCF-7 cells were transfected with NLRX1 and control vector followed by treatment with TNF-α and clonogenic activity was assessed by counting number of colony forming units and plotted as plating efficiency (n = 2). (C and C') MCF-7 cells were transfected with NLRX1 and vector constructs and treated with TNF-α. The soft agar assay was performed and colonies in soft agar were observed under DIC mode in fluorescence microscope after 25 days. The colonies areas were measured using Image J 1.45 software (n = 2). (D) MCF-7 cells, transfected with NLRX1 and control vector were subjected to TNF-α treatment and scratch assay was performed as indicated in the Materials and methods section (n = 2). Data in (B)–(D) depict mean ± SEM. Asterisk (*) indicates that p value < 0.05, for SEM.

receptor TNFR1, predominantly expressed on plasma membranes of many different cell types. Following the binding of TNF-α, a proximal membrane bound complex-I is assembled by the recruitment of TRADD adaptor protein, TRAF2, RIP1 and cIAPs. The complex-I is known to activate NF-κB and promotes cell survival. During TNF-α induced apoptosis, complex-I is internalized and recruits Caspase-8 and FADD adaptor protein thereby forming a pro-apoptotic complex-II in

the cytoplasm [18]. The exact composition and regulation of the assembly of complex-II during the TNF-α induced apoptosis is not well understood. The results in the current study obtained by measuring cell death and immunoprecipitation demonstrate the association of NLRX1 with Caspase-8 and TRAF2, subunits of complex-II, in the presence of TNF-α. The recruitment of different Ub E3 ligases [35,39,40] at this step may ubiquitinate NLRX1 [33] and may regulate the assembly of the
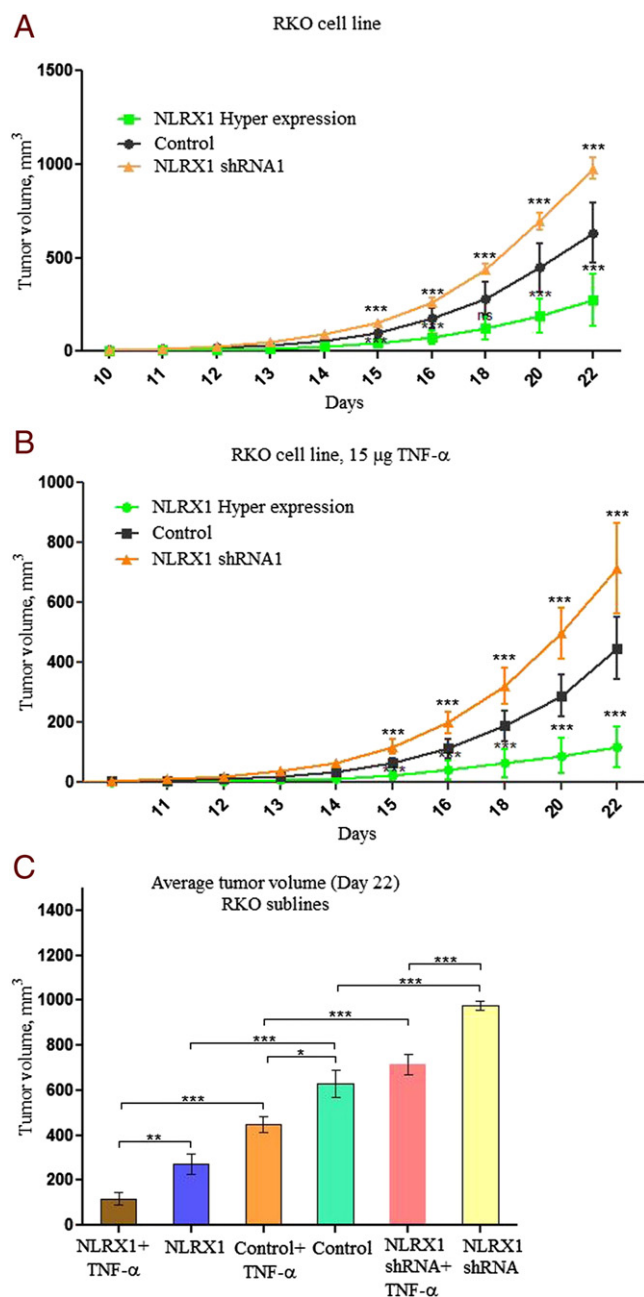
Fig. 8. NLRX1 expression decreases tumorigenic potential of transformed cells in vivo. RKO colon carcinoma cells with stable hyper expression and knockdown of NLRX1 gene were used to study xenograft tumor formation in nude mice. (A) and (B) kinetics of tumor growth in nude mice after injection of RKO cells with hyper expression and stable knockdown of NLRX1 with or without treatment of TNF-α (15 μg/ml) 24 h after administration of cancer cell line. (C) Tumor volume from untreated and TNF-α treated mice was measured every two days. Average tumor volume at day 22 was measured and plotted against each RKO sublines. Data in (A)–(C) depict mean ± SEM of values (n = 3). Asterisk (*) indicates that p value < 0.05, for SEM.

complex and Caspase-8 activation, hence sensitizing the cells to the TNF-α induced cell death.

Caspase-8 is a multifunctional protease and translocates to different subcellular locations during stress conditions. During ischemia conditions, Caspase-8 translocates to the nucleus and cleaves PARP2 [20]. Previous reports also describe the translocation of Caspase-8, TRAF2 and RIP1 to mitochondria during the TNF-α induced apoptosis. Evidences obtained in the current study suggest that NLRX1 may regulate the association of active subunits of Caspase-8 with mitochondria in the presence of TNF-α. NLRX1 may regulate

the formation of pro-apoptotic complex-II and mediate activation of Caspase-8 at the mitochondria to control metabolic functions in the presence of TNF-α. This observation is in consonance with earlier report showing that Caspase-8 may form a native macromolecular complex with Bid at the mitochondria [47], although the functional significance of the association was not understood. Our results suggest that NLRX1 and Caspase-8 crosstalk is important for the regulation of mitochondrial ROS, as the inhibition of Caspase-8 and knockdown of NLRX1 attenuate the TNF-α induced mitochondrial ROS. The dysregulation of redox balance in response to TNF-α or certain pathological conditions result in leakage of electrons from Complex I and Complex III to molecular oxygen, thus serving as a primary source of superoxide anion radical. The observed mitochondria-localized association of NLRX1 with activated Caspase-8 suggests that the activity of Caspase-8 may inhibit the mitochondrial ETC Complex I and Complex III. A previous report also suggests that NDUFS1, a 75 kDa protein of mitochondrial Complex I subunit is a substrate of Caspase-3 during apoptosis and is critical event of mitochondrial dysfunction during apoptosis, [41] suggesting caspase mediated regulation of ETC during stress conditions. Similarly, a recent report suggests that Caspase-8 is an important bioenergetic determinant and a key regulator of cellular ATP levels [48]. The results obtained here also allow to hypothesize that NLRX1 may regulate the Caspase-8 activity on mitochondria in the presence of TNF-α. The activated Caspase-8 associated with mitochondria may cleave subunit of mitochondrial respiratory Complex I or Complex III. The association of NLRX1 with UQCRC2, an integral member of the Complex III also known as the mitochondrial cytochrome bc1 complex, is consistent with the hypothesis [49]. The observed TNF-α mediated decrease in the activity of Complex III along with the increase in mitochondria-generated ROS in the NLRX1 expressing cells suggest that activated Caspase-8 may target components of respiratory Complex III. The additional studies are required to understand the association of NLRX1 and Caspase-8 with mitochondrial ETC complexes and its role in metabolism.

Cancer cells are often endowed with high intrinsic ROS generation and constitutive NF-κB activation. Increased ROS generation coincides with upregulated glucose metabolism under hypoxic conditions, a phenomenon characteristic of fast proliferating cancer cells [50,51]. The increased activities of mitochondrial Complex I and Complex III and elevated ATP levels observed in the NLRX1 knockdown cells treated with TNF-α suggest an increase in mitochondrial metabolic activity and energy production. This assumption is supported by a previous report showing that TNF-α regulates the expression of key metabolic enzymes, such as glycogen phosphorylase (PYGL) and glutamate dehydrogenase 1 (GLUD1). PYGL increases the flux of glucose from glycogen reserves whereas GLUD1 activity provides the substrates for anaplerotic metabolism [52]. The current study demonstrates that NLRX1 expression inhibits the activity of mitochondrial respiratory chain, generates ROS and sensitizes cells to TNF-α induced death. Altogether, these results implicate that NLRX1 has a tumor suppressor activity. In breast carcinoma cells, MCF-7 and T47D, the expression of NLRX1 is compromised. We show that the ectopic expression of NLRX1 in MCF-7 cells compromised the clonogenic ability in vitro. In other human carcinoma cell lines RKO, we observed that expression of NLRX1 also decreases clonogenic ability in vitro and tumor formation in a nude mice xenograft assay in vivo. Increased levels of TNF-α observed in tumor microenvironment and loss of NLRX1 expression may facilitate the metabolic reprogramming to meet the anaplerotic demands of tumor cells. The higher expression of NLRX1 was observed in MDA-MB-231, a highly metastatic cell line and HBL-100, a SV40 mediated immortalized cell line. The observations in the current study are supported by the findings of Soares et al. [38]. The authors analyzed WT versus KO cells, rather than scramble versus knockdown cells and found a phenotype between WT and KO cells only in transformed cells that already express very low levels of NLRX1 in WT, rather than in WT versus KO primary

cells that have higher levels of NLRX1 in WTs. It is possible that low expression of NLRX1 in KD cells changes the overall outcome of the sensitivity to TNF-α/CHX.

This strongly suggests that NLRX1 may have a different role in the altered tumor microenvironment. Recent evidence suggests that aggressive and metastatic properties of MDA-MB-231 cells are attributed to autophagy-dependence. These cells are addicted to autophagy for survival even in nutrient rich conditions [53]. Similarly, previous reports suggest that NLRX1 acts as a positive regulator of autophagy during antiviral signaling [54]. Altogether, these evidences raise the possibility that the up-regulated expression of NLRX1 may synergistically regulate metabolism and autophagy for highly invasive growth of the autophagy addicted MDA-MB-231 breast cancer cells. Therefore, the tumor suppressor role of NLRX1 may be cell type dependent and will be highly specific to tumor microenvironment. The heterogeneity observed in the breast cancer cells in tumor microenvironment further strengthens the hypothesis [55]. The responsiveness of these cell lines to TNF-α induced cell death as well as metabolic reprogramming in different cancer types need additional studies.

5. Conclusion

The results obtained in the present study suggest the role of NLRX1 in regulating the cross talk of inflammation, metabolism and tumorigenesis. The proteins discovered at the interface of mitochondria and ER, such as MAVS, MITA and NLRX1, had recently been shown to play important roles in innate immune responses. A previous report from our lab as well as the current study suggest that proteins regulating NF-κB and IFN pathways may be critically linked to metabolism and cell death [56]. The evidences presented here suggest that loss of NLRX1 may confer dual advantage for the cells in the tumor microenvironment, as they acquire resistance to TNF-α induced cell death, while their metabolic pathways are being reprogrammed to meet the high energy and anaplerotic demands. Further studies in this direction would help to understand the intimate connection between inflammation, metabolism and tumor progression.

Acknowledgments

Appendix A. Supplementary data

Supplementary data to this article can be found online at http://dx.doi.org/10.1016/j.bbamcr.2015.01.016.

References

[1] D.H. Dapito, A. Mencin, G.Y. Gwak, J.P. Pradere, M.K. Jang, I. Mederacke, J.M. Caviglia, H. Khiabanian, A. Adeyemi, R. Bataller, J.H. Lefkowitch, M. Bower, R. Friedman, R.B. Sartor, R. Rabadan, R.F. Schwabe, Promotion of hepatocellular carcinoma by the intestinal microbiota and TLR4, Cancer Cell 21 (2012) 504–516.

[2] F.M. Robertson, M. Bondy, W. Yang, H. Yamauchi, S. Wiggins, S. Kamrudin, S. Krishnamurthy, H. Le-Petross, L. Bidaut, A.N. Player, S.H. Barsky, W.A. Woodward, T. Buchholz, A. Lucci, N.T. Ueno, M. Cristofanilli, Inflammatory breast cancer: the disease, the biology, the treatment, CA Cancer J. Clin. 60 (2010) 351–375.

[3] J. Terzic, S. Grivennikov, E. Karin, M. Karin, Inflammation and colon cancer, Gastroenterology 138 (2010) 2101–2114 (e2105).

[4] N. Uemura, S. Okamoto, S. Yamamoto, N. Matsumura, S. Yamaguchi, M. Yamakido, K. Taniyama, N. Sasaki, R.J. Schlemper, Helicobacter pylori infection and the development of gastric cancer, N. Engl. J. Med. 345 (2001) 784–789.

[5] B.E. Lippitz, Cytokine patterns in patients with cancer: a systematic review, Lancet Oncol. 14 (2013) e218–e228.

[6] T. Ashizawa, R. Okada, Y. Suzuki, M. Takagi, T. Yamazaki, T. Sumi, T. Aoki, S. Ohnuma, T. Aoki, Clinical significance of interleukin-6 (IL-6) in the spread of gastric cancer: role of IL-6 as a prognostic factor, Gastric Cancer Off. J. Int. Gastric Cancer Assoc. Japan. Gastric Cancer Assoc. 8 (2005) 124–131.

[7] M. Ikeguchi, T. Hatada, M. Yamamoto, T. Miyake, T. Matsunaga, Y. Fukumoto, Y. Yamada, K. Fukuda, H. Saito, S. Tatebe, Serum interleukin-6 and -10 levels in patients with gastric cancer, Gastric Cancer Off. J. Int. Gastric Cancer Assoc. Japan. Gastric Cancer Assoc. 12 (2009) 95–100.

[8] T. Kawabata, T. Ichikura, T. Majima, S. Seki, K. Chochi, E. Takayama, H. Hiraide, H. Mochizuki, Preoperative serum interleukin-18 level as a postoperative prognostic marker in patients with gastric carcinoma, Cancer 92 (2001) 2050–2055.

[9] O. Kayacan, D. Karnak, S. Beder, E. Gullu, H. Tutkak, F.C. Senler, D. Koksal, Impact of TNF-alpha and IL-6 levels on development of cachexia in newly diagnosed NSCLC patients, Am. J. Clin. Oncol. 29 (2006) 328–335.

[10] L. Kozlowski, I. Zakrzewska, P. Tokajuk, M.Z. Wojtukiewicz, Concentration of interleukin-6 (IL-6), interleukin-8 (IL-8) and interleukin-10 (IL-10) in blood serum of breast cancer patients, Rocz. Akad. Med. Bialymst. 48 (2003) 82–84.

[11] J.C. Lee, K.M. Lee, D.W. Kim, D.S. Heo, Elevated TGF-beta1 secretion and down-modulation of NKG2D underlies impaired NK cytotoxicity in cancer patients, J. Immunol. 172 (2004) 7335–7340.

[12] Y. Lin, S. Kikuchi, Y. Obata, K. Yagyu, C. Tokyo, Research group on prevention of gastric, serum levels of transforming growth factor beta1 are significantly correlated with venous invasion in patients with gastric cancer, J. Gastroenterol. Hepatol. 21 (2006) 432–437.

[13] N.I. Nikiteas, N. Tzanakis, M. Gazouli, G. Rallis, K. Daniilidis, G. Theodoropoulos, A. Kostakis, G. Peros, Serum IL-6, TNFalpha and CRP levels in Greek colorectal cancer patients: prognostic implications, World J. Gastroenterol. WJG 11 (2005) 1639–1643.

[14] Y. Ren, R.T. Poon, H.T. Tsui, W.H. Chen, Z. Li, C. Lau, W.C. Yu, S.T. Fan, Interleukin-8 serum levels in patients with hepatocellular carcinoma: correlations with clinicopathological features and prognosis, Clin. Cancer Res. Off. J. Am. Assoc. Cancer Res. 9 (2003) 5996–6001.

[15] K.S. Shim, K.H. Kim, W.S. Han, E.B. Park, Elevated serum levels of transforming growth factor-beta1 in patients with colorectal carcinoma: its association with tumor progression and its significant decrease after curative surgical resection, Cancer 85 (1999) 554–561.

[16] S.I. Grivennikov, F.R. Greten, M. Karin, Immunity, inflammation, and cancer, Cell 140 (2010) 883–899.

[17] W.W. Lin, M. Karin, A cytokine-mediated link between innate immunity, inflammation, and cancer, J. Clin. Invest. 117 (2007) 1175–1183.

[18] O. Micheau, J. Tschopp, Induction of TNF receptor I-mediated apoptosis via two sequential signaling complexes, Cell 114 (2003) 181–190.

[19] L. Wang, F. Du, X. Wang, TNF-alpha induces two distinct caspase-8 activation pathways, Cell 133 (2008) 693–703.

[20] A. Benchoua, C. Couriaud, C. Guegan, L. Tartier, P. Couvert, G. Friocourt, J. Chelly, J. Menissier-de Murcia, B. Onteniente, Active caspase-8 translocates into the nucleus of apoptotic cells to inactivate poly(ADP-ribose) polymerase-2, J. Biol. Chem. 277 (2002) 34217–34222.

[21] L. Scorrano, Caspase-8 goes cardiolipin: a new platform to provide mitochondria with microdomains of apoptotic signals? J. Cell Biol. 183 (2008) 579–581.

[22] D. Chandra, G. Choy, X. Deng, B. Bhatia, P. Daniel, D.G. Tang, Association of active Caspase 8 with the mitochondrial membrane during apoptosis: potential roles in cleaving BAP31 and Caspase 3 and mediating mitochondrion–endoplasmic reticulum cross talk in etoposide-induced cell death, Mol. Cell. Biol. 24 (2004) 6592–6607.

[23] J.J. Kim, S.B. Lee, J.K. Park, Y.D. Yoo, TNF-alpha-induced ROS production triggering apoptosis is directly linked to Romo1 and Bcl-X(L), Cell Death Differ. 17 (2010) 1420–1434.

[24] H. Nohl, L. Gille, K. Staniek, Intracellular generation of reactive oxygen species by mitochondria, Biochem. Pharmacol. 69 (2005) 719–723.

[25] E. Gottlieb, M.G. Vander Heiden, C.B. Thompson, Bcl-x(L) prevents the initial decrease in mitochondrial membrane potential and subsequent reactive oxygen species production during tumor necrosis factor alpha-induced apoptosis, Mol. Cell. Biol. 20 (2000) 5680–5689.

[26] D.S. Straus, TNFalpha and IL-17 cooperatively stimulate glucose metabolism and growth factor production in human colorectal cancer cells, Mol. Cancer 12 (2013) 78.

[27] D. Arnoult, F. Soares, I. Tattoli, S.E. Girardin, Mitochondria in innate immunity, EMBO Rep. 12 (2011) 901–910.

[28] R.B. Seth, L. Sun, C.K. Ea, Z.J. Chen, Identification and characterization of MAVS, a mitochondrial antiviral signaling protein that activates NF-kappaB and IRF 3, Cell 122 (2005) 669–682.

[29] Y. Zhao, X. Sun, X. Nie, L. Sun, T.S. Tang, D. Chen, Q. Sun, COX5B regulates MAVS-mediated antiviral signaling through interaction with ATG5 and repressing ROS production, PLoS Pathog. 8 (2012) e1003086.

[30] H. Ishikawa, G.N. Barber, STING is an endoplasmic reticulum adaptor that facilitates innate immune signalling, Nature 455 (2008) 674–678.

[31] K. Bhatelia, A. Singh, D. Tomar, K. Singh, L. Sripada, M. Chagtoo, P. Prajapati, R. Singh, M.M. Godbole, R. Singh, Antiviral signaling protein MITA acts as a tumor suppressor in breast cancer by regulating NF-kappaB induced cell death, Biochim. Biophys. Acta 1842 (2014) 144–153.

[32] C.B. Moore, D.T. Bergstralh, J.A. Duncan, Y. Lei, T.E. Morrison, A.G. Zimmermann, M.A. Accavitti-Loper, V.J. Madden, L. Sun, Z. Ye, J.D. Lich, M.T. Heise, Z. Chen, J.P. Ting, NLRX1 is a regulator of mitochondrial antiviral immunity, Nature 451 (2008) 573–577.

[33] X. Xia, J. Cui, H.Y. Wang, L. Zhu, S. Matsueda, Q. Wang, X. Yang, J. Hong, Z. Songyang, Z.J. Chen, R.F. Wang, NLRX1 negatively regulates TLR-induced NF-kappaB signaling by targeting TRAF6 and IKK, Immunity 34 (2011) 843–853.

[34] L. Sripada, D. Tomar, P. Prajapati, R. Singh, A.K. Singh, R. Singh, Systematic analysis of small RNAs associated with human mitochondria by deep sequencing: detailed analysis of mitochondrial associated miRNA, PLoS ONE 7 (2012) e44873.

[35] D. Tomar, P. Prajapati, L. Sripada, K. Singh, R. Singh, A.K. Singh, R. Singh, TRIM13 regulates Caspase-8 ubiquitination, translocation to autophagosomes and activation during ER stress induced cell death, Biochim. Biophys. Acta 1833 (2013) 3134–3144.

[36] T. Cheng, J. Sudderth, C. Yang, A.R. Mullen, E.S. Jin, J.M. Mates, R.J. DeBerardinis, Pyruvate carboxylase is required for glutamine-independent growth of tumor cells, Proc. Natl. Acad. Sci. U. S. A. 108 (2011) 8674–8679.

[37] D. D'Amours, F.R. Sallmann, V.M. Dixit, G.G. Poirier, Gain-of-function of poly(ADP-ribose) polymerase-1 upon cleavage by apoptotic proteases: implications for apoptosis, J. Cell Sci. 114 (2001) 3771–3778.

[38] F. Soares, I. Tattoli, M.A. Rahman, S.J. Robertson, A. Belcheva, D. Liu, C. Streutker, S. Winer, D.A. Winer, A. Martin, D.J. Philpott, D. Arnoult, S.E. Girardin, The mitochondrial protein NLRX1 controls the balance between extrinsic and intrinsic apoptosis, J. Biol. Chem. 289 (2014) 19317–19330.

[39] F. Gonzalvez, D. Lawrence, B. Yang, S. Yee, R. Pitti, S. Marsters, V.C. Pham, J.P. Stephan, J. Lill, A. Ashkenazi, TRAF2 sets a threshold for extrinsic apoptosis by tagging Caspase-8 with a ubiquitin shutoff timer, Mol. Cell 48 (2012) 888–899.

[40] Z. Jin, Y. Li, R. Pitti, D. Lawrence, V.C. Pham, J.R. Lill, A. Ashkenazi, Cullin3-based polyubiquitination and p62-dependent aggregation of Caspase-8 mediate extrinsic apoptosis signaling, Cell 137 (2009) 721–735.

[41] J. Huai, F.N. Vogtle, L. Jockel, Y. Li, T. Kiefer, J.E. Ricci, C. Borner, TNFalpha-induced lysosomal membrane permeability is downstream of MOMP and triggered by caspase-mediated NDUFS1 cleavage and ROS formation, J. Cell Sci. 126 (2013) 4015–4025.

[42] R.B. Hamanaka, N.S. Chandel, Mitochondrial reactive oxygen species regulate cellular signaling and dictate biological outcomes, Trends Biochem. Sci. 35 (2010) 505–513.

[43] F.J. Lopez-Hernandez, M.A. Ortiz, Y. Bayon, F.J. Piedrafita, Z-FA-fmk inhibits effector caspases but not initiator caspases 8 and 10, and demonstrates that novel anticancer retinoid-related molecules induce apoptosis via the intrinsic pathway, Mol. Cancer Ther. 2 (2003) 255–263.

[44] T. Geiger, A. Wehner, C. Schaab, J. Cox, M. Mann, Comparative proteomic analysis of eleven common cell lines reveals ubiquitous but varying expression of most proteins, Mol. Cell. Proteomics MCP 11 (2012) 014050 (M111).

[45] D. Hanahan, R.A. Weinberg, Hallmarks of cancer: the next generation, Cell 144 (2011) 646–674.

[46] I. Tattoli, L.A. Carneiro, M. Jehanno, J.G. Magalhaes, Y. Shu, D.J. Philpott, D. Arnoult, S.E. Girardin, NLRX1 is a mitochondrial NOD-like receptor that amplifies NF-kappaB and JNK pathways by inducing reactive oxygen species production, EMBO Rep. 9 (2008) 293–300.

[47] Z.T. Schug, F. Gonzalvez, R.H. Houtkooper, F.M. Vaz, E. Gottlieb, BID is cleaved by caspase-8 within a native complex on the mitochondrial membrane, Cell Death Differ. 18 (2011) 538–548.

[48] N.J. Lanning, B.D. Looyenga, A.L. Kauffman, N.M. Niemi, J. Sudderth, R.J. DeBerardinis, J.P. MacKeigan, A mitochondrial RNAi screen defines cellular bioenergetic determinants and identifies an adenylate kinase as a key regulator of ATP levels, Cell Rep. 7 (2014) 907–917.

[49] D. Arnoult, F. Soares, I. Tattoli, C. Castanier, D.J. Philpott, S.E. Girardin, An N-terminal addressing sequence targets NLRX1 to the mitochondrial matrix, J. Cell Sci. 122 (2009) 3161–3168.

[50] G. He, M. Karin, NF-kappaB and STAT3 — key players in liver inflammation and cancer, Cell Res. 21 (2011) 159–168.

[51] P.P. Hsu, D.M. Sabatini, Cancer cell metabolism: Warburg and beyond, Cell 134 (2008) 703–707.

[52] D.W. Zhang, J. Shao, J. Lin, N. Zhang, B.J. Lu, S.C. Lin, M.Q. Dong, J. Han, RIP3, an energy metabolism regulator that switches TNF-induced cell death from apoptosis to necrosis, Science 325 (2009) 332–336.

[53] P. Maycotte, C.M. Gearheart, R. Barnard, S. Aryal, J.M. Mulcahy Levy, S.P. Fosmire, R.J. Hansen, M.J. Morgan, C.C. Porter, D.L. Gustafson, A. Thorburn, STAT3-mediated autophagy dependence identifies subtypes of breast cancer where autophagy inhibition can be efficacious, Cancer Res. 74 (2014) 2579–2590.

[54] Y. Lei, H. Wen, Y. Yu, D.J. Taxman, L. Zhang, D.G. Widman, K.V. Swanson, K.W. Wen, B. Damania, C.B. Moore, P.M. Giguere, D.P. Siderovski, J. Hiscott, B. Razani, C.F. Semenkovich, X. Chen, J.P. Ting, The mitochondrial proteins NLRX1 and TUFM form a complex that regulates type I interferon and autophagy, Immunity 36 (2012) 933–946.

[55] A.S. Cleary, T.L. Leonard, S.A. Gestl, E.J. Gunther, Tumour cell heterogeneity maintained by cooperating subclones in Wnt-driven mammary cancers, Nature 508 (2014) 113–117.

[56] K. Bhatelia, K. Singh, R. Singh, TLRs: Linking inflammation and breast cancer, Cell. Signal. 26 (2014) 2350–2357.

NLRX1 resides in mitochondrial RNA granules and regulates mitochondrial RNA processing and bioenergetic adaptation

Kritarth Singh[a], Lakshmi Sripada[a], Anastasia Lipatova[c], Milton Roy[a], Paresh Prajapati[b], Dhruv Gohel[a], Khyati Bhatelia[a], Peter M. Chumakov[c,d], Rajesh Singh[a,*]

[a] *Department of Biochemistry, Faculty of Science, The M.S. University of Baroda, Vadodara, 390002, Gujarat, India*
[b] *SCoBIRC Department of Neuroscience, University of Kentucky, 741S.Limestone, BBSRB, Lexington, KY 40536, USA*
[c] *Engelhardt Institute of Molecular Biology, Russian Academy of Sciences, Vavilov Street 32, 119991 Moscow, Russia*
[d] *Chumakov Institute of Poliomyelitis and Viral Encephalitides, Federal Scientific Center on Research and Development of Immunobiology Products, Russian Academy of Sciences, 142782 Moscow, Russia*

ARTICLE INFO

ABSTRACT

The role of mitochondria is emerging in regulation of innate immunity, inflammation and cell death beyond its primary role in energy metabolism. Mitochondria act as molecular platform for immune adaptor protein complexes, which participate in innate immune signaling. The mitochondrial localized immune adaptors are widely expressed in non-immune cells, however their role in regulation of mitochondrial function and metabolic adaption is not well understood. NLRX1, a member of NOD family receptor proteins, localizes to mitochondria and is a negative regulator of anti-viral signaling. However, the submitochondrial localization of NLRX1 and its implication in regulation of mitochondrial functions remains elusive. Here, we confirm that NLRX1 translocates to mitochondrial matrix and associates with mitochondrial FASTKD5 (Fas-activated serine-threonine kinase family protein-5), a bonafide component of mitochondrial RNA granules (MRGs). The association of NLRX1 with FASTKD5 negatively regulates the processing of mitochondrial genome encoded transcripts for key components of complex-I and complex-IV, to modulate its activity and supercomplexes formation. The evidences, here, suggest an important role of NLRX1 in regulating the post-transcriptional processing of mitochondrial RNA, which may have an important implication in bioenergetic adaptation during metabolic stress, oncogenic transformation and innate immunity.

1. Introduction

ATP generation through oxidative phosphorylation (OxPhos) is one of the major function of mitochondria, besides its additional important roles in numerous biosynthetic reactions, maintaining intracellular ion homeostasis, apoptosis and innate immune signaling [1]. Mitochondrial outer membrane and mitochondrial contact sites serve as molecular platform for the assembly of dynamic signaling complexes that forms during viral infection [2]. Mitochondrial outer membrane proteins namely, MAVS and STING act as adaptors for the downstream activation of anti-viral signaling [3, 4]. NLRX1 (Nod-Like Receptor (NLR) protein family member) negatively regulates innate immune responses during viral infections. Recent reports from our lab and others have shown that mitochondrial immune signaling proteins are widely expressed in non-immune cells and their levels are altered during tumor progression [5, 6]. Similarly, the role of NLRX1 in controlling mitochondrial metabolic functions and apoptosis during inflammatory condition and tissue injury is emerging [7, 8]. However, its sub-mitochondrial localization and molecular mechanism(s) of regulating mitochondrial function is not well understood.

The OxPhos system, embedded in inner mitochondrial membrane, is composed of five multiprotein complexes forming the mitochondrial respiratory chain (MRC). The MRC complexes are assembled from nearly 100 protein subunits, of which approximately 90 subunits are encoded by nuclear genes and imported into mitochondria. The remaining 13 subunits are encoded by mitochondrial DNA (mtDNA) [9]. In addition, mitochondrial genome encodes 22 tRNAs and 12S and 16S mt-rRNAs that are essential for the synthesis of mitochondria-encoded proteins. As all protein factors involved in the expression of mitochondrial genome are nuclear encoded, a strict coordination between nuclear and mitochondrial gene expression programs is necessary, especially during physiological responses requiring changes in energy demands, such as conditions of altered carbon sources [10]. The regulatory mechanisms of mitochondrial gene expression and its

modulation through nuclear-encoded factors in different patho-physiological stimuli are not well understood.

mtDNA-encoded subunits of respiratory chain complex are transcribed on both strands to form three continuous polycistronic transcripts [11]. These precursor transcripts are usually punctuated by tRNAs that are further excised by RNase P at the 5′ and by RNase Z at the 3′ ends of the tRNAs [12, 13]. The post-transcriptional processing of mt-mRNAs and mitoribosome assembly is spatially organized within distinct foci termed as mitochondrial RNA granules (MRGs) [14–16]. These are dynamic mitochondrial sub-domains to which mt-RNAs processing enzymes such as RNase P, RNase Z, GRSF1, RNA methyl transferases and other unidentified proteins are recruited [17, 18]. MRGs interactome capture studies have identified novel class of nuclear encoded RNA binding proteins that translocate to mitochondria and lack the canonical RNA binding domain, however, interacts with mt-mRNAs in human cells [14, 19, 20]. Mutations in genes encoding these proteins have been associated with a range of heritable disorders with overlapping phenotypes, as observed in mitochondrial monogenic diseases [21, 22].

Human Fas-activated serine/threonine kinase (FASTK) family, an emerging class of RNA-binding proteins, acts as a central regulator of mitochondrial post-transcriptional RNA processing [23]. The family comprises of six structurally related proteins named FASTK and its homologs FASTKD1-5. All members share an N-terminal mitochondrial targeting signal and a putative RNA-binding module, RAP domain (RNA-binding domain abundant in Apicomplexans) [24]. FASTKD1, FASTKD2 and FASTKD5 have been shown to localize within MRGs, which differentially regulate the processing of mitochondrial RNAs [14, 25, 26]. Distinct role of FASTK family proteins and recruitment of other RNA-binding proteins to regulate processing and maturation of mitochondrial RNA during patho-physiological condition is still lacking.

A recent study suggested that NLRX1 may directly associate with ssRNA through its C-terminal LRR (leucine-rich repeat) motif, which may be connected to its role in anti-viral immunity [27]. Therefore, we hypothesized that NLRX1 may associate with mitochondrial RNA and form a part of MRGs. We, therefore, tested whether NLRX1 can interact with FASTKD5 and regulate maturation of mitochondrial precursor transcripts. We show that NLRX1 specifically interacts with FASTKD5, a bonafide component of MRGs, and colocalizes with MRGs. Ectopic expression of NLRX1 inhibits the processing of mtDNA encoded mRNAs and results in alterations in the assembly of OxPhos system.

2. Material and methods

2.1. Cell culture, transfection and reagents

HEK293, MCF-7, T47D and HeLa cell lines were cultured in Dulbecco's modified Eagle's media (DMEM, Thermo Fisher Scientific Inc., USA). Media were supplemented with 10% (v/v) heat-inactivated fetal bovine serum (Thermo Fisher Scientific Inc.), 1% penicillin, streptomycin and neomycin (PSN) antibiotic mixture (Thermo Fisher Scientific Inc.). Full length NLRX1 (isoform 1, 975 amino acids), NLRX1 ΔN-ter (amino acids 156–975) and LRR (amino acids 564–975) cloned into pcDNA3.1 vector were provided by Dr. Stephen. Girardin (University of Toronto, Ontario, Canada). NLRX1-ΔLRR (amino acids 1-680) was generated by PCR using forward primer 5′-CTTGGTACCATG AGGTGGGGCCACCAT-3′ and reverse primer 5′-AGACTCGAGGAAGAG GTGGTCAAGGAG-3′ and sub-cloned into pcDNA3.1 vector in frame at the KpnI and XhoI cut sites. NLRX1-GFP was cloned into pLCMV-tagGFP2-Puro vector. Lentiviral construct expressing NLRX1-specific shRNA was purchased from Sigma-Aldrich Inc., USA (Sigma TRCN0000129459). pDsRed2-mito vector (hereafter mtRFP) was purchased from Takara-Bio, Japan. pSpCas9(BB)-2A-Puro (PX459) V2.0 was a gift from Dr. Feng Zhang (Addgene plasmid #62988). FASTKD5-Flag-HA, FASTKD5-myc and FASTKD5-RFP were kind gifts from Dr. María Simarro (Edificio de Ciencias de la Salud, Valladolid, Spain).

pECFP-Mito (hereafter mtCFP) construct was gifted by Dr. Jean-Claude Martinou (University of Geneva, Switzerland). Details of the antibodies used in current studies along with their sources are given in Supplementary Table S1.

Proteinase K, puromycin, sodium azide, rotenone, antimycin A, uridine, 5-bromouridine, digitonin, cytochrome c, NADH, sodium succinate, 2,6-Dichlorophenolindophenol sodium salt hydrate (DCPIP), EZview™ Red Anti-Flag M2 Affinity Gel and EZview™ Red Anti-HA Affinity Gel were purchased from Sigma-Aldrich, USA. Tetramethyl rhodamine methyl ester (TMRM), G418, Opti-MEM, Yeast tRNA, MicroAmp Fast Optical 96-Well Reaction Plate, MicroAmp Optical Adhesive Film and Pierce Protein A/G Agarose were procured from Thermo Fisher Scientific Inc., USA. SYBR green and complementary DNA (cDNA) isolation kits were purchased from Takara Bio Inc., Japan. Nitrotetrazolium Blue chloride (NTB) and diaminobenzidine (DAB) were purchased from Sisco Research Laboratories (SRL), India.

HEK293 and HeLa cells were transfected using standard calcium phosphate transfection method and Lipofectamine 2000 reagent (Thermo Fisher Scientific Inc., USA). MCF-7 and T47D cells were transfected using Biotool DNA transfection reagent and X-tremeGENE™ 9 DNA transfection reagent (Roche GmbH, Germany) respectively, as per manufacturer's protocol.

2.2. Isolation of mitochondria, mitoplasts, integral proteins of the inner mitochondrial membrane, and proteinase K protection assay

Mitochondria were isolated from HeLa cells or transfected HEK293 cells. HeLa cells or HEK293 cells were resuspended in mitochondria isolation buffer (0.25 M sucrose, 10 mM Tris/HCl, pH 7.4, 1× protease inhibitor cocktail (Sigma-Aldrich, USA) and incubated on ice for 5 min. The cells were disrupted by passing through a 24G sterile syringe needle and centrifuged at 600g for 15 min to separate nuclei and cell debris. The supernatant (cytosolic fraction) was collected and centrifuged again at 8000g for 10 min. The pellet (mitochondrial fraction) were washed twice and resuspended in isolation buffer. Mitoplast was isolated by incubating mitochondria to a final concentration of 1 mg/ml in PBS with 2.7 mg/ml digitonin for 20 min on ice. The sample was further centrifuged at 10,000g for 10 min and the final pellet containing mitoplasts was washed twice with PBS. For alkaline carbonate extraction, mitoplasts were incubated in 100 mM Na_2CO_3 (final solution pH 11.5) for 60 min on ice. Separation of the pellet (integral protein of the inner membrane) and supernatant (soluble and matrix proteins) was achieved by centrifugation at 47,000 rpm for 2 h at 4 °C in an ultracentrifuge (SW60 Ti rotor, Beckman Coulter Instruments).

Mitochondrial or mitoplasts pellet from HeLa cells were resuspended in digestion buffer (25 mM Tris/HCl, pH 7.5, 125 mM sucrose, 1 mM $CaCl_2$). The samples were incubated with proteinase K (50 μg/ml) with or without 0.1% (v/v) Triton X-100 for indicated time. Proteinase K activity was quenched with 2 mM phenylmethylsulphonyl fluoride (PMSF) for 10 min on ice. After centrifugation, the pellet and the supernatant were collected and analyzed by western blotting.

2.3. Confocal live cell microscopy and image quantitation

To study the subcellular localization of different proteins MCF-7, HeLa, SH-SY5Y and mtRFP-HEK293 cells were seeded at density of 2–4 × 10^5 cells into 35 mm glass bottom dishes and transfected with NLRX1-GFP. After transfection, MCF-7, HeLa and SH-SY5Y cells were loaded with 100 nM TMRM for 15 min for mitochondrial staining. Images of live cells expressing NLRX1-GFP were acquired with inverted Leica TCS SP8 confocal microscope system (Leica Microsystems GmbH, Germany) equipped with an air-cooled argon laser at 488 nm and 561 nm and a HC PL APO CS2 63×/1.40 differential interference contrast objective including a HyD detector, PMT and a PMT Trans detector. Images were collected for each channel sequentially at 1024 × 1024 pixels, 8-bit depth, 1 AU pinhole and 3× magnification.

Detectors gain, offset levels and laser power were calibrated at identical levels and remain unchanged for a set of experiment. All figure images were processed, pseudo colored and analyzed for intensity profile using Application Suite X (LASX v2.0.2). For imaging quantitation and analysis, percent correlation values were calculated using JACoP plugin in ImageJ v1.45 (NIH, MD, USA) and represented as mean colocalization and error, SD. Sample size $n \geq 5$ NLRX1-GFP positive cells.

2.4. 3D-SIM super-resolution microscopy

MCF-7 cells were co-transfected with NLRX1-GFP and FASTKD5-RFP. Twenty-four hours post transfection, cells were washed twice with DPBS and fixed with 4% paraformaldehyde solution. Imaging was performed at room temperature using a CFI Apochromat TIRF $100\times/$ 1.49 NA oil immersion objective lens on an N-SIM microscope (Nikon Instruments, Inc.) equipped with a Andor iXon3 DU-897E EMCCD camera, PFS and SIM Illuminator using 488 nm and 561 nm lasers. Raw images were acquired and reconstructed using NIS-Elements software. The exposure time was set to 100 ms for each raw data capture. The image stacks were acquired in 200 nm intervals for 8–12 Z planes over a range of 3 μm. In each plane 9 images were acquired with a rotating illumination pattern (3 phases, 3 angles) in two color channels (488 nm and 561 nm) independently. SIM images were analyzed with NIS-Elements and ImageJ.

2.5. Mitochondrial respiratory complexes enzyme activities

Mitochondrial complex I activity was determined as described previously [7]. Mitochondrial complex II and complex IV enzyme activity were monitored using NanoPhotometer® P-300 (Implen GmbH, Germany). The following extinction coefficients were used to calculate relative enzyme activities from absorption values: 2,6-dichlorphenol-indophenol (DCPIP): $\varepsilon_{610nm} = 22.0\,mM^{-1}\,cm^{-1}$ and cytochrome c: $\varepsilon_{550nm} = 19.0\,mM^{-1}\,cm^{-1}$. Briefly, MCF-7 cells were seeded at density of 1×10^6 cells in 60 mm dishes. After overnight incubation, cells were transfected and treated as indicated. The cells were washed with cold DPBS and resuspended in 0.4 ml of 20 mM hypotonic potassium phosphate buffer (pH 7.5) and incubated on ice for 10 min. Cells were disrupted with 24G sterile syringe needle and lysates were subjected to 2–3 freeze–thaw cycles. For complex II activity, lysates were preincubated with sodium succinate (200 mM) at 37 °C for 15 min and further incubated in complex II assay buffer (0.1 M potassium phosphate buffer, pH 7.5, 50 mg/ml fatty acid-free BSA, 100 mM NaN$_3$ and 0.015% (wt/v) DCPIP). The reaction was initiated by adding 12.5 mM decylubiquinone (DUB) and decrease in absorbance at 600 nm was monitored.

To assay complex IV activity, samples were processed as indicated above and resuspended in complex IV assay buffer (50 mM potassium phosphate buffer, pH 7.0 and 1 mM reduced cytochrome c). Cytochrome c was freshly reduced as described earlier [28]. The reaction was initiated by adding 80 μg of lysate to the assay buffer and baseline activity was monitored at 550 nm for 2 min. Complex IV activity was measured by monitoring the decrease in absorbance at 550 nm. Specificity of complex IV activity was recorded by addition of 100 mM NaN$_3$ to the reaction mixture.

2.6. BN-PAGE, in-gel assays and immunoblotting

BN-PAGE was performed on Native PAGE Novex 3%–12% Bis-Tris Protein Gels (Thermo Fisher Scientific Inc., USA) with minor modification. Briefly, mitochondria from MCF-7 cells were isolated in Tris-Sucrose buffer as described above and 50 μg pellets were solubilized as per manufacturer's protocol (Thermo Fisher Scientific Inc., USA) and run at room temperature. In-gel enzyme activity of different OXPHOS complexes were carried on gradient Bis-Tris gels as previously described [29]. For immunoblotting, proteins were transferred on PVDF

membrane at 50 V, 4–7 °C and probed with an antibody cocktail comprising anti-NDUFS2, anti-huATPase6 and anti-holoCOX.

2.7. Co-immunoprecipitation and western blotting

For protein interaction study, immunoprecipitation experiments were performed as reported earlier [29]. Briefly, HEK293 and MCF-7 cells were plated at density of 2×10^6 per 90 mm dish and co-transfected with indicated constructs. After 24 h of transfection, cells were washed with ice-cold DPBS (Thermo Fisher Scientific Inc., USA), and resuspended in NP40 lysis buffer (100 mM NaCl, 50 mM Tris/HCl, 10% Glycerol, 0.1% Nonidet P-40) containing complete protease inhibitor cocktail and incubated on ice for 1 h with occasional vortexing, and centrifuged at 13,000 rpm for 15 min at 4 °C. Cell lysates were collected and incubated overnight with anti-Flag affinity gel on a roller shaker at 4 °C. For immunoprecipitation of FASTKD5, HeLa cell lysates were precleared with Protein A/G Agarose beads for 2 h at 4 °C. After preclearing, the cell lysates were incubated overnight with anti-FASTKD5 antibody (1:200 dilution) on a roller shaker at 4 °C. After overnight incubation, the precipitate was mixed with blocked Protein A/G Agarose beads for 2 h at 4 °C. Finally, anti-Flag and agarose beads were washed three times with NP40 IP lysis buffer, resuspended in $5\times$ SDS-PAGE sample buffer, resolved on 12% SDS-PAGE and analyzed by western blotting using specific antibodies.

2.8. Bromouridine (BrU) staining, immunocytochemistry and imaging quantitation

For visualizing nascent mitochondrial transcript, BrU pulse was performed using 2.5 mM 5-bromouridine for 60 min in transfected mtCFP-HEK293 stable cells. Cells were washed twice with DPBS and fixed with 4% paraformaldehyde solution. Immunocytochemistry was performed in PBS containing 5% BSA, 0.1% Triton X-100, and 0.1% Tween-20. The permeabilized cells were incubated with primary antibody for 3 h at room temperature. After incubation cells were washed five times with PBST and incubated with secondary antibody for 1 h at the room temperature. BrU-labeled RNA was detected using anti-BrdU antibody. DyLight™ 594-conjugated anti-rabbit secondary antibody was used at a dilution of 1:500. Fixed cell images were acquired with Leica TCS SP8 confocal microscope equipped with air-cooled argon laser at 458 nm, 488 nm, DPSS laser at 561 nm, HeNe laser at 594 nm and a HC PL APO CS2 63 X/1.40 objective using a HyD detector with narrow and wide band pass filters. The image acquisition settings were kept same as described above except that four-channel sequential line scanning was used to avoid bleach through and crosstalk between the fluorophores. All figure images were processed and analyzed as mentioned above. To quantify BrU-NLRX1-FASTKD5 foci-foci colocalization approximately 15 foci in > 5 cells per experiment (> 75 foci in total) were analyzed by intensity correlation analysis and Coloc2 plugin in ImageJ. The frequency of overlap with BrU foci were calculated as mean colocalization. The colocalization values were calculated and plotted as mean colocalization, error, SD.

2.9. RNA isolation and expression analysis

RNA from total cell was isolated using RNAiso Plus reagent (Takara Bio Inc., Japan). cDNA was transcribed with Primescript™ First Strand cDNA synthesis kit (Takara Bio Inc., Japan) using random 6-mer primers in two steps. The initial primer annealing was performed at 65 °C for 5 min followed by addition of reverse transcriptase and incubation at 37 °C for 60 min in the second step. qRT-PCR was performed with cDNA as template and specific primers using SYBR Premix Ex Taq™ (Takara Bio Inc., Japan) as per the manufacturer's instructions. Three biological replicates were performed per experiment. The relative levels of mitochondrial DNA encoded transcripts were determined by the $2^{-\Delta\Delta CT}$ method. GAPDH was taken as endogenous control. The reaction

conditions were 95 °C for 2 min followed by 35 cycles of 95 °C for 5 s and 60 °C for 34 s (the data was acquired at this step). The generation of specific PCR products was confirmed by melt-curve analysis and relative expression with standard error was plotted. The details of primer are listed in Table S2.

2.10. Mitochondrial DNA quantification

Mitochondrial DNA copy number was determined by analyzing the relative quantity of mitochondrial genome with respect to nuclear genome. Briefly, MCF-7 and HEK293 cells were collected post transfection. Genomic DNA was isolated from cells by phenol-choloroform purification method. The relative quantity of mitochondrial genome to nuclear genome was analyzed using RNaseP specific primer as nuclear genome marker (Fwd: CCCCGTTCTCTGGGAACTC and Rev.: TGTATG AGACCACTCTTTCCCATA) and a hypervariable region (HVR) specific primer in the D-loop of mitochondrial DNA (Fwd: CACTTTCCACACA GACATCA and Rev.: TGGTTAGGCTGGTGTTAGGG).

2.11. Analysis of mitochondrial RNA processing

The processing of mitochondrial transcripts and maturation defects were analyzed by PCR amplification of mitochondrial mRNA regions. MCF-7 cells were transfected and treated as indicated. After treatment, RNA was isolated and cDNA synthesized as mentioned above. The regions flanking adjacent mitochondrial genes were amplified from cDNA using 2× Emerald GT PCR Master mix (Takara Bio Inc., Japan) at 95 °C, 5 min; 35 cycles of 95 °C for 20 s, 56 °C for 20 s and 72 °C for 40 s; 72 °C for 5 min and accumulation of unprocessed transcripts and intermediates was visualized on 1% agarose gel. The details of primer combinations are listed in Table S3.

2.12. RNA immunoprecipitation

To identify the mitochondrial RNA species bound, NLRX1, NLRX1-ΔLRR and FASTKD5 was immunoprecipitated from mitochondria of HEK293 cells and coimmunoprecipitated RNA was isolated and analyzed. Briefly, HEK293 cells were transfected with NLRX1, NLRX1-ΔLRR and FASTKD5 and mitochondria was isolated post transfection from HEK293 cells or from control sgRNA and FASTKD5 knockdown HeLa cells. Mitochondria (200 μg) were resuspended in 200 μl of extraction buffer (50 mM Tris/HCl, pH 7.5, 150 mM NaCl, 1 mM MgCl₂, 100 U/ml RNase inhibitor, 1% NP-40, and 1× complete protease inhibitors without EDTA) on ice for 40 min, with occasional vortexing. The extract was centrifuged at 20,000*g* at 4 °C for 45 min and supernatant collected. The anti-FLAG M2 affinity beads (for IP of NLRX1 and NLRX1-ΔLRR) or EZview™ Red Anti-HA Affinity Gel (for IP of FASTKD5) (Sigma-Aldrich, USA) were washed thrice in extraction buffer and blocked with 1% BSA and 100 μg/ml yeast tRNA for 2 h at room temperature. After blocking, beads were washed and were incubated with supernatant on a roller shaker at 4 °C for 4 h. For endogenous IP, the mitochondrial lysate from HeLa cells were precleared with Protein A/G Agarose beads for 1 h and incubated overnight with indicated antibodies (1: 100 dilution) on a roller shaker at 4 °C. After incubation, the precipitates were mixed with blocked Protein A/G Agarose beads for 2 h at 4 °C. To isolate RNA following immunoprecipitation, beads were washed five times with extraction buffer and supplemented with EDTA (5 mM) and yeast tRNA (1 μg). Further, RNA was isolated, cDNA was synthesized, qRT-PCR was performed and relative association of mitochondrial RNA transcripts with respect to input with standard error was calculated and plotted as mentioned above.

2.13. Analysis of translation of mtDNA-encoded genes by Click-iT® assay

Nascent mtDNA-encoded protein synthesis was evaluated in intact cells using the Click-iT AHA protein labeling kit (Thermo Fisher Scientific Inc., USA). Briefly, transfected MCF-7 and HeLa cells were incubated with methionine-free RPMI for 10 min at 37 °C and cotreated with 100 μg/ml cycloheximide to inhibit cytosolic translation for 30 min. After incubation, 100 μM L-azidohomoalanine (AHA, a methionine analog) was added and incubated further for 3 h. AHA-labeled cells were harvested and lysed in 20 mM Tris-HCl pH 8.0, 1% SDS and 250 U/ml benzonase nuclease (Sigma-Aldrich, USA) and protein concentration was estimated by Bradford assay. The cycloaddition of biotin-tagged alkyne molecule to AHA-labeled proteins was carried out according to the manufacturer's protocol. Equal proteins were loaded and resolved on 12% SDS-PAGE and analyzed by western blotting using anti-biotin antibody.

2.14. Generation of stable cell lines

HEK293-MTRFP and HEK293-MTCFP stable cell line was generated to study mitochondrial localization of proteins as previously described [30].

2.15. Generation of knockout lines using CRISPR/Cas9 gene editing

To generate NLRX1 or FASTKD5 knockout cell line, CRISPR/Cas9 guide RNAs were designed using CRISPRko sgRNA design tool [31]. The sgRNA targeting fourth exon with pick order score of 1 was selected and synthesized. Synthesized oligos were annealed and cloned into *Bbs*I -linearized pSpCas9(BB)-2A-Puro (PX459) vector essentially as described earlier [32]. NLRX1 and FASTKD5 sgRNA clone was transformed into competent Stbl3 *E. coli* strain and the transformants were screened by colony PCR, using U6 sequencing primer and antisense sgRNA. Positive clones were finally confirmed by Sanger DNA sequencing. NLRX1 and FASTKD5 sgRNA constructs were transfected into HEK293 cells using lipofectamine 2000. After 48 h of transfection, transfected cells were selected with 2 μg/ml puromycin. The puromycin-supplemented medium was replaced every 24 h until single colonies were visible. The colonies were harvested and transferred to 96-well plate to obtain single clone using serial dilution method. Each single clone was further grown and transferred to 12 well plate and maintained in puromycin medium. Positive stable clones were identified by a western blot screening for the loss of NLRX1 or FASTKD5 gene product. The NLRX1 and FASKD5-specific sgRNA sequence and colony PCR primers are listed in Supplementary Table S4.

2.16. Cell proliferation assay

Cell proliferation assay was performed to study the growth rate of NLRX1 transfected T47D and MCF-7 cells and NLRX1 KO cell line in customized substrate selective media. Briefly, cells growing in log phase were transfected and incubated overnight. After 24 h of transfection, MCF-7 and T47D cells were seeded in 48-well plate at 20000 cells/well whereas NLRX1 KO cells were plated at 10000 cells/well. Cells were washed twice with DPBS and customized glycolytic and oxidative media was added in the presence and absence of antimycin (100 nM). The customized media was prepared by using base DMEM solution that lacks glucose, pyruvate, and glutamine (Thermo Fisher Scientific Inc., catalog #A14430) and supplemented with 10% FBS, 10 mM glucose, 4 mM glutamine, and 1% PSN (Glycolytic medium). Galactose-containing (oxidative) media were generated by DMEM supplemented with 10% FBS, 10 mM galactose, 4 mM glutamine, and 1% PSN. Cells were trypsinized after 24 h cycle and cell number was counted and growth curve generated. For all conditions, the seeding densities used allowed exponential proliferation for four days and final cell counts were measured four days after treatment. The experiment was replicated two times per condition. Proliferation rate was determined using the following formula:

Proliferation Rate (Doublings per day)

$$= \log_2(\text{Final cell count (D5)/Initial cell count(D1))/D4}.$$

2.17. Statistical analysis

Data are shown as either mean ± SEM or mean ± SD for *n* observations. The data sets were normalized considering the values of controls as 100%. The comparisons between data sets were performed by unpaired two-tailed Student's *t*-test to determine the levels of significance for each data set GraphPad Prism® 5. The experiments were repeated minimum of two to three times independently, probability values of *p* < 0.05 were considered as statistically significant. All figure images were prepared with Adobe Photoshop©8 CS.

3. Results

3.1. NLRX1 is a mitochondrial matrix protein

Human NLRX1 is a ubiquitously expressed highly conserved multi-domain protein of 975 amino acids [33] having N-terminal mitochondria-targeting sequence (MTS), a central nucleotide-binding and oligomerization domain (NOD) and a C-terminal putative ligand-binding and regulatory leucine-rich repeat (LRR) domain (Fig. S1A). NLRX1 is known to translocate to mitochondria [34], however its sub-mitochondrial localization is not well established. The expression analysis showed high levels of NLRX1 in some cancer cell lines, such as MDA-MB-231, SHSY-5Y, HepG2 and HeLa, whereas its levels were low in HEK293 and MCF-7 and absent in T47D cells (Fig.1A and B).

We expressed full length (FL) NLRX1 (1–975 aa), NLRX1 ΔN-ter (160–975 aa) and LRR (564–975 aa) constructs in HEK293 cells and analyzed its subcellular localization by western blotting. Full length NLRX1 localized predominantly to mitochondrial fraction although low levels of NLRX1 were also detected in the cytosol (Fig. 1C). N-terminal deletion (NLRX1 ΔN-ter) and LRR domain variants of NLRX1 were found exclusively in cytosolic fraction confirming that the N-terminal domain of NLRX1 is essential for its translocation to mitochondria.

To further examine the submitochondrial localization of NLRX1, mitoplasts from HeLa cells were prepared by selective disruption of the mitochondrial outer membrane with digitonin and analyzed by western blotting. A band of 110 kDa corresponding to NLRX1 was detected in mitoplast fraction. Similarly, 45 kDa and 25 kDa bands corresponding to Citrate Synthase (CS, mitochondrial matrix protein), and ATPase6 (inner mitochondrial membrane protein), respectively, (Fig. 1D) were detected in mitoplast fraction. As expected, the outer membrane protein Tom20, the intermembrane protein AIF and the cytosolic protein RPS9 were not observed in mitoplasts fraction. Similar to CS and ATPase6 proteins, NLRX1 remained intact when mitoplast pellet was digested in the Proteinase K protection assay (Fig. 1E) but acquired a full sensitivity to Proteinase K after permeabilization with Triton X-100. In contrast, Tom20 was sensitive to digestion even in the absence of Triton X-100. The alkaline carbonate extraction of isolated mitoplast demonstrated that NLRX1 is not an intrinsic inner membrane protein but was extractable alongside soluble protein CS (Fig. 1F). Altogether, these results suggested that NLRX1 is a soluble mitochondrial matrix protein.

We also analyzed the subcellular localization of NLRX1 by live-cell imaging. MCF-7 cells were transfected with NLRX1-GFP and mitochondria were visualized by staining cells with TMRM, a cell-permeant cationic fluorescent dye which accumulates in mitochondria. We observed a partial but distinct overlap of the GFP signal with the TMRM positive mitochondrial network (up to 60%) (Fig. 1G). The intensity profile analysis revealed a near-complete overlay of NLRX1-GFP and TMRM fluorescence, suggesting that NLRX1 exclusively localizes to mitochondria. Recently, by diffraction-unlimited stimulated emission depletion (STED) imaging revealed that TMRM was found

preferentially at the inner mitochondrial membrane, rather than in the matrix [35]. We transiently expressed a mitochondrial matrix-targeted red fluorescent protein (mtRFP) in HeLa cells and observed a punctate distribution of NLRX1 (shown in grayscale) colocalizing with mitochondria (Fig. 1H). The colocalization analysis revealed > 70% overlap of distinct green puncta of NLRX1-GFP with positive red signals from mtRFP. These evidences strongly suggest the predominant localization of NLRX1 to mitochondrial matrix in cells of different origin.

3.2. NLRX1 interacts with FASTKD5 and colocalizes with mitochondrial RNA granules

The functional significance of localization of NLRX1 to mitochondrial matrix is not understood. In a high throughput proteome study of the human innate immunity network, the interaction of NLRX1 with FASTKD5 was predicted [36] hence this was further analyzed. NLRX1 and FASTKD5 were co-transfected and co-immunoprecipitation experiments were performed. The immunoprecipitation of FASTKD5 revealed a band of 110 kDa corresponding to NLRX1 suggesting their interaction in normal cellular condition (Fig. 2A). This interaction appears to be specific as another mitochondrial RNA granule protein LRPPRC (leucine-rich pentatricopeptide repeat containing protein) and translation elongation factor, EF-Tu were not detected in the FASTKD5 immunoprecipitates. Similarly, we immunoprecipitated NLRX1 and detected a band of 87 kDa corresponding to FASTKD5, as an NLRX1 interacting protein both in HEK293 and MCF-7 cells (Fig. 2B).

We further investigated the co-localization of NLRX1-GFP and FASTKD5-RFP in HEK293 cells that stably express a cyan fluorescent protein targeted to mitochondrial matrix (mtCFP) by confocal microscopy. Analysis of the fluorescence profiles showed almost complete overlap in the distribution pattern of NLRX1-GFP and FASTKD5-RFP (Fig. 2C). The triple color composite image revealed distinct co-localization (up to 80%) of NLRX1-GFP and FASTKD5-RFP. Both NLRX1-GFP and FASTKD5-RFP appeared as distinct puncta across the tubular distribution of mtCFP positive signal. To characterize the size and distribution of distinct punctate morphology exhibited by NLRX1 and FASTKD5, we performed dual-color 3D-SIM (three-dimensional structured illumination microscopy) super-resolution imaging of MCF-7 cells ectopically expressing NLRX1-GFP and FASTKD5-RFP (Fig. 2D). Both NLRX1 and FASTKD5 were concentrated in discrete foci and overlapped by 60%. The colocalization of NLRX1 and FASTKD5 was also observed in XZ-plane with size of focal structures varying between 50 and 100 nm in the axial direction. The intensity profile showed complete overlap of NLRX1-GFP and FASTKD5-RFP with size of colocalizing foci ranging from 30 to 100 nm.

The emerging evidence suggests that FASTKD5 is an integral component of the mitochondrial RNA granules (MRGs) [14]. The colocalization of FASTKD5 and NLRX1 suggest their direct recruitment to the site of MRGs in mitochondrial matrix. To test this hypothesis, we performed an indirect immunofluorescence staining with antibodies against BrU-labeled nascent mt-mRNAs and analyzed the degree of colocalization with NLRX1-GFP and FASTKD5-RFP. We observed discrete MRGs foci along with a tubular mitochondrial network of mitochondria, where NLRX1-GFP and FASTKD5-RFP colocalized (65.2% and 62.7% respectively) (Figs. 2E and S2A). The fluorescence intensity profile showed the punctate structure of NLRX1 (in gray scale) overlapping with BrU-labeled nascent mt-mRNAs. A cross-correlation analysis of composite images revealed a gaussian distribution profile with Pearson's coefficient of $P_{NLRX1-BrU} = 0.961$ and $P_{FASTKD5-BrU} = 0.935$ at the ΔX values approaching zero suggesting that both NLRX1 and FASTKD5, the bonafide RNA granule protein, co-localize to MRGs (Fig. S2B and C). The co-localization of NLRX1 and FASTKD5 within the MRGs suggest their possible role in regulating post-transcriptional processing of mt-mRNAs.

We further co-imaged the NLRX1-GFP and FASTKD5-RFP with the BrU-labeled MRGs in the mtCFP-expressing HEK293 cells. As observed
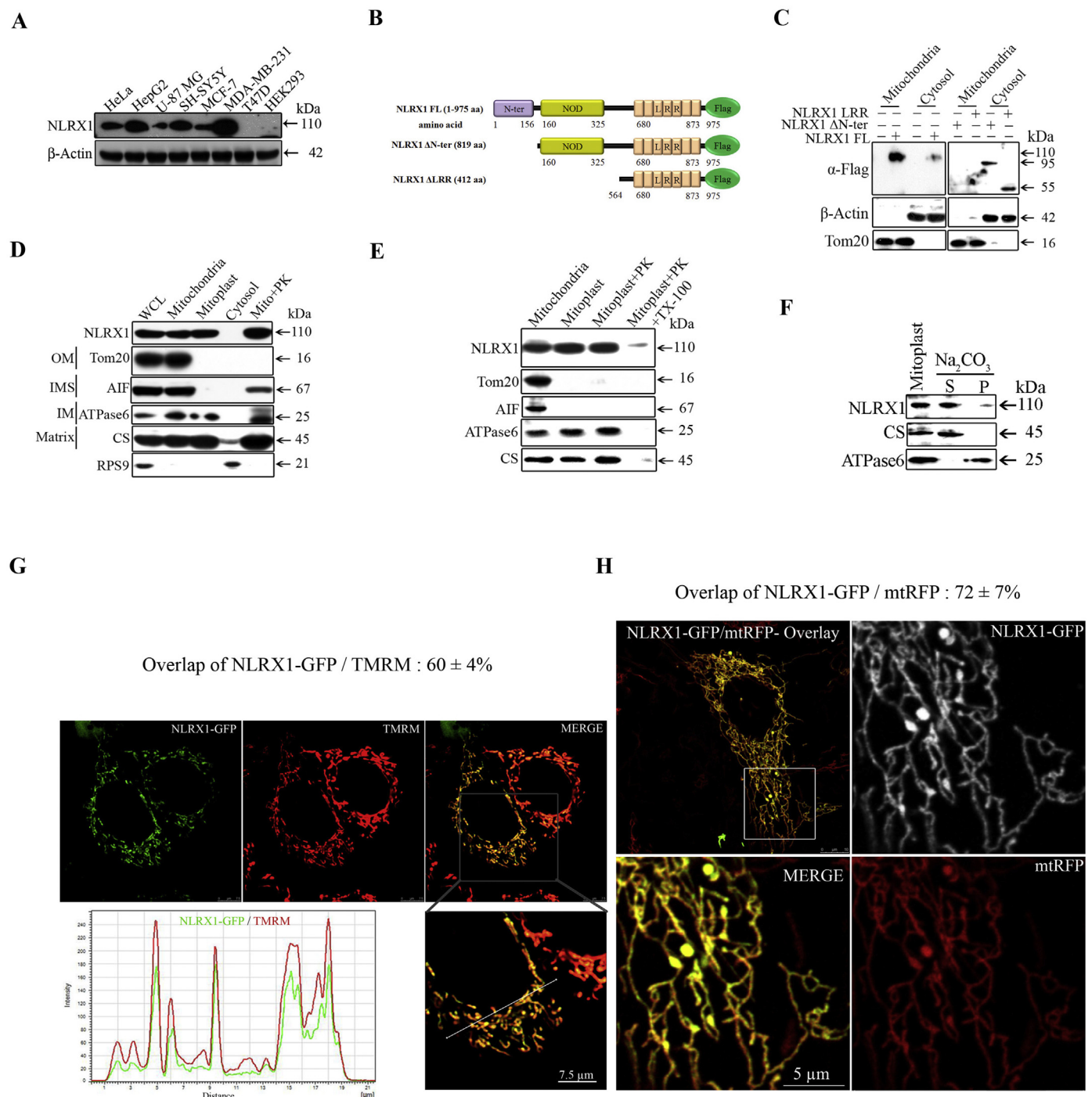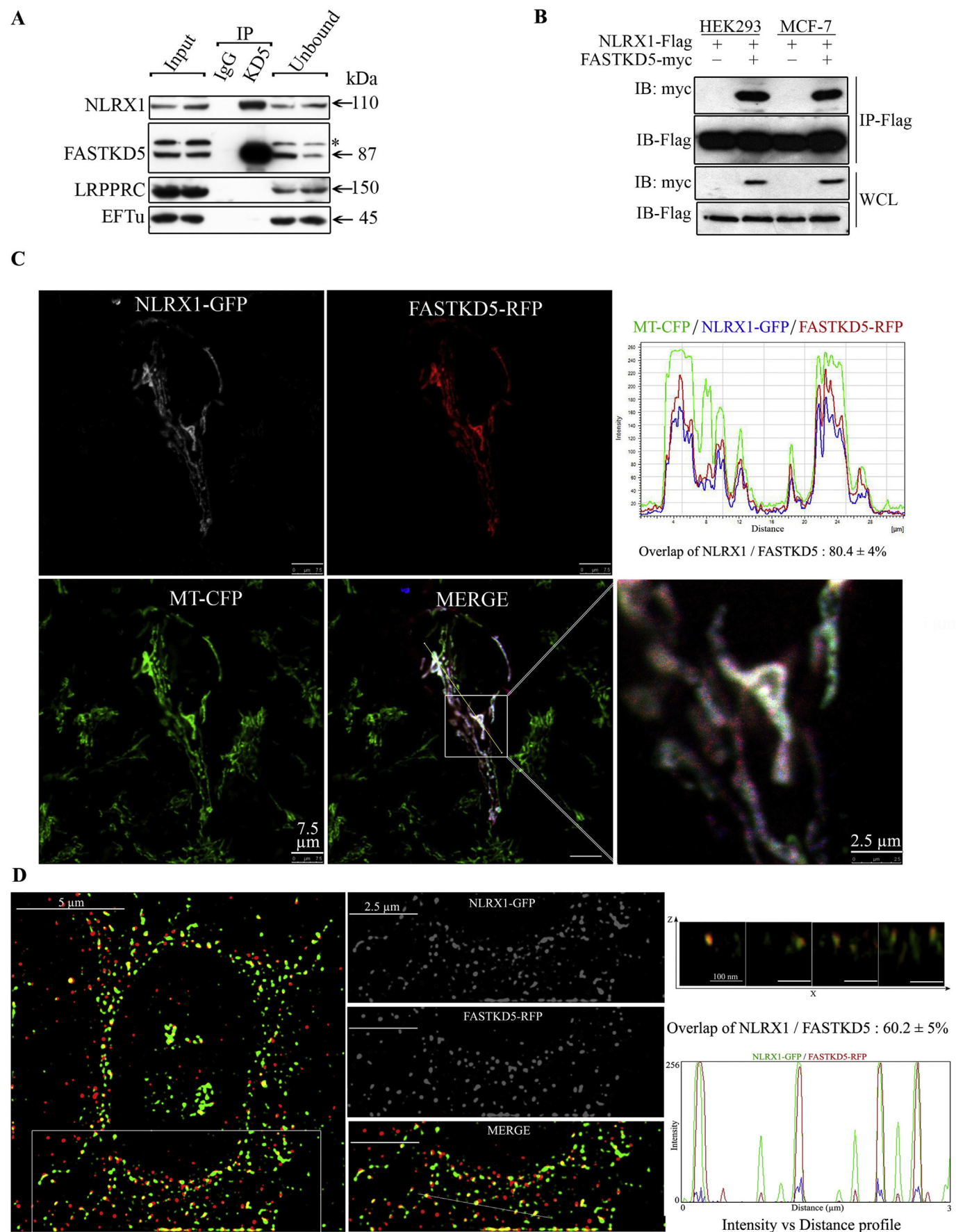
Fig. 1. NLRX1 localizes to mitochondrial matrix. (A) Endogenous level of NLRX1 in different cell lines was detected by western blotting using anti-NLRX1 antibody. (B) Schematic representation of the deletion constructs of NLRX1 used in the study. (C) Subcellular distribution of NLRX1, HEK293 cells were transfected with indicated constructs, heavy membrane (mitochondria) and light membrane (cytosol) fractions were isolated and analyzed by western blotting using indicated antibodies. (D) Mitochondrial and cytosolic fractions were isolated from HeLa cells mitoplasts were digested with Proteinase K as described in Materials and methods and analyzed by western blotting using indicated antibodies. (E) Mitoplast fraction (pellet) from HeLa cells were treated with Proteinase K in the presence of Triton X-100 treatment and analyzed by western blotting. (F) Mitoplasts pellet was subjected to alkaline extraction and ultra-centrifugation to allow the separation of soluble matrix protein (S) and integral protein of inner membrane (P). (G and H) Live cell imaging was performed to visualize mitochondrial localization of NLRX1. MCF-7 cells were transfected with NLRX1-GFP and mitochondria were stained with TMRM and analyzed by confocal microscopy. Scale bar, 7.5 μm (Merge and inset image). Pixel intensity distribution profile depicts colocalization of NLRX1 and TMRM fluorescence. HeLa cells were co-transfected with mtRFP and NLRX1-GFP and observed under confocal microscope. Scale bar, 10 μm (Merge image) and 5 μm (inset image). Pearson's correlation coefficients for NLRX1-GFP/TMRM and NLRX1-GFP/mtRFP are represented as percent mean ± SD value from $n \geq 5$ NLRX1-GFP positive cells.

earlier, both FASTKD5-RFP and NLRX1-GFP appeared as punctate substructures within mitochondria (shown in grayscale, Fig. 2F). More than 50% of FASTKD5-RFP and NLRX1-GFP positive structures co-

localized with BrU-labeled foci suggesting that both FASTKD5 and NLRX1 associates with nascent mRNAs in mitochondria (Fig. 2G). The analysis of fluorescence intensity profiles revealed a major overlap of

Overlap of NLRX1 / FASTKD5 : 80.4 ± 4%

Overlap of NLRX1 / FASTKD5 : 60.2 ± 5%

Intensity vs Distance profile

(caption on next page)

Fig. 2. NLRX1 associates with FASTKD5 and localizes to mitochondrial RNA granules. (A) Co-immunoprecipitation of FASTKD5 was performed using control IgG or anti-FASTKD5 antibody and interacting proteins were analyzed by western blotting using indicated antibodies. Asterisk (*) indicate a non-specific band. (B) FASTKD5 co-immunoprecipitate with NLRX1 in a reciprocal IP. HEK293 cells were co-transfected with NLRX1-Flag and FASTKD5-myc and co-IP was performed using anti-Flag antibody and analyzed by western blotting using indicated antibodies. WCL represents expression of proteins in whole-cell lysates. (C) mtCFP-HEK293 stable cells were co-transfected with NLRX1-GFP and FASTKD5-RFP, fixed with 4% paraformaldehyde and visualized by confocal microscope ($n = 3$). Fluorescence intensity distribution profile demonstrates colocalization of NLRX1 and FASTKD5 with mitochondria. Scale bar, 7.5 µm (Merge image) and 2.5 µm (inset image). Quantification of NLRX1 overlap with FASTKD5 from ≥ 3 cells is shown as mean ± SD alongside intensity profile. (D) Dual-color 3D-SIM image analysis of MCF-7 cells co-transfected with NLRX1-GFP and FASTKD5-RFP. Enlarged view of boxed region in (D) is shown on right with Pearson's correlation coefficients for NLRX1-GFP/FASTKD5-RFP represented as percent mean ± SD value. Line scan shows the pixel intensity profile of each fluorescence signal along a line of 3 µm. Colocalization of NLRX1-GFP/FASTKD5-RFP foci along the line scan is shown in a 200 nm thick XZ plane. Scale bar, 5 µm (Merge image) and 2.5 µm (inset image). (E) NLRX1 accumulates in mitochondrial RNA granules. HeLa cells were transfected with either NLRX1-GFP or immunofluorescence was performed using anti-BrdU antibody. Quantification of NLRX1 overlap with BrU from ≥ 4 cells is shown as mean ± SD. Fluorescence intensity distribution profile demonstrates the overlap of NLRX1-GFP signal with BrU. Scale bar, 10 µm (Merge image) and 2.5 µm (inset image). (F) mtCFP-HEK293 stable cells were co-transfected with NLRX1-GFP and FASTKD5-RFP and immunofluorescence was performed using anti-BrdU antibody and observed under confocal microscope. Scale bar, 5 µm. (G) Quantification of BrU foci with mtCFP, NLRX1 and FASTKD5 signal (arrowheads) for inset image of (F). Data are shown as mean ± SEM ($N ≥ 5$ cells with ≥ 15 foci per cell; in total 75 foci were analyzed). (H) Intensity profiles demonstrate the spatial overlap of NLRX1 and FASTKD5 with BrU signal along the line scan.

NLRXI-GFP and FASTKD5-RFP fluorescence with the BrU signal across CFP-labeled mitochondria (Fig. 2H). To examine the effect of NLRX1 on RNA granule stability, we knocked down NLRX1 in HeLa cells and visualized for the BrU positive foci. The relative number and distribution of the BrU positive foci remained unaltered in the NLRX1 KD HeLa cells indicating that NLRX1 is not essential for the formation of MRGs (Fig. S2D, E and F). These results suggest that NLRX1 is a novel protein component of the mitochondrial RNA granules where it interacts with FASTKD5 and co-localizes with nascent mitochondrial RNAs.

3.3. NLRX1 regulates post-transcriptional processing of non-canonical precursor transcripts

The interaction of NLRX1 with FASTKD5 and its localization to MRGs suggests its potential involvement in the post-transcriptional processing of mitochondrial mRNAs. Therefore, we measured steady-state levels of mature mt-RNAs by qPCR upon NLRX1 knockdown. Depletion of NLRX1 in HeLa cells upregulated the levels of COX I, COX II, ATP8, ATP6, COX III, ND5 and cyt b mRNAs (Figs. 3A, S3A and B). We observed a marked increase in the levels of ATP8, ATP6, COX III, ND5 and cyt b genes which are products of non-canonical mt-mRNAs processing. Conversely, NLRX1 expression in HEK293 cells decreased the levels of 16S rRNA and all mature mt-mRNAs except those for ND2, ND4, ND4L, ND3 and ND6 genes. Transfection of NLRX1 ΔN-ter showed no significant alterations in the steady-state levels of mt-mRNAs and 16SrRNA as compared to vector control (Figs. 3B and S3C). We further investigated the alteration in relative copy number of mtDNA in NLRX1 transfected cells. NLRX1 expression did not showed significant changes in level of mtDNA content, thus, ruling out the possibility of mtDNA depletion as a mechanism for the observed decrease in steady-state levels of mitochondrial transcripts in NLRX1 transfected cells (Fig. S3D). The results indicate that NLRX1 may participate in a selective regulation of steady-state levels of a subset of mt-mRNAs.

We further tested the possibility that NLRX1 may regulate the post-transcriptional processing of precursor mt-mRNAs downstream of mtDNA replication. The precursor mRNA regions corresponding to pairs of adjacent genes were selectively amplified by PCR as described previously [37]. In cells, transfected with NLRX1, we detected an increased accumulation of 1523-bp and 1015-bp PCR products corresponding to the processing intermediates of ATP8 + COX III and ND5 + cyt b non-junctional heavy strand transcripts (Figs. 3C and S3E). The levels of the remaining pairs of adjacent genes, such as 16S rRNA-ND1, ND1-ND2 and ND2-COX I, remained unaffected. Depletion of FASTKD5 in HEK293 cells showed a similar processing defect resulting in accumulation of ATP8/6 + COX III and ND5 + cyt b heavy-strand transcripts (Fig. S3F and G) as previously reported [14]. We confirmed this observation using a qPCR approach to quantify the levels of processing intermediates of fused transcripts in a non-strand specific manner in T47D cells. It was observed that unprocessed form of ATP8/6 + COX III and ND5 transcript were two and three-fold higher

respectively in NLRX1 transfected cells (Figs. 3D and S3H). However, the COX I + COX II transcript punctuated by tRNA^{Ser} and tRNA^{Asp} as well as ND6 and cyt b transcript punctuated by tRNA$^{Glu.}$ was processed normally. Taken together, these data demonstrate that NLRX1 may regulate the post-transcriptional processing of non-canonical heavy strand transcript of ATP8/6 + COX III and ND5 + cyt b mRNAs.

3.4. The binding of mitochondrial RNA transcripts to FASTKD5 is regulated by NLRX1

To further explain the apparent decrease in the steady state levels of heavy strand transcripts caused by NLRX1, we co-transfected HEK293 cells with FASTKD5 and NLRX1 either alone or in combination and analyzed the enrichment of target transcripts bound by FASTKD5 or NLRX1 using RNA-IP. The analysis of FASTKD5 immunoprecipitate revealed more than twenty-fold enrichment of almost all long-lived COX I, COX II, COX III mRNAs and 16S rRNA except for ATP8 and ATP6 (Figs. 4A and S4A). We also observed a low but significant enrichment of short-lived ND5 and cyt b mRNAs with the exception of ATP6 (long-lived). In contrast, the analysis of NLRX1 immunoprecipitate revealed more than five-fold enrichment of ND5 and cyt b mRNAs but bound weakly to COX I, COX II, ATP8 mRNAs and 16S rRNA. Interestingly, the analysis of FASTKD5 immunoprecipitate from cells co-transfected with both NLRX1 and FASTKD5, revealed a loss in the enrichment of all FASTKD5-target RNAs. These results indicate that NLRX1 inhibits the binding of mitochondrial transcripts to FASTKD5.

To further confirm if association of NLRX1 with FASTKD5 modulates its mitochondrial transcript binding under endogenous conditions, we performed RNA-IP of endogenous NLRX1 and FASTKD5 from mitochondrial lysates of control and FASTKD5 knockdown HeLa cells. As a control, we also immunoprecipitated LRPPRC alongside NLRX1 and FASTKD5. The analysis of protein fractions by western blotting confirmed the knockdown of FASTKD5 (Fig. 4B). The pulldown of both NLRX1 and FASTKD5 was observed in respective immunoprecipitates of control cells while none of them co-immunoprecipitated with LRPPRC as observed in Fig. 2A. As previously reported, the analysis of bound RNA from LRPPRC immunoprecipitate indicated a strong association with COX I, COX II and COX III mRNAs and knockdown of FASTKD5 did not altered this association, further validating LRPPRC as mtRNA-binding protein (Fig. S4B and C) in addition to our experimental approach. Importantly, the analysis of endogenous FASTKD5 immunoprecipitate from control cells showed a similar enrichment of 16S rRNA, COX I, ATP8, ATP6 and COX III mRNAs in agreement with the pulldown by ectopically expressed FASTKD5 except ND5 and cyt b. This enrichment was drastically reduced in FASTKD5 knockdown cells (Fig. 4C and D). The analysis of endogenous NLRX1 immunoprecipitate showed a weaker but significant enrichment of all five target RNAs of FASTKD5 in control cells. In contrast, analysis of NLRX1 immunoprecipitate from FASTKD5 knockdown cells, revealed a strong and significant enrichment of ATP8, ATP6, COX III, ND5 and cyt b mRNAs.
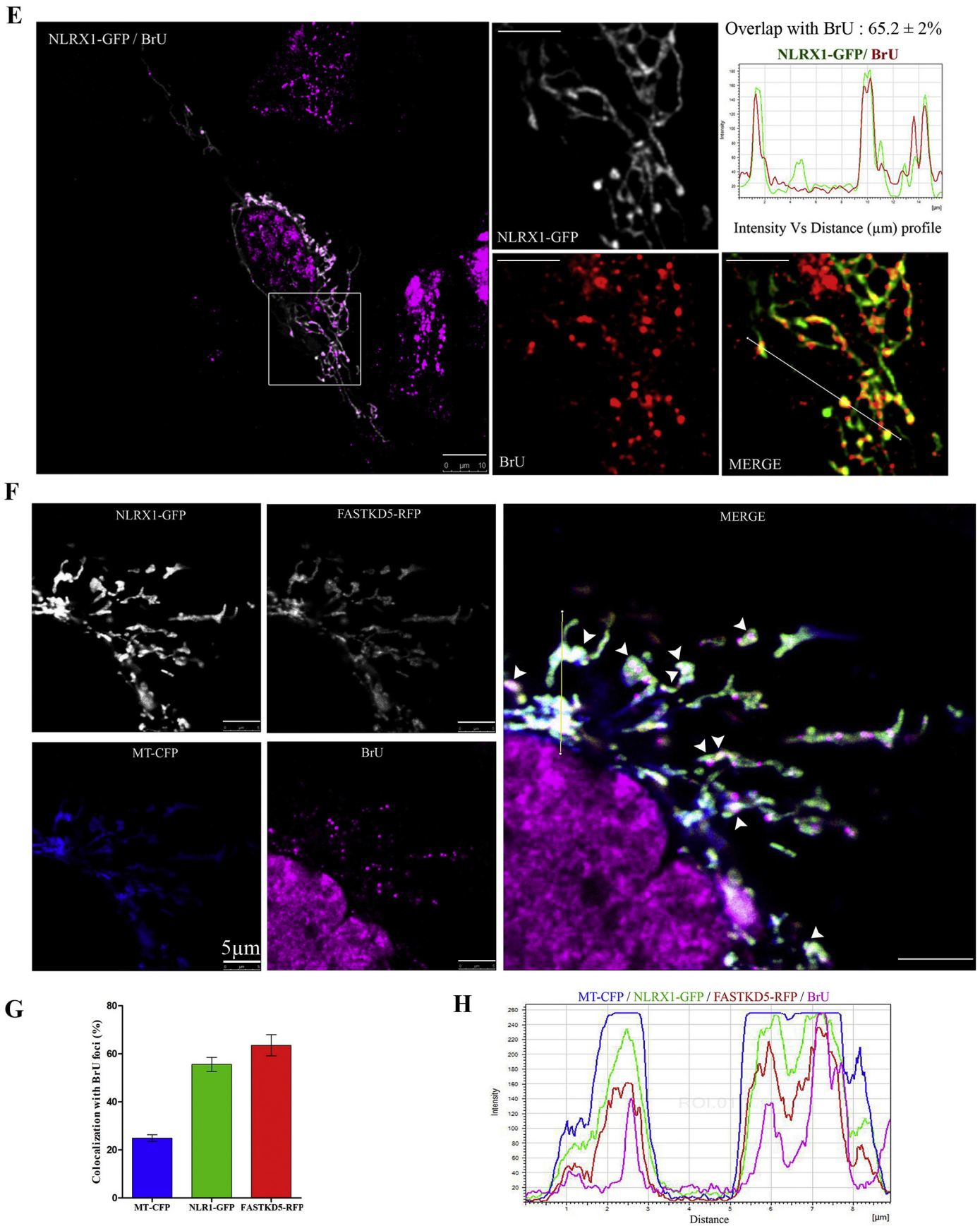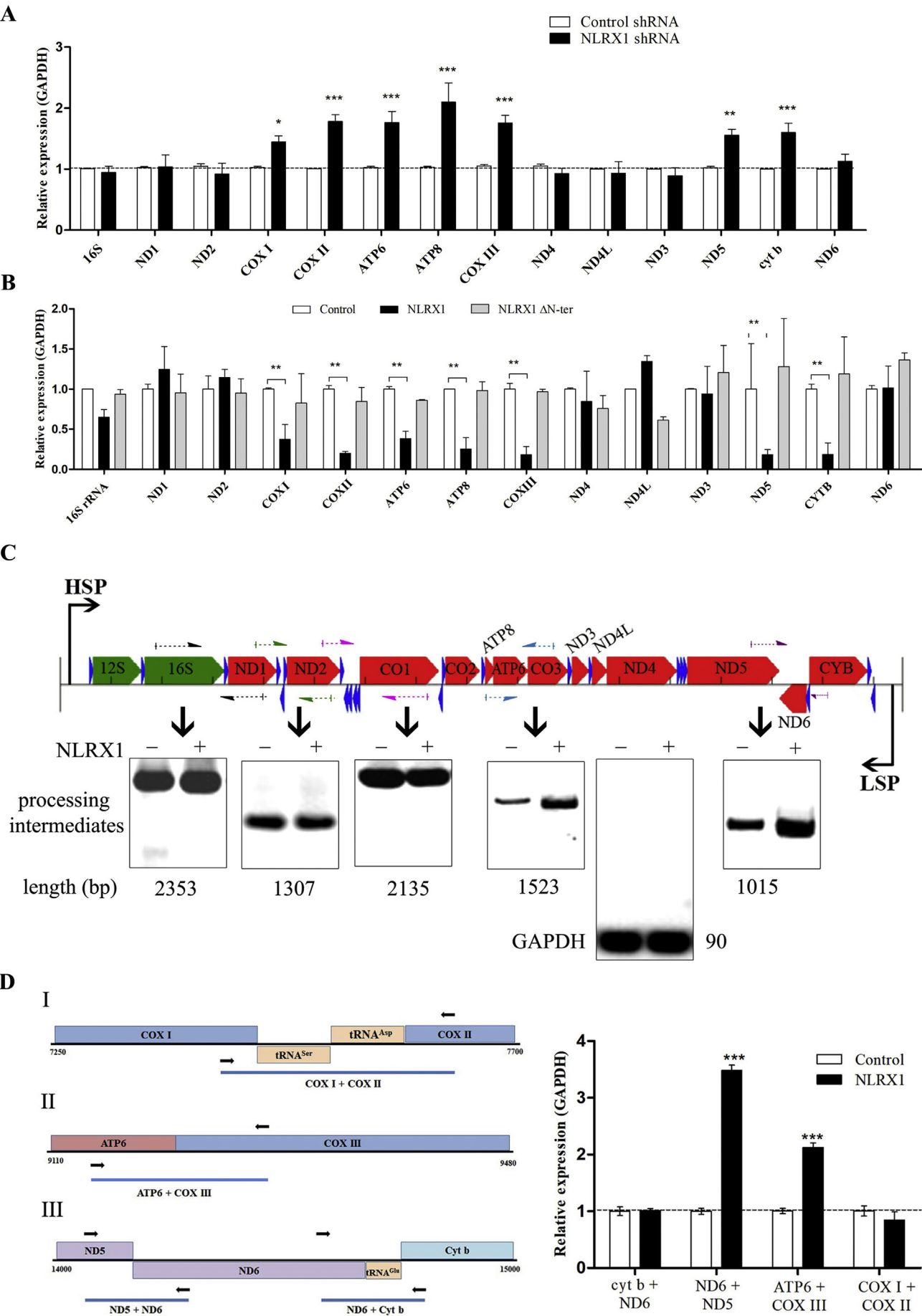
Fig. 2. (continued)

(caption on next page)

Fig. 3. NLRX1 affects the processing of mitochondrial RNA regulated by FASTKD5. (A) HeLa cells were transfected with Control shRNA and NLRX1 shRNA and levels of mature mitochondrial genome-encoded transcripts were determined by qPCR. Data are shown as mean ± SD ($n = 3$). (B) HEK293 cells were transfected with control vector, full length NLRX1 and N-terminal deletion mutant of NLRX1 (NLRX1 ΔN-ter) and levels of mature mitochondrial genome-encoded transcripts were determined by qPCR. Data are shown as mean ± SD (n = 3). (C) Linear representation of the mitochondrial genome. Green, rRNA; red, mRNA; blue, tRNA. HSP, heavy-strand promoter. LSP, light-strand promoter. Color-coded and half-headed arrow pair represents the PCR amplifying RNA regions. Black, 16S rRNA-ND1; green, ND1-ND2; pink, ND1-COX I; blue, ATP8-COX III and purple, ND5 + cyt b. HEK293 cells were transfected with NLRX1 and the levels of processing intermediates indicated on linear mitochondrial genome map were analyzed as described in materials and methods. GAPDH was included as nuclear control. (D) Strategy for PCR- quantification of junction-less transcripts: I- COX I + COX II indicated primer sets generating amplification product only when tRNA^{Ser} and tRNA^{Asp} are unprocessed. II-ATP6 + COX III indicate primer pair for the fragment when the adjacent COXIII and ATPase6 transcripts are unprocessed. III-ND5 + ND6 and ND6 + cyt b indicate primer sets generating product when their respective antisense strands are unprocessed. T47D cells were transfected with vector control and quantitation of expression using these primer pairs (Table S3) relative to nuclear control (GAPDH) was performed. Data are representative of three independent experiments, and the results are expressed as mean ± SD. Asterisk (*) denotes significant differences with $p < 0.05$.

Fig. 4. Association of NLRX1 with FASTKD5 negatively regulates mitochondrial transcript binding. (A) HEK293 cells were transfected with NLRX1 and FASTKD5 either alone or in combination and RNA-IP was performed as described in Materials and methods. The enrichment of 16S rRNA and mt-mRNAs were quantified by qPCR and relative expression levels were represented by Heat map, ($n = 4$). Blue and white represents strong and weak enrichment respectively. (B) Mitochondrial lysates from FASTKD5 knockdown HeLa cells (Clone D, Fig. S3E) and control sgRNA cells were immunoprecipitated for endogenous FASTKD5, NLRX1 and LRPPRC and their pull down and input levels in IP, IgG control and mitochondrial lysate, were determined by western blotting using indicated antibody. (C) and (D) Analysis of immunoprecipitated proteins in Fig. B from control sgRNA and FASTKD5 knockdown cells for bound RNA was performed as described in Materials and methods. The enrichment of mitochondrial transcripts was quantified by qPCR. Data are shown as mean ± SD (n = 3). Asterisk (*) denotes significant differences with $p < 0.05$.
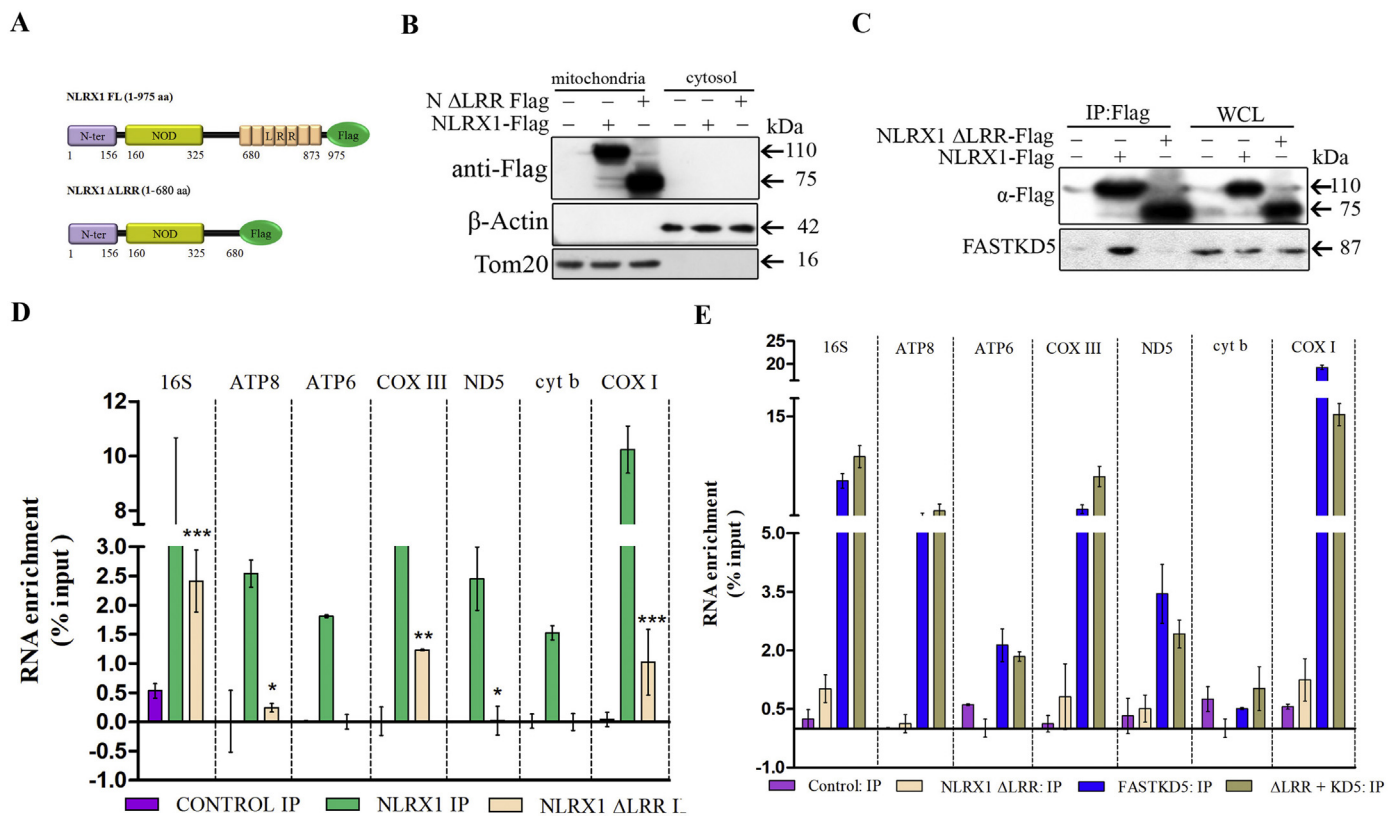
Fig. 5. NLRX1 binds to mitochondrial RNA and associates with FASTKD5 through the LRR domain. (A) Schematic representation of the LRR domain deleted construct of C-terminal Flag tag-NLRX1 generated for further study. (B) HEK293 cells were transfected with NLRX1-Flag and NLRX1-ΔLRR-Flag constructs and their subcellular localization was determined by cellular fractionation and western blotting as described in Materials and methods using indicated antibodies. (C) Co-immunoprecipitation of NLRX1, NLRX1-ΔLRR by anti-Flag beads and FASTKD5 by anti-HA beads were performed from mitochondrial lysates of HEK293 cells lysate transfected with these constructs and analyzed by western blotting using indicated antibodies. (D) and (E) IP Beads from Fig. C were further analyzed by RNA-IP as described in Materials and methods. The enrichment of mitochondrial RNA was quantified using qPCR. Data are shown as mean ± SD, (n = 3). Asterisk (*) denotes significant differences with $p < 0.05$.

These results suggested that NLRX1 preferentially associates with ATP8/6 + COX III and ND5 + cyt b transcripts with high affinity and negatively regulates FASTKD5-mediated processing.

3.5. The LRR domain of NLRX1 is required for its association with FASTKD5 and mitochondrial RNA

Among the conserved domain of NOD family receptors, LRR domain has been reported to sense and bind to its cognate ligands. The c-terminal LRR domain of NLRX1 has been shown to bind RNA *ex situ* [27]. Therefore, to validate our hypothesis, we generated a NLRX1 mutant lacking LRR domain (NLRX1-ΔLRR-Flag) and probed its localization in HEK293 cells by anti-flag antibody (Fig. 5A and B). Subcellular fractionation revealed that both NLRX1 and NLRX1-ΔLRR were exclusively localized to mitochondria. Finally, we immunoprecipitated NLRX1 and NLRX1-ΔLRR from mitochondrial lysates of HEK293 cells and assessed the mtRNA enrichment in respective immunoprepites. As a control, we immunoprecipitated FASTKD5 alongside NLRX1 and NLRX1-ΔLRR. The analysis of protein fractions by western blotting confirmed the immunoprecipitation of both NLRX1 and NLRX1-ΔLRR in the IP fraction (Fig. 5C). Importantly, FASTKD5 co-precipitated only with full length NLRX1, suggesting that LRR domain is essential for their interaction.

The analysis of bound RNA in NLRX1 immunoprecipitate showed a similar enrichment of 16S rRNA, COX I, ATP8, ATP6, COX III, ND5 and cyt b mRNAs indistinguishable from FASTKD5 immunoprecipitates (Figs. 5D and S5A). In contrast, deletion of LRR domain showed a significant decrease in enrichment of all mRNAs of heavy strand

transcripts in NLRX1-ΔLRR immunoprecipitates. These results suggested that NLRX1 binds to mtRNA through the LRR domain. We further investigated if LRR domain of NLRX1 essential for its interaction with FASTKD5 could also affect FASTKD5-RNA binding. Therefore, we immunoprecipitated FASTKD5 from cells with or without co-expressed NLRX1-ΔLRR and analyzed the enrichment of target transcripts (Fig. 5E). We did not observe any significant decrease in enrichment of the heavy strand transcripts by FASTKD5 immunoprecipitates from cells transfected with FASTKD5 alone or in combination with NLRX1-ΔLRR in contrast to Fig. 4A where co-expression of full length NLRX1 significantly decreases the enrichment by FASTKD5. The above results suggest that NLRX1 recognizes and associates with the non-junctional heavy strand transcripts specifically ND5 and cyt b mRNAs through LRR domain and negatively regulates the levels of 16S rRNA, COX I, ATP8, ATP6 and COX III mRNAs *via* its interaction with FASTKD5.

3.6. NLRX1 regulates translation of mtDNA-encoded proteins and assembly of respiratory supercomplexes

To reveal the functional consequences of NLRX1-mediated control of mt-RNA processing we studied the assembly and activity of MRC complexes. By Click azide/alkyne reaction, we monitored the changes in the levels of mtDNA-encoded nascent protein subunits in NLRX1 expressing MCF-7 cells. A global decline in the levels of mitochondrial translation products was observed in NLRX1 transfected cells which is consistent with the decrease in steady state levels of mt-mRNAs and 16S rRNA (Fig. 6A). However, the decrease in the levels of mitochondrial protein subunits was not uniform. Levels of non-canonical ATP8 + COX
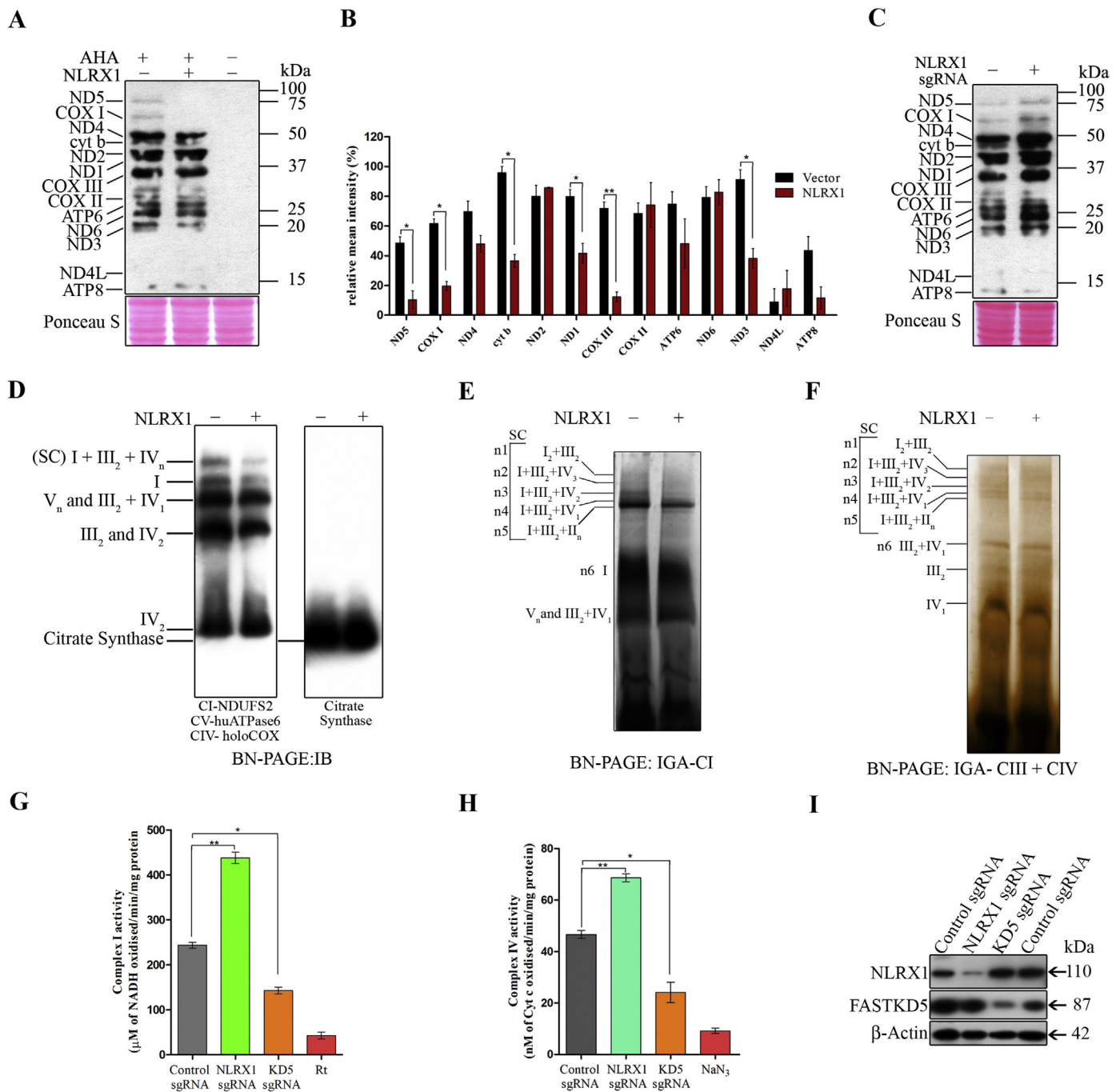
Fig. 6. NLRX1 decreases the levels of mtDNA-encoded protein subunits, OxPhos activity and assembly. (A) MCF-7 cells were transfected with control vector and NLRX1 and the levels of nascent mitochondrial protein subunits were determined after AHA (Methionine homologue) incorporation followed by analysis using Click-iT® AHA chemistry and immunoblotting with anti-biotin antibody. Normal methionine incorporated (without AHA) cells were used as positive control (B) Quantification of band intensity of (A) detected by western blotting was performed by densitometric analysis using ImageJ v1.45 (NIH, MD, USA) software. (C) HeLa cells were transfected with control sgRNA and NLRX1 sgRNA and were labeled and processed as described in (A). PVDF membranes were stained with Ponceau S to assess equal protein loading. (D) MCF-7 cells were transfected with control vector and NLRX1 and levels of respirasomes ($I + III_2 + IV_n$) and supercomplex of CIII and CIV as well as individual levels were detected by BN-PAGE followed by immunoblotting with indicated antibodies. Citrate Synthase was used as loading control. (E) Assembly and activity of CI containing supercomplexes and individual CI were determined by BN-PAGE followed by in-gel activity staining specific for CI. (F) Assembly and activity of CIII and CIV containing supercomplexes and individual CIII and CIV were determined by BN-PAGE followed by in-gel activity staining specific for CIII + CIV. (G) and (H) Hela cells were transfected with control sgRNA, NLRX1 sgRNA or FASTKD5 sgRNA and enzyme activity of CI and CIV were quantified using spectrophotometer. (I) Confirmation of the NLRX1 and FASTKD5 knockdown in HeLa cells was assessed by western blotting using indicated antibodies. Data in (B), (G) and (H) are shown as mean ± SEM ($n ≥ 3$). Asterisk (*) denotes significant differences with $p < 0.05$.

III and ND5 + cyt b precursor products, ND5, cyt b and COXIII subunits were substantially decreased (Fig. 6B). Similarly, levels of ND1, ND3 and COX1 were decreased, whereas levels of the remaining protein subunits were not significantly altered. Conversely, depletion of NLRX1 in HeLa cells increased the levels of mtDNA encoded proteins subunits (Fig. 6C).

mtDNA-encoded protein subunits are indispensable for the assembly of functional individual MRCs, as well as their supercomplexes [38, 39].

The individual CI, CIII, and CIV associate to form intermediate supramolecular assemblies known as supercomplexes (SCs) or respirasomes. We tested levels and organization of respirasomes in NLRX1 transfected MCF-7 cells by western blots probed for NDUFS2, a nuclear encoded subunit of CI. The level of SCs composed of $CI + CIII_2 + CIV_n$ and $CIII_2 + CIV$ decreased in the NLRX1 expressing cells (Fig. 6D) as compared to vector transfected cells. Levels of free CI and dimeric CIII and CIV also decreased, whereas levels of monomeric CIV remained unaltered.

We further analyzed the functional levels of supercomplexes by BN-PAGE and in-gel activity staining for CI and CIII + CIV. The in-gel activity assay for CI in control MCF-7 cells revealed NADH dehydrogenase activity in all bands, corresponding to supercomplexes (bands n1 to n5), and to the individual CI (band n6). The expression of NLRX1 decreased the activity of free CI and the supercomplexes (Fig. 6E). Similarly, the in-gel staining for CIII + CIV was present in all bands of SCs (n1 to n5 and n6), whereas the maximum signal was detected for the monomeric CIV in control MCF-7 cells (Fig. 6F). In contrast, the activity of SCs (band n1 to n5), CIII dimers and monomeric CIV decreased in NLRX1-expressing cells. The enzyme activity of CI and CIV in NLRX1 expressing MCF-7 cells also decreased (Fig. S6A and B). However, the expression of NLRX1 in MCF-7 cells did not affect the enzyme activity of CII (Fig. S6C and D). Conversely, CRISPR-Cas9 mediated knockdown of NLRX1 in HeLa cells increased the enzyme activity of CI and CIV while knockdown of FASTKD5 significantly downregulated this activity (Fig. 6G, H and I). Collectively, these results demonstrate that NLRX1 modulates the organization of functional mitochondrial supercomplexes.

3.7. NLRX1 regulates OxPhos-dependent cell proliferation

To understand the physiological implications of NLRX1-regulated function in mitochondria, we analyzed growth rates of the NLRX1 expressing T47D and MCF-7 breast cancer cells and HEK293 cells in a medium containing alternative nutrient carbon sources, namely glucose or galactose. In high-glucose medium, the growth rate of the NLRX1 transfected T47D, MCF-7 and HEK293cells showed no change, up to day five (Fig. S7A, B and C). Supposedly, the energy deficit due to the impaired OxPhos inNLRX1 expressing cells could be compensated by an increased glycolysis in the high glucose medium. This is consistent with the observation that NLRX1 was able to increase cellular proliferation by activating the glycolytic metabolism [40].

The growth rate of control cells in the galactose-containing medium was lower, as compared to the high glucose medium (Figs. 7A, C and S7D). Apparently, the NADH consuming and energetically less efficient conversion of galactose to glucose-1-phosphate fails to provide the high energy demands of proliferating cells making the cells more dependent on mitochondrial respiration [41]. In agreement, we observed an overall decrease in growth rate of the NLRX1 expressing T47D, MCF-7 and HEK293 cells in the galactose medium. The cells demonstrated an unchanged proliferation rate during the initial 48 h, thereafter rate gradually declined and stopped proliferating after day 5 suggesting a compromised OxPhos activity.

We further monitored the role of NLRX1 in growth kinetics of MCF-7 and T47D cells in presence of glucose or galactose containing medium (Fig. 7B and D). The vector-transfected control cells showed similar proliferation rates in both medium, but NLRX1 transfected cells exhibited a retarded proliferation in the galactose medium. Furthermore, after treatment with antimycin A, the CIII inhibitor, there was a severe decrease in proliferation rate of cells growing in the galactose medium, but the cells growing in high glucose medium proliferated normally. Therefore, the NLRX1-expressing cells with dysfunctional mitochondrial respiratory function are unable to proliferate in the galactose medium. Similarly, the CRISPR-Cas9 mediated loss of NLRX1 could reverse the growth limitation of HEK293 cells in the galactose medium (Figs. 7E and E', S7E and F). These results confirmed that NLRX1 attenuates mitochondrial respiration making cell proliferation more

dependent on the glycolysis.

4. Discussion

The submitochondrial localization of NLRX1 and its role in regulation of mitochondrial function is not only critical for understanding the metabolic reprogramming during innate immune activation but also for the homeostasis of cellular bioenergetics. In the present study, we demonstrated that association of NLRX1 and FASTKD5 negatively regulates the mitochondrial RNA processing and metabolic adaptation.

Here, we systematically characterized the sub-mitochondrial localization of NLRX1. We show that NLRX1 is predominantly present in mitochondrial fraction, specifically in mitochondrial matrix. This conclusion is in agreement with Arnoult et al. suggesting that NLRX1 is targeted to mitochondrial matrix [34]. Our live-cell imaging data further confirmed the mitochondrial matrix localization of NLRX1 in different cell lines. The lower levels of cytoplasmic NLRX1 detected in our study potentially explains the discrepancy in the localization and function of NLRX1 reported by other groups [42, 43]. It is possible that the cytoplasmic pool of NLRX1 may interact and initiate the degradation of MAVS at the mitochondrial outer membrane, thereby negatively regulate type-I IFN and NF-κB activation during antiviral signaling [44]. Additional studies are needed to investigate whether the mitochondrial localization of NLRX1 is important for innate immune signaling, or the cytoplasmic NLRX1 is alone sufficient.

Effector functions and potential ligands of NLRX1 within mitochondria is still unknown. Mitochondria maintain mt-mRNAs at distinct steady-state levels that vary in their abundance across different tissues to ensure proper OxPhos complex stoichiometry [45, 46]. The polycistronic mRNAs encoded by mtDNA are processed within MRGs to generate mature mitochondrial mRNAs [18]. In the current study, we confirmed the interaction of NLRX1 with FASKD5 in mitochondria by co-immunoprecipitation experiments. By confocal and super-resolution imaging, we confirmed the colocalization of NLRX1 and FASTKD5 with MRGs and analyzed its size and punctate distribution within mitochondria. Our results strongly indicate that NLRX1 is a novel component of MRGs where it dynamically associates with FASTKD5. The analysis of mature mitochondrial transcripts revealed a significant reduction in the steady-state levels of non-canonical mt-mRNAs, such as COX I, ATP8/6, COX III, ND5, cyt b in NLRX1 expressing cells. A deletion of the N-terminal mitochondria targeting sequence prevented the accumulation of NLRX1 to mitochondria leaving levels of mature mt-mRNAs unchanged. This strongly suggests that localization of NLRX1 in the mitochondrial matrix is essential for the regulation of RNA processing within MRGs. FASTKD5 is known to be required for the processing of three non-canonical heavy-strand precursor transcripts (5'end-COX I, ATP8/6 + COX III, and ND5 + cyt b), as depletion of FASTKD5 resulted in an accumulation of unprocessed precursor RNAs and defective complex IV [14]. The steady state levels of ATP8/6, COX III, ND5 and cyt b mRNAs is decreased in NLRX1 expressing cells preventing their maturation by binding directly to these transcripts as shown by RNA-IP of NLRX1. It is also possible that NLRX1 may modulate the processing and maturation of non-canonical precursor transcripts through its interaction with FASTKD5. Additionally, in the absence of FASTKD5, NLRX1 competitively binds to ATP8/6, COX III, ND5 and cyt b mRNAs and negatively regulates the transcripts mature levels. This observation is further supported by accumulation of ATP8/6 + COX III, and ND5 + cyt b unprocessed heavy strand transcripts upon FASTKD5 knockdown as reported earlier [14].

NLRX1 possesses a C-terminal LRR domain (residues 629–975, cNLRX1), which is responsible for the compact hexameric architecture stabilized by inter-subunit and inter-domain interactions. It has been demonstrated that cNLRX1 can directly bind to ssRNA analogue *ex situ* [27], although no data with live cells and its implication in cellular function has been reported. In the present study, by co-immunoprecipitation of NLRX1, we demonstrated an enrichment of a
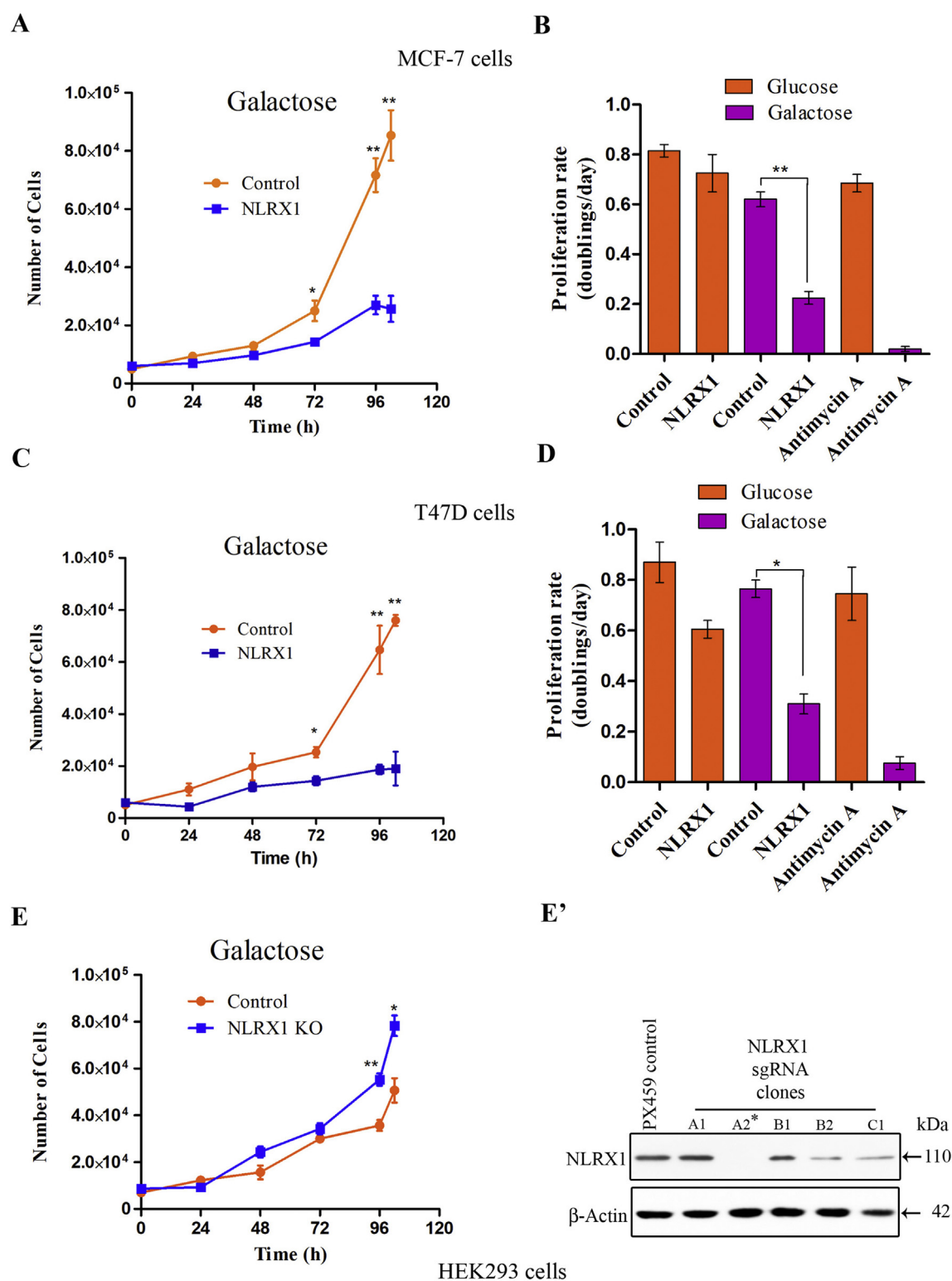
Fig. 7. NLRX1 decreases the proliferation of OxPhos-deficient cells. (A) and (C) MCF-7 and T47D cells were transfected with vector and NLRX1 and seeded in galactose-containing medium with or without antimycin A (100 nM). Growth curves were determined by cell count normalized to cell number at $t = 0$ when media conditions were applied, were assessed for five consecutive days and used to calculate proliferation rate. (B) and (D) Proliferation rates of the cells in respective medium were determined as described in Materials and methods. (E) and (E') HEK293 cell were transfected with PX459 control and NLRX1 sgRNA vector. Stable cell clones were selected and cultured as described in Materials and method. The clone A2 marked with an asterisk is referred to as NLRX1 knockout cell line and was used for cell proliferation assay (E'). Control and NLRX1 KO HEK293 cells were seeded in galactose containing medium and growth curves were obtained (E). Data are representative of three independent experiments, and the results are expressed as mean ± SEM. Asterisk (*) denotes significant differences with $p < 0.05$.

distinct set of mt-mRNAs, as compared to FASTKD5, however, deletion of LRR domain showed no enrichment strongly suggesting that LLR domain of NLRX1 is essential for binding to RNA as well as its interaction with FASTKD5. These evidences suggest that NLRX1 may directly bind to mitochondrial transcripts and regulate its processing and maturation, as well as indirectly by sequestering FASTKD5.

Mature mt-mRNAs are translated to 13 essential protein subunits of the enzyme complexes constituting the OxPhos system. Although, levels of mtDNA-encoded protein subunits generally declined in NLRX1 expressing cells, we observed a specific decrease in the mtDNA-encoded CI (ND1, ND3 and ND5), CIII (cyt b) and CIV (COX I and COX III) protein subunits. The expression of NLRX1 decreased levels of mature 16SrRNA suggesting that the mitochondrial ribosome biogenesis may be affected. The sequestration or binding of NLRX1 to FASTKD5 may inhibit mito-ribosome assembly and thereby decrease the translation of mt-mRNA. The previous report demonstrating the role of FASTKD5 in mitochondrial ribosome biogenesis [14] and its association with NLRX1 further supports this hypothesis. Similarly, association of NLRX1 with TUFM (Tu translation elongation factor, mitochondrial) and its role in antiviral response has been reported [47], however its implication on mitochondrial translation has not been investigated. Our findings here suggest that NLRX1 in mitochondria may be important for RNA processing and mito-ribosome biogenesis and translation.

mtDNA-encoded protein subunits are essential for the assembly of MRC complexes. The overall decrease in mitochondrial protein synthesis suggests a combined defect in the assembly of OxPhos supercomplexes containing CI, CIII and CIV including individual complexes. An impaired assembly of respirasomes is known to induce oxidative stress by an excessive generation of ROS [48]. We and others have previously reported the increased generation of ROS in response to an overexpression of NLRX1 [7, 33]. Here, we found that NLRX1 can selectively decrease the enzyme activity of CIV in supercomplex, or in its uncomplexed state. A defective OxPhos assembly compromises mitochondrial respiration, which is supported by our observation that NLRX1 expressing cells proliferate poorly in the medium containing galactose instead of glucose.

5. Conclusions

In conclusion, our study establishes a critical role of NLRX1in regulating the post-transcriptional processing of mitochondrial precursor mRNAs to modulate the steady state levels of mature mitochondrial RNAs, thus, controlling the activity and organization of OxPhos complexes. These findings will have important implication in understanding bioenergetic adaptations in infection and cancer. We and others have reported that NLRX1 may act as a potential tumor suppressor in breast and colorectal cancer [7, 49]. NLRX1-mediated regulation of mitochondrial gene expression may play an important role in metabolic reprogramming of tumor cells. However, this observation needs to be further studied and validated in different experimental models of cancer.

Conflict of interest

The authors declare that no conflict of interest exists.

Author contribution

K.S., R.S., and L.S. conceptualized and designed the work; K.S., L.S., M.R., A.L., P.P., D.G., and K.B. discussed and performed the experiments; K.S., L.S., M.R., and P.P. analyzed the data; K.S. and R.S. wrote the original draft of manuscript; R.S. and P.M.C. revised and edited the manuscript; R.S. and P.M.C. acquired the funding for research work; R.S. supervised the entire study.

Transparency document

The http://dx.doi.org/10.1016/j.bbamcr.2018.06.008 associated with this article can be found, in online version.

Appendix A. Supplementary data

Supplementary data to this article can be found online at https://doi.org/10.1016/j.bbamcr.2018.06.008.

References

[1] W.J. Koopman, P.H. Willems, J.A. Smeitink, Monogenic mitochondrial disorders, N. Engl. J. Med. 366 (2012) 1132–1141.

[2] D. Arnoult, F. Soares, I. Tattoli, S.E. Girardin, Mitochondria in innate immunity, EMBO Rep. 12 (2011) 901–910.

[3] K. Bhatelia, K. Singh, R. Singh, TLRs: linking inflammation and breast cancer, Cell. Signal. 26 (2014) 2350–2357.

[4] M. Monlun, C. Hyernard, P. Blanco, L. Lartigue, B. Faustin, Mitochondria as molecular platforms integrating multiple innate immune signalings, J. Mol. Biol. 429 (2017) 1–13.

[5] T. Xia, H. Konno, J. Ahn, G.N. Barber, Deregulation of STING signaling in colorectal carcinoma constrains DNA damage responses and correlates with tumorigenesis, Cell Rep. 14 (2016) 282–297.

[6] K. Bhatelia, A. Singh, D. Tomar, K. Singh, L. Sripada, M. Chagtoo, P. Prajapati, R. Singh, M.M. Godbole, R. Singh, Antiviral signaling protein MITA acts as a tumor suppressor in breast cancer by regulating NF-kappaB induced cell death, Biochim. Biophys. Acta 1842 (2014) 144–153.

[7] K. Singh, A. Poteryakhina, A. Zheltukhin, K. Bhatelia, P. Prajapati, L. Sripada, D. Tomar, R. Singh, A.K. Singh, P.M. Chumakov, R. Singh, NLRX1 acts as tumor suppressor by regulating TNF-alpha induced apoptosis and metabolism in cancer cells, Biochim. Biophys. Acta 1853 (2015) 1073–1086.

[8] G. Stokman, L. Kors, P.J. Bakker, E. Rampanelli, N. Claessen, G.J.D. Teske, L. Butter, H. van Andel, M.A. van den Bergh Weerman, P.W.B. Larsen, M.C. Dessing, C.J. Zuurbier, S.E. Girardin, S. Florquin, J.C. Leemans, NLRX1 dampens oxidative stress and apoptosis in tissue injury via control of mitochondrial activity, J. Exp. Med. 214 (2017) 2405–2420.

[9] D.J. Pagliarini, S.E. Calvo, B. Chang, S.A. Sheth, S.B. Vafai, S.E. Ong, G.A. Walford, C. Sugiana, A. Boneh, W.K. Chen, D.E. Hill, M. Vidal, J.G. Evans, D.R. Thorburn, S.A. Carr, V.K. Mootha, A mitochondrial protein compendium elucidates complex I disease biology, Cell 134 (2008) 112–123.

[10] M.T. Couvillion, I.C. Soto, G. Shipkovenska, L.S. Churchman, Synchronized mitochondrial and cytosolic translation programs, Nature 533 (2016) 499–503.

[11] J. Montoya, G.L. Gaines, G. Attardi, The pattern of transcription of the human mitochondrial rRNA genes reveals two overlapping transcription units, Cell 34 (1983) 151–159.

[12] D. Ojala, J. Montoya, G. Attardi, tRNA punctuation model of RNA processing in human mitochondria, Nature 290 (1981) 470–474.

[13] O. Rackham, T.R. Mercer, A. Filipovska, The human mitochondrial transcriptome and the RNA-binding proteins that regulate its expression, Wiley Interdiscip. Rev. RNA 3 (2012) 675–695.

[14] H. Antonicka, E.A. Shoubridge, Mitochondrial RNA granules are centers for post-transcriptional RNA processing and ribosome biogenesis, Cell Rep. 10 (2015) 920–932.

[15] A.A. Jourdain, M. Koppen, M. Wydro, C.D. Rodley, R.N. Lightowlers, Z.M. Chrzanowska-Lightowlers, J.C. Martinou, GRSF1 regulates RNA processing in mitochondrial RNA granules, Cell Metab. 17 (2013) 399–410.

[16] Y.T. Tu, A. Barrientos, The human mitochondrial DEAD-box protein DDX28 resides in RNA granules and functions in mitoribosome assembly, Cell Rep. 10 (2015) 854–864.

[17] A.A. Jourdain, E. Boehm, K. Maundrell, J.C. Martinou, Mitochondrial RNA granules: compartmentalizing mitochondrial gene expression, J. Cell Biol. 212 (2016)

611–614.

[18] S.F. Pearce, P. Rebelo-Guiomar, A.R. D'Souza, C.A. Powell, L. Van Haute, M. Minczuk, Regulation of mammalian mitochondrial gene expression: recent advances, Trends Biochem. Sci. 42 (2017) 625–639.

[19] H. Antonicka, K. Choquet, Z.Y. Lin, A.C. Gingras, C.L. Kleinman, E.A. Shoubridge, A pseudouridine synthase module is essential for mitochondrial protein synthesis and cell viability, EMBO Rep. 18 (2017) 28–38.

[20] A.G. Baltz, M. Munschauer, B. Schwanhausser, A. Vasile, Y. Murakawa, M. Schueler, N. Youngs, D. Penfold-Brown, K. Drew, M. Milek, E. Wyler, R. Bonneau, M. Selbach, C. Dieterich, M. Landthaler, The mRNA-bound proteome and its global occupancy profile on protein-coding transcripts, Mol. Cell 46 (2012) 674–690.

[21] V. Boczonadi, R. Horvath, Mitochondria: impaired mitochondrial translation in human disease, Int. J. Biochem. Cell Biol. 48 (2014) 77–84.

[22] L. Van Haute, S.F. Pearce, C.A. Powell, A.R. D'Souza, T.J. Nicholls, M. Minczuk, Mitochondrial transcript maturation and its disorders, J. Inherit. Metab. Dis. 38 (2015) 655–680.

[23] A.A. Jourdain, J. Popow, M.A. de la Fuente, J.C. Martinou, P. Anderson, M. Simarro, The FASTK family of proteins: emerging regulators of mitochondrial RNA biology, Nucleic Acids Res. 45 (2017) 10941–10947.

[24] M. Simarro, A. Gimenez-Cassina, N. Kedersha, J.B. Lazaro, G.O. Adelmant, J.A. Marto, K. Rhee, S. Tisdale, N. Danial, C. Benarafa, A. Orduna, P. Anderson, Fast kinase domain-containing protein 3 is a mitochondrial protein essential for cellular respiration, Biochem. Biophys. Res. Commun. 401 (2010) 440–446.

[25] E. Boehm, S. Zaganelli, K. Maundrell, A.A. Jourdain, S. Thore, J.C. Martinou, FASTKD1 and FASTKD4 have opposite effects on expression of specific mitochondrial RNAs, depending upon their endonuclease-like RAP domain, Nucleic Acids Res. 45 (2017) 6135–6146.

[26] E. Boehm, M. Zornoza, A.A. Jourdain, A. Delmiro Magdalena, I. Garcia-Consuegra, R. Torres Merino, A. Orduna, M.A. Martin, J.C. Martinou, M.A. De la Fuente, M. Simarro, Role of FAST kinase domains 3 (FASTKD3) in post-transcriptional regulation of mitochondrial gene expression, J. Biol. Chem. 291 (2016) 25877–25887.

[27] M. Hong, S.I. Yoon, I.A. Wilson, Structure and functional characterization of the RNA-binding element of the NLRX1 innate immune modulator, Immunity 36 (2012) 337–347.

[28] M. Spinazzi, A. Casarin, V. Pertegato, L. Salviati, C. Angelini, Assessment of mitochondrial respiratory chain enzymatic activities on tissues and cultured cells, Nat. Protoc. 7 (2012) 1235–1246.

[29] P. Jha, X. Wang, J. Auwerx, Analysis of mitochondrial respiratory chain supercomplexes using blue native polyacrylamide gel electrophoresis (BN-PAGE), Current Protocols in Mouse Biology, 6 2016, pp. 1–14.

[30] D. Tomar, P. Prajapati, J. Lavie, K. Singh, S. Lakshmi, K. Bhatelia, M. Roy, R. Singh, G. Benard, R. Singh, TRIM4; a novel mitochondrial interacting RING E3 ligase, sensitizes the cells to hydrogen peroxide (H$_2$O$_2$) induced cell death, Free Radic. Biol. Med. 89 (2015) 1036–1048.

[31] J.G. Doench, N. Fusi, M. Sullender, M. Hegde, E.W. Vaimberg, K.F. Donovan, I. Smith, Z. Tothova, C. Wilen, R. Orchard, H.W. Virgin, J. Listgarten, D.E. Root, Optimized sgRNA design to maximize activity and minimize off-target effects of CRISPR-Cas9, Nat. Biotechnol. 34 (2016) 184–191.

[32] F.A. Ran, P.D. Hsu, J. Wright, V. Agarwala, D.A. Scott, F. Zhang, Genome engineering using the CRISPR-Cas9 system, Nat. Protoc. 8 (2013) 2281–2308.

[33] I. Tattoli, L.A. Carneiro, M. Jehanno, J.G. Magalhaes, Y. Shu, D.J. Philpott, D. Arnoult, S.E. Girardin, NLRX1 is a mitochondrial NOD-like receptor that amplifies NF-kappaB and JNK pathways by inducing reactive oxygen species production, EMBO Rep. 9 (2008) 293–300.

[34] D. Arnoult, F. Soares, I. Tattoli, C. Castanier, D.J. Philpott, S.E. Girardin, An N-terminal addressing sequence targets NLRX1 to the mitochondrial matrix, J. Cell Sci. 122 (2009) 3161–3168.

[35] M. Ishigaki, M. Iketani, M. Sugaya, M. Takahashi, M. Tanaka, S. Hattori, I. Ohsawa, STED super-resolution imaging of mitochondria labeled with TMRM in living cells, Mitochondrion 28 (2016) 79–87.

[36] S. Li, L. Wang, M. Berman, Y.Y. Kong, M.E. Dorf, Mapping a dynamic innate immunity protein interaction network regulating type I interferon production, Immunity 35 (2011) 426–440.

[37] L. Sripada, K. Singh, A.V. Lipatova, A. Singh, P. Prajapati, D. Tomar, K. Bhatelia, M. Roy, R. Singh, M.M. Godbole, P.M. Chumakov, R. Singh, hsa-miR-4485 regulates mitochondrial functions and inhibits the tumorigenicity of breast cancer cells, J. Mol. Med. 95 (2017) 641–651.

[38] R. Acin-Perez, P. Fernandez-Silva, M.L. Peleato, A. Perez-Martos, J.A. Enriquez, Respiratory active mitochondrial supercomplexes, Mol. Cell 32 (2008) 529–539.

[39] E. Lapuente-Brun, R. Moreno-Loshuertos, R. Acin-Perez, A. Latorre-Pellicer, C. Colas, E. Balsa, E. Perales-Clemente, P.M. Quiros, E. Calvo, M.A. Rodriguez-Hernandez, P. Navas, R. Cruz, A. Carracedo, C. Lopez-Otin, A. Perez-Martos, P. Fernandez-Silva, E. Fernandez-Vizarra, J.A. Enriquez, Supercomplex assembly determines electron flux in the mitochondrial electron transport chain, Science 340 (2013) 1567–1570.

[40] F. Soares, I. Tattoli, M.A. Rahman, S.J. Robertson, A. Belcheva, D. Liu, C. Streutker, S. Winer, D.A. Winer, A. Martin, D.J. Philpott, D. Arnoult, S.E. Girardin, The mitochondrial protein NLRX1 controls the balance between extrinsic and intrinsic apoptosis, J. Biol. Chem. 289 (2014) 19317–19330.

[41] B.H. Robinson, R. Petrova-Benedict, J.R. Buncic, D.C. Wallace, Nonviability of cells with oxidative defects in galactose medium: a screening test for affected patient fibroblasts, Biochem. Med. Metab. Biol. 48 (1992) 122–126.

[42] M. Rebsamen, J. Vazquez, A. Tardivel, G. Guarda, J. Curran, J. Tschopp, NLRX1/NOD5 deficiency does not affect MAVS signalling, Cell Death Differ. 18 (2011) 1387.

[43] F. Soares, I. Tattoli, M.E. Wortzman, D. Arnoult, D.J. Philpott, S.E. Girardin, NLRX1 does not inhibit MAVS-dependent antiviral signalling, Innate Immun. 19 (2013) 438–448.

[44] Y. Qin, B. Xue, C. Liu, X. Wang, R. Tian, Q. Xie, M. Guo, G. Li, D. Yang, H. Zhu, NLRX1 mediates MAVS degradation to attenuate hepatitis C virus-induced innate immune response through PCBP2, J. Virol. 91 (2017) e01264–17.

[45] G. Benard, B. Faustin, E. Passerieux, A. Galinier, C. Rocher, N. Bellance, J.P. Delage, L. Casteilla, T. Letellier, R. Rossignol, Physiological diversity of mitochondrial oxidative phosphorylation, Am. J. Phys. Cell Phys. 291 (2006) C1172–C1182.

[46] T.R. Mercer, S. Neph, M.E. Dinger, J. Crawford, M.A. Smith, A.M. Shearwood, E. Haugen, C.P. Bracken, O. Rackham, J.A. Stamatoyannopoulos, A. Filipovska, J.S. Mattick, The human mitochondrial transcriptome, Cell 146 (2011) 645–658.

[47] Y. Lei, H. Wen, J.P. Ting, The NLR protein, NLRX1, and its partner, TUFM, reduce type I interferon, and enhance autophagy, Autophagy 9 (2013) 432–433.

[48] I. Lopez-Fabuel, J. Le Douce, A. Logan, A.M. James, G. Bonvento, M.P. Murphy, A. Almeida, J.P. Bolanos, Complex I assembly into supercomplexes determines differential mitochondrial ROS production in neurons and astrocytes, Proc. Natl. Acad. Sci. U. S. A. 113 (2016) 13063–13068.

[49] A. Lei, K.J. Maloy, Colon cancer in the land of NOD: NLRX1 as an intrinsic tumor suppressor, Trends Immunol. 37 (2016) 569–570.

Antiviral signaling protein MITA acts as a tumor suppressor in breast cancer by regulating NF-κB induced cell death

Khyati Bhatelia [a], Aru Singh [b], Dhanendra Tomar [a], Kritarth Singh [a], Lakshmi Sripada [a], Megha Chagtoo [b], Paresh Prajapati [a], Rochika Singh [a], Madan M. Godbole [b], Rajesh Singh [c,*]

[a] Department of Cell Biology, School of Biological Sciences and Biotechnology, Indian Institute of Advanced Research, Gandhinagar, India
[b] Deptartment of Endocrinology, Sanjay Gandhi Postgraduate Institute of Medical Sciences, Lucknow 226014, UP, India
[c] Department of Bio-Chemistry, The M. S. University of Baroda, Vadodara 390005, Gujarat, India

ARTICLE INFO

ABSTRACT

Emerging evidences suggest that chronic inflammation is one of the major causes of tumorigenesis. The role of inflammation in regulation of breast cancer progression is not well established. Recently Mediator of IRF3 Activation (MITA) protein has been identified that regulates NF-κB and IFN pathways. Role of MITA in the context of inflammation and cancer progression has not been investigated. In the current report, we studied the role of MITA in the regulation of cross talk between cell death and inflammation in breast cancer cells. The expression of MITA was significantly lower on estrogen receptor (ER) positive breast cancer cells than ER negative cells. Similarly, it was significantly down regulated in tumor tissue as compared to the normal tissue. The overexpression of MITA in MCF-7 and T47D decreases the cell proliferation and increases the cell death by activation of caspases. MITA positively regulates NF-κB transcription factor, which is essential for MITA induced cell death. The activation of NF-κB induces TNF-α production which further sensitizes MITA induced cell death by activation of death receptor pathway through capsase-8. MITA expression decreases the colony forming units and migration ability of MCF-7 cells. Thus, our finding suggests that MITA acts as a tumor suppressor which is down regulated during tumorigenesis providing survival advantage to tumor cell.

© 2013 Elsevier B.V. All rights reserved.

1. Introduction

Breast cancer is the second most common form of cancer worldwide. About 1.3 million women are diagnosed with breast cancer annually and more than 400,000 women die from the disease around the world [1,2]. In spite of extensive efforts, there is significant morbidity and mortality associated; therefore, understanding the pathogenesis of breast cancer is of immense importance.

Evidences support the view that chronic inflammation contributes to initiation and progression of cancer [3–5]. The patients with ulcerative colitis and Crohn's disease are at increased risk for developing colorectal cancer. Similarly, inflammation and infection of liver are associated with increased risk of hepatic cancer [6,7]. The experimental evidences demonstrating association of inflammation and breast cancer are emerging. Chronic inflammation plays a critical role in breast cancer occurrence/recurrence [8]. Inflammatory Breast Cancer (IBC) is one of the most aggressive types of breast cancer. The symptoms of IBC like swelling, skin redness, and an orange peel like texture of the skin are similar to inflammation. IBC is often misdiagnosed as mastitis
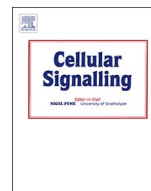
and even antibiotics are prescribed to the patients [9]. These observations suggest that there is a strong linkage between inflammation and breast cancer. The biochemical mechanisms regulating inflammation in breast tissue and their association with breast cancer are not understood.

NF-κB and IFNs are important cellular pathways associating inflammation and cancer. The regulation of NF-κB and IFN pathways is extensively studied; however, its modulation in stimulus specific manner and its significance to tumorigenesis are still not clear. Recent studies suggest that sub-cellular organelles, specifically mitochondria and ER, provide novel signaling platform for the assembly of signalosomes. Mitochondria are emerging as a central regulator of viruses and bacteria induced inflammatory pathways. The discovery of mitochondria associated viral signaling protein (MAVS) on the outer membrane of mitochondria and its role in regulating NF-κB and IFN pathway during viral and bacterial infections suggested a strong linkage between mitochondria and inflammation [10]. Similarly, ER associated protein MITA is another link that might help understand the linkage between ER, mitochondria and inflammation.

MITA plays an important role in inflammation through regulation of NF-κB and IFN [11]. MITA interacts with RIG-I, and MAVS associated signalosome. This further activates downstream kinase complexes: the 'non-canonical' IKK-related kinase TBK1 or IKK complex [12]. The TBK1 complex induces the phosphorylation and dimerization of the transcription factors (IRF3 and IRF7), which translocate to the nucleus

ELSEVIER

MITA modulated autophagy flux promotes cell death in breast cancer cells

CrossMark

Khyati Bhatelia, Kritarth Singh, Paresh Prajapati, Lakshmi Sripada, Milton Roy, Rajesh Singh*

Department of Biochemistry, Faculty of Science, The Maharaja Sayajirao University of Baroda, Sayajigunj, Vadodara 390002, Gujarat, India

ARTICLE INFO

ABSTRACT

The crosstalk between inflammation and autophagy is an emerging phenomenon observed during tumorigenesis. Activation of NF-κB and IRF3 plays a key role in the regulation of cytokines that are involved in tumor growth and progression. The genes of innate immunity are known to regulate the master transcription factors like NF-κB and IRF3. Innate immunity pathways at the same time regulate the genes of the autophagy pathway which are essential for tumor cell metabolism. In the current study, we studied the role of MITA (Mediator of IRF3 Activation), a regulator of innate immunity, in the regulation of autophagy and its implication in cell death of breast cancer cells. Here, we report that MITA inhibits the fusion of autophagosome with lysosome as evident from different autophagy flux assays. The expression of MITA induces the translocation of p62 and NDP52 to mitochondria which further recruits LC3 for autophagosome formation. The expression of MITA decreased mitochondrial number and enhances mitochondrial ROS by increasing complex-I activity. The enhancement of autophagy flux with rapamycin or TFEB expression normalized MITA induced cell death. The evidences clearly show that MITA regulates autophagy flux and modulates mitochondrial turnover through mitophagy.

1. Introduction

The tumor microenvironment is complex milieu having the cells of different origin, including immune cells [1,2]. The tumor cells show increased levels of definite pattern of cytokines which probably helps the tumor cells to reprogramme gene expression pattern and metabolism for their survival [3,4]. Interestingly, the origin of the increased level of cytokines is attributed to the immune cells that are recruited to the tumor microenvironment. The role of the tumor cells themselves in regulation of inflammation is not yet clear and needs to be established in order to modulate different metabolic and signaling pathways to inhibit tumor cells proliferation and metastasis.

NF-κB and IFNs are key regulators of distinct set of anti- and pro-inflammatory cytokines. The regulators of these pathways are critical in different innate immune pathways. It is observed that during the cellular transformation, the genes regulating antitumorigenic cytokines are lost from the tumor cells. MITA, for example, is downregulated or functionally inactivated in different types of cancer including breast cancer, acute myeloid leukemia and prostate cancer [5–7]. Interestingly, the adaptor proteins like MAVS and MITA, antiviral signaling proteins, are localized on the mitochondria and ER-mitochondria contact site respectively [8,9]. During viral infection, RNA and DNA viruses are recognized by distinct proteins like RIG1 and cyclic GMP-AMP synthase (cGAS) respectively which further interact with MITA [10,11]. The interaction recruits downstream signaling proteins and
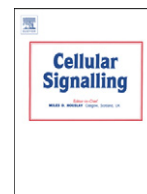
activate NF-κB and IFN that induces antiviral response. Moreover, the evidences also suggest that these proteins regulate mitochondrial functions during infection [12]. The specific localization of these proteins on mitochondria suggests their role beyond innate immunity in metabolism under normal physiological conditions.

It is observed that critical innate immunity pathways (NF-κB and IFN) are also involved in the regulation the expression of the genes involved in autophagy [13–15]. NF-κB regulates the expression of p62 that is essential for the regulation of selective elimination of defective mitochondria called as mitophagy [13]. The increased level of autophagy is important for the tumor cell metabolism and adaptation for increased rate of cell division [16,17]. The selective elimination of the defective organelles via autophagy is important for the cellular homeostasis [18–20]. The degradation of mitochondria may down regulate the levels of several mitochondrial and mitochondrial associated membrane resident proteins like MAVS and MITA hence downregulating and maintaining inflammation in physiological limits.

Autophagy (macroautophagy) is a sequential process of degradation of cytoplasmic material as well as organelles through lysosomes. The first step involves the formation of autophagophore membrane which encloses the portion of cytoplasm to form autophagosome [21]. The outer membrane of autophagosomes fuses with lysosomes and forms autophagolysosomes [22,23]. The lysosomal enzymes degrade the enclosed cytoplasmic material and inner membrane of autophagosome [24]. Defect in autophagy leads to several diseased conditions including

Review

TLRs: Linking inflammation and breast cancer

CrossMark

Khyati Bhatelia, Kritarth Singh, Rajesh Singh *

Department of Bio-Chemistry, The M.S. University of Baroda, Vadodara 390002, Gujarat, India

ARTICLE INFO

ABSTRACT

Breast cancer is one of the leading causes of mortality in the females. Intensive efforts have been made to understand the molecular mechanisms of pathogenesis of breast cancer. The physiological conditions that lead to tumorigenesis including breast cancer are not well understood. Toll like receptors (TLRs) are essential components of innate immune system that protect the host against bacterial and viral infection. The emerging evidences suggest that TLRs are activated through pathogen associated molecular patterns (PAMPs) as well as endogenous molecules, which lead to the activation of inflammatory pathways. This leads to increased levels of several pro-inflammatory cytokines and chemokines mounting inflammation. Several evidences support the view that chronic inflammation can lead to cancerous condition. Inflammation aids in tumor progression and metastasis. Association of inflammation with breast cancer is emerging. TLR mediated activation of NF-κB and IRF is an essential link connecting inflammation to cancer. The recent reports provide several evidences, which suggest the important role of TLRs in breast cancer pathogenesis and recurrence. The current review focuses on emerging studies suggesting the strong linkages of TLR mediated regulation of inflammation during breast cancer and its metastasis emphasizing the initiation of the systematic study.

© 2014 Elsevier Inc. All rights reserved.

Contents

1. Introduction

Breast cancer is the second most common cancer diagnosed worldwide. More than 1.3 million women worldwide are diagnosed with breast cancer each year [1]. Breast cancer rate has increased by 0.4% per year from 1975 to 1990; however its death rate decreased thereafter by 2.2% from 1990 to 2007 [2]. In spite of decrease in breast cancer incidence, about half-a-million women still die because of breast cancer each year [1,3]. The high figures of incidences and mortality, even with the advancement of primary screening and diagnosis, suggest the need to systematically investigate the cause and pathogenesis of breast cancer.

The physiological conditions that stimulate proliferation and growth of somatic cells leading to neoplasia and carcinoma are not well understood. The relationship between inflammation and cancer is emerging. The inflammatory diseases increase the risk of developing cancer [2, 4–7]. For example, patients with ulcerative colitis and Crohn's disease are at increased risk for developing colorectal cancer [8]. Similarly,

* Corresponding author at: Department of Bio-Chemistry, Faculty of Science, The M.S. University of Baroda, Vadodara 390002, Gujarat, India. Tel.: +91 265 2759594.
E-mail address: singhraj1975@gmail.com (R. Singh).

JMolMed CrossMark

ORIGINAL ARTICLE

hsa-miR-4485 regulates mitochondrial functions and inhibits the tumorigenicity of breast cancer cells

Lakshmi Sripada[1] · Kritarth Singh[1] · Anastasiya V. Lipatova[2] · Aru Singh[3] ·
Paresh Prajapati[1] · Dhanendra Tomar[4] · Khyati Bhatelia[1] · Milton Roy[1] ·
Rochika Singh[5] · Madan M. Godbole[3] · Peter M. Chumakov[2] · Rajesh Singh[1]

Abstract The modulation of mitochondrial functions is important for maintaining cellular homeostasis. Mitochondria essentially depend on the import of RNAs and proteins encoded by the nuclear genome. MicroRNAs encoded in the nucleus can translocate to mitochondria and target the genome, affecting mitochondrial function. Here, we analyzed the role of miR-4485 in the regulation of mitochondrial functions. We showed that miR-4485 translocated to mitochondria where its levels varied in response to different stress conditions. A direct binding of miR-4485 to mitochondrial 16S rRNA was demonstrated. MiR-4485 regulated the processing of pre-rRNA at the 16S rRNA-ND1 junction and the translation of downstream transcripts. MiR-4485 modulated mitochondrial complex I activity, the production of ATP, ROS levels, caspase-3/7 activation, and apoptosis. Transfection of a miR-4485 mimic downregulated the expression of regulatory glycolytic pathway genes and reduced the clonogenic

ability of breast cancer cells. Ectopic expression of miR-4485 in MDA-MB-231 breast carcinoma cells decreased the tumorigenicity in a nude mouse xenograft model. Furthermore, levels of both precursor and mature miR-4485 are decreased in tumor tissue of breast cancer patients. We conclude that the mitochondria-targeted miR-4485 may act as a tumor suppressor in breast carcinoma cells by negatively regulating mitochondrial RNA processing and mitochondrial functions.

Keywords Mitochondria · miR-4485 · Breast cancer · Tumor suppressors · RNA processing · Mouse xenograft

✉ Rajesh Singh
    singhraj1975@gmail.com

1   Department of Biochemistry, The Maharaja Sayajirao University of Baroda, Vadodara, Gujarat 390002, India

2   Engelhardt Institute of Molecular Biology, Russian Academy of Sciences, Moscow, Russia

3   Department of Endocrinology, Sanjay Gandhi Postgraduate Institute of Medical Sciences, Lucknow, Uttar Pradesh 226014, India
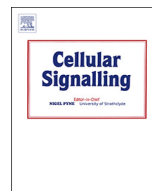
4   Center for Translational Medicine, Temple University, Philadelphia, PA 19140, USA

5   Department of Cell Biology, School of Biological Sciences and Biotechnology, Indian Institute of Advanced Research, Koba Institutional Area, Gandhinagar, Gujarat 382007, India

Introduction

Mitochondria are indispensable for energy production, lipid and carbohydrate metabolism, redox regulation, calcium signaling, and cell death. Mitochondria have also been implicated in the regulation of innate immunity, inflammation, and antiviral signaling [1, 2]. Mitochondrial dysfunction is associated with numerous pathologies, including metabolic and neurodegenerative disorders, cardiomyopathies, cancer, and aging [3, 4]. Reprogramming of mitochondrial functions is one of the major hallmarks of tumor cell metabolism [5, 6]. To cope with growing bioenergetic demands of rapid proliferation, cancer cells can switch from an efficient but slow mitochondrial respiration to the less efficient but rapid aerobic glycolysis [7–10]. Some of the key intermediates, such as citrate and glycerol, are redirected from the Krebs cycle to meet increased demands of tumor cells in macromolecular synthesis [11, 12]. Although mechanisms of metabolic reprogramming in rapidly dividing cancer cells are being extensively studied, many of the processes remain elusive.

Proteomics studies have revealed that the human mitochondrion contains more than a thousand distinct

TRIM8 regulated autophagy modulates the level of cleaved Caspase-3 subunit to inhibit genotoxic stress induced cell death

Milton Roy[a], Dhanendra Tomar[b], Kritarth Singh[a], Sripada Lakshmi[a,1], Paresh Prajapati[a,2], Khyati Bhatelia[a], Dhruv Gohel[a], Rajesh Singh[a,*]

[a] Department of Biochemistry, Faculty of Science, The Maharaja Sayajirao University of Baroda, Vadodara, Gujarat 390002, India
[b] Center for Translational Medicine, Temple University, Philadelphia, PA 19140, USA

ABSTRACT

In cancer patients, treatment modalities like chemotherapy and radiation exert their anticancer effects by inducing DNA damage. The cancer cells can survive under genotoxic stress by inducing DNA damage response (DDR) or can undergo cell death. The process of autophagy is emerging as crucial regulator of cell survival during different stress conditions. Post translational modification through ubiquitin plays an essential role in DDR during genotoxic stress conditions. Ubiquitin ligases regulate autophagy and cell death pathways however their role during genotoxic stress conditions is not understood. In the current study we identified TRIM8, RING E3 Ligase, as a novel regulator of autophagy during DDR. TRIM8 regulates lysosomal biogenesis and autophagy flux. The turnover of TRIM8 is high and is stabilized during genotoxic stress conditions. TRIM8 regulated autophagy is essential for its cytoprotective role during genotoxic stress induced cell death. TRIM8 stabilizes the turnover of XIAP during genotoxic stress and forms complex with XIAP and caspase-3 to inhibit its activation in presence of etoposide. TRIM8 mediated autophagy promotes degradation of cleaved caspase-3 subunits. This study described TRIM8, as a novel regulator of DDR-autophagy crosstalk, which may play role in survival of cancer cells in presence of genotoxic agents.

1. Introduction

The cell has evolved DNA damage response (DDR) to ensure genomic integrity and cell survival. DDR includes sensing of the DNA damage, recruitment of DNA repair proteins and repair. During DNA damage response (DDR), cell cycle check points are activated leading to either repair or cell death in irreversible DNA damage conditions. DNA double stranded breaks (DSBs) detection by ATM (ataxia telangiectasia mutated) and ATR (ataxia telangiectasia and Rad3 related) promotes activation of apoptosis by inducing p53 [1] however many other regulators still needs to be identified. The DNA repair process and cell survival/death pathway are intricately linked to maintain cellular homeostasis [2,3]. Any defect in this process can lead to genomic aberrations including chromosomal translocations, mutations deletions/additions leading to malignant transformation of the cells. Cancer cells often have compromised DDR which help them in avoiding cellular checkpoints and proliferate. During radiation and chemotherapy of cancer patients, the genomic DNA of malignant cells is the target and

DDR induced apoptosis is initiated to eliminate cancer cells [4]. The mechanism of cross talk of different cell survival and death pathways and their regulators during genotoxic stress in cancer cells needs to be identified and investigated.

Genotoxic agent induced autophagy have been implicated both in initiation of cell death as well as cell survival, hence its role further needs more investigation for targeted therapeutic intervention [5,6]. The crosstalk between autophagy and apoptosis is crucial as apoptosis acts as the last resort for cells in severe or persistent genotoxic stress [7]. Autophagy maintains cellular fitness by elimination of defective organelles, dysfunctional proteins and aggregates [8–10]. Interestingly, autophagy has also been shown essential for removal of DNA damage induced extranuclear DNA that can lead to activation of inflammatory pathways. It is observed that damaged DNA is exported outside the nucleus and its autophagy mediated degradation in lysosomes is essential for cell survival. Failure in clearance of extranuclear DNA leads to activation of inflammatory pathways by intracellular DNA sensors like cGAS/STING [11]. It had been observed that knockout of p62/

Original contribution

TRIM4; a novel mitochondrial interacting RING E3 ligase, sensitizes the cells to hydrogen peroxide (H$_2$O$_2$) induced cell death

Dhanendra Tomar [a,b,1], Paresh Prajapati [c], Julie Lavie [b], Kritarth Singh [c], Sripada Lakshmi [c], Khyati Bhatelia [c], Milton Roy [c], Rochika Singh [a], Giovanni Bénard [b,*], Rajesh Singh [c,*]

[a] Department of Cell Biology, School of Biological Sciences and Biotechnology, Indian Institute of Advanced Research, Gandhinagar, India
[b] Université de Bordeaux, Laboratoire Maladie Rares: Genetique et metabolisme, Hopital Pellegrin, 33076 Bordeaux, France
[c] Department of Biochemistry, Faculty of Science, The M.S. University of Baroda, Vadodara 390002, Gujarat, India

ABSTRACT

The emerging evidences suggest that posttranslational modification of target protein by ubiquitin (Ub) not only regulate its turnover through ubiquitin proteasome system (UPS) but is a critical regulator of various signaling pathways. During ubiquitination, E3 ligase recognizes the target protein and determines the topology of ubiquitin chains. In current study, we studied the role of TRIM4, a member of the TRIM/RBCC protein family of RING E3 ligase, in regulation of hydrogen peroxide (H$_2$O$_2$) induced cell death. TRIM4 is expressed differentially in human tissues and expressed in most of the analyzed human cancer cell lines. The subcellular localization studies showed that TRIM4 forms distinct cytoplasmic speckle like structures which transiently interacts with mitochondria. The expression of TRIM4 induces mitochondrial aggregation and increased level of mitochondrial ROS in the presence of H$_2$O$_2$. It sensitizes the cells to H$_2$O$_2$ induced death whereas knockdown reversed the effect. TRIM4 potentiates the loss of mitochondrial transmembrane potential and cytochrome c release in the presence of H$_2$O$_2$. The analysis of TRIM4 interacting proteins showed its interaction with peroxiredoxin 1 (PRX1), including other proteins involved in regulation of mitochondrial and redox homeostasis. TRIM4 interaction with PRX1 is critical for the regulation of H$_2$O$_2$ induced cell death. Collectively, the evidences in the current study suggest the role of TRIM4 in regulation of oxidative stress induced cell death.

© 2015 Elsevier Inc. All rights reserved.

1. Introduction

The studies in the last two decades suggest that beside metabolism, mitochondria plays crucial role in other cellular processes like cell death, inflammation and differentiation [1–3]. The regulation of mitochondrial function is required for cellular homeostasis and its dysregulation had been implicated in various pathological conditions like neurodegeneration, ageing, inflammation, infection and cancer [4–6]. The understanding of the regulation of mitochondrial functions is important to modulate its function in associated pathological condition.

Mitochondria are one of the primary sites of the production of reactive oxygen species (ROS) during physiological and pathological conditions [7,8]. The regulated level of ROS plays critical role in different cellular processes like cell cycle, proliferation,

differentiation, migration [9–11]; however, its excess leads to the activation of cell death pathways [12,13]. The physiological level of ROS is maintained by redox reactions and activity of several antioxidant enzymes like glutathione peroxidases (GPX), thioredoxins (TRX) and peroxiredoxins (PRX) [14–16]. PRXs are member of low molecular weight peroxidases, involved in regulation of redox signaling [16]. PRX scavenge low concentrations of H$_2$O$_2$, hence acts as modulator of H$_2$O$_2$ signaling [16,17]. The regulation of different antioxidant enzymes and their selective role in oxidative stress induced cell death is less understood.

The emerging evidences suggest that ubiquitin mediated posttranslational modifications plays critical role in the regulation of redox pathways [18,19]. The ubiquitin E3 ligases are terminal protein during ubiquitination and provide specificity to this process as it recognizes the substrate and transfer Ub moiety to the target [20]. Ubiquitin E3 ligase, E6AP, regulates the cellular response during oxidative stress condition by modulating the turnover of PRX1 [21]. The role of specific E3 ligase, their recruitment to mitochondria and regulation of redox signaling, cell death during oxidative stress is less understood.

TRIM proteins are members of RING family of ubiquitin E3

CrossMark

Systemic Analysis of miRNAs in PD Stress Condition: miR-5701 Modulates Mitochondrial–Lysosomal Cross Talk to Regulate Neuronal Death

Paresh Prajapati[1] · Lakshmi Sripada[1] · Kritarth Singh[1] · Milton Roy[1] · Khyati Bhatelia[1] · Pooja Dalwadi[1] · Rajesh Singh[1]

Abstract Parkinson's disease (PD) is complex neurological disorder and is prevalent in the elderly population. This is primarily due to loss of dopaminergic neurons in the substantia nigra pars compacta (SNc) region of the brain. The modulators of the selective loss of dopaminergic neurons in PD are still not well understood. The small non-coding RNAs specifically miRNAs fine-tune the protein levels by post-transcriptional gene regulation. The role of miRNAs in PD pathogenesis is still not well characterized. In the current study, we identified the miRNA expression pattern in 6-OHDA-induced PD stress condition in SH-SY5Y, dopaminergic neuronal cell line. The targets of top 5 miRNAs both up- and down regulated were analyzed by using StarBase. The putative pathways of identified miRNAs included neurotrophin signaling, neuronal processes, mTOR, and cell death. The level of miR-5701 was significantly downregulated in the presence of 6-OHDA. The putative targets of miR-5701 miRNA include genes involved in lysosomal biogenesis and mitochondrial quality control. The transfection of miR-5701 mimic decreased the transcript level of VCP, LAPTM4A, and ATP6V0D1. The expression of miR-5701 mimic induces mitochondrial dysfunction, defect in autophagy flux, and further sensitizes SH-SY5Y cells to 6-OHDA-induced cell death. To our knowledge, the evidence in the current study demonstrated the dysregulation of specific pattern of miRNAs in PD stress conditions. We further characterized the role of miR-5701, a novel miRNA, as a potential regulator of the mitochondrial and lysosomal function determining the fate of neurons which has important implication in the pathogenesis of PD.

Keywords Autophagy flux · Lysosome · miRNA · Parkinson's disease · Mitochondria

Introduction

Parkinson's disease (PD) is a second most common neurodegenerative movement disorder in elderly population. This is clinically characterized by resting tremor, rigidity, bradykinesia, and postural instability due to preferential loss of dopamine-producing neurons in the *substantia nigra pars compacta* region of the midbrain [1]. The other pathological hallmark of PD is the presence of intracytoplasmic proteinaceous deposits termed as Lewy bodies (LBs) and dystrophic neurites (Lewy neurites) in surviving neurons. These aggregates consist of fibrillar α-synuclein, molecular chaperones, ubiquitin, and neurofilaments [2]. The mechanisms of further progression and selective loss of dopaminergic neurons in PD had been a focus of research for the last several years; however, it is still not well understood. There is no effective therapy, and dopamine (DA) supplementation only provides symptomatic relief. It is important to indentify the modulators of selective neuronal loss in PD to find the next generation of therapeutic strategies.

Now there are established evidences suggesting mitochondrial dysfunction is one of the major causative factors of PD [3–5]. The first evidence of association of mitochondrial dysfunction with PD came from the observation of 1-methyl-4-phenyl-1,2,5,6-tetrahydropyridine (MPTP), which causes symptoms of PD during drug abuse and produces severe

✉ Rajesh Singh
singhraj1975@gmail.com

1 Department of Biochemistry, Faculty of Science, The Maharaja Sayajirao University of Baroda, Vadodara, Gujarat 390002, India

TNF-α regulates miRNA targeting mitochondrial complex-I and induces cell death in dopaminergic cells

Paresh Prajapati [a,b], Lakshmi Sripada [a,b], Kritarth Singh [a,b], Khyati Bhatelia [a,b], Rochika Singh [a], Rajesh Singh [b,*]

[a] Department of Cell Biology, School of Biological Sciences and Biotechnology, Indian Institute of Advanced Research (IIAR), Koba Institutional Area, Gandhinagar 382007, Gujarat, India
[b] Department of Biochemistry, Faculty of Science, The M. S. University of Baroda, Vadodara 390002, Gujarat, India

ABSTRACT

Parkinson's disease (PD) is a complex neurological disorder of the elderly population and majorly shows the selective loss of dopaminergic (DAergic) neurons in the substantia nigra pars compacta (SNpc) region of the brain. The mechanisms leading to increased cell death of DAergic neurons are not well understood. Tumor necrosis factor-alpha (TNF-α), a pro-inflammatory cytokine is elevated in blood, CSF and striatum region of the brain in PD patients. The increased level of TNF-α and its role in pathogenesis of PD are not well understood. In the current study, we investigated the role of TNF-α in the regulation of cell death and miRNA mediated mitochondrial functions using, DAergic cell line, SH-SY5Y (model of dopaminergic neuron degeneration akin to PD). The cells treated with low dose of TNF-α for prolonged period induce cell death which was rescued in the presence of zVAD.fmk, a caspase inhibitor and N-acetyl-cysteine (NAC), an antioxidant. TNF-α alters mitochondrial complex-I activity, decreases adenosine triphosphate (ATP) levels, increases reactive oxygen species levels and mitochondrial turnover through autophagy. TNF-α differentially regulates miRNA expression involved in pathogenesis of PD. Bioinformatics analysis revealed that the putative targets of altered miRNA included both pro/anti apoptotic genes and subunits of mitochondrial complex. The cells treated with TNF-α showed decreased level of nuclear encoded transcript of mitochondrial complexes, the target of miRNA. To our knowledge, the evidences in the current study demonstrated that TNF-α is a potential regulator of miRNAs which may regulate mitochondrial functions and neuronal cell death, having important implication in pathogenesis of PD.

© 2014 Elsevier B.V. All rights reserved.

1. Introduction

Parkinson's disease (PD) is the most common neurodegenerative disorder, affecting millions of elderly individuals worldwide [1,2]. The increase in aging population is already showing exponential rise in PD cases. The mechanisms leading to PD had been the focus of research for the last several years; however, there is no effective therapy or any potential marker for monitoring the progression of PD. Neuropathological examination of the post-mortem brain suggests that several regions of the brain are affected, however the loss of dopaminergic (DAergic) neurons in the substantia nigra pars compacta (SNpc) is one of the most prominent features of PD [3]. At the time of clinical presentation approximately 50–70% of DAergic neurons in the nigrostriatal system are already lost [4]. The mechanisms leading to degeneration of DAergic neurons are still not well understood.

Inflammation and its association with neurodegenerative diseases are emerging [5,6]. Several studies provide strong evidences for the association of inflammation with sporadic and familial forms of the PD. The studies of post-mortem human brain obtained from PD patients

provided direct evidence of the association with inflammation with PD. HLA-DR-positive reactive microglia were clearly observed within the substantia nigra of PD patients [7]. The increased levels of several pro-inflammatory cytokines (IL1-β, IL-2, IL-6, TNF-α and IFN-γ) were observed in the DAergic nigrostriatal system and the regions outside the SN in PD patients [8–13]. TNF-α is one of the important pleiotropic cytokines and had been implicated in both neuronal survival and death. TNF-α is known to induce ROS (reactive oxygen species) generation in mitochondria [14]. The mitochondrial complex I and complex III are the primary sites of ROS generation. The homeostasis of mitochondria is maintained through selective elimination of defective mitochondria by the process of selective autophagy called as mitophagy [15]. The role of TNF-α in regulation of mitochondrial dysfunction, generation of ROS and implication in mitophagy during PD conditions is not well understood.

The optimal functioning of mitochondria requires more than 1000 proteins. Hence >1000 resident proteins and critical non-coding RNAs (RNaseP, RNA component of MRP and 5S rRNA) are encoded from nuclear genome and are imported into mitochondria for their optimal function [16]. The miRNAs, emerging class of small non-coding RNAs, play important role in the regulation of mRNA copy number and protein level in the narrow physiological range [17]. Recently, our group

TRIM13 regulates caspase-8 ubiquitination, translocation to autophagosomes and activation during ER stress induced cell death

Dhanendra Tomar, Paresh Prajapati, Lakshmi Sripada, Kritarth Singh, Rochika Singh, Arun Kumar Singh, Rajesh Singh *

Department of Cell Biology, School of Biological Sciences and Biotechnology, Indian Institute of Advanced Research, Gandhinagar, Gujarat, India

ABSTRACT

The emerging evidences suggest that endoplasmic (ER) stress is involved in onset of many pathological conditions like cancer and neurodegeneration. The persistent ER stress results in misfolded protein aggregates, which are degraded through the process of autophagy or lead to cell death through activation of caspases. The regulation of crosstalk of autophagy and cell death during ER stress is emerging. Ubiquitination plays regulatory role in crosstalk of autophagy and cell death. In the current study, we describe the role of TRIM13, RING E3 ubiquitin ligase, in regulation of ER stress induced cell death. The expression of TRIM13 sensitizes cells to ER stress induced death. TRIM13 induced autophagy is essential for ER stress induced caspase activation and cell death. TRIM13 induces K63 linked poly-ubiquitination of caspase-8, which results in its stabilization and activation during ER stress. TRIM13 regulates translocation of caspase-8 to autophagosome and its fusion with lysosome during ER stress. This study first time demonstrated the role of TRIM13 as novel regulator of caspase-8 activation and cell death during ER stress.

© 2013 Elsevier B.V. All rights reserved.

1. Introduction

The endoplasmic reticulum (hereafter ER) is the primary site for synthesis and folding of proteins in eukaryotes. The accumulation of misfolded proteins and its aggregation leads to unfolded protein response (UPR) which prevents further protein burden and damage to the cell [1,2]. Unfolded proteins in the ER are generally tagged with ubiquitin and degraded by ubiquitin proteasome system (UPS), known as ER associated degradation system-I (ERAD-I) [3,4]. It has been observed that accumulation of misfolded proteins in ER may lead to formation of protein aggregates, which are toxic to cell. The process of autophagy, also known as ERAD-II/macroautophagy clears these protein aggregates [5,6]. Specialized sensors like IREα, PERK and ATF6, sense the persistent ER stress to maintain either ER homeostasis or initiate cell death pathways [1,7]. Recent evidences suggest that autophagy may be adaptive response during ER stress leading to either cell death or survival. The cross talk of autophagy and cell death during ER stress has implication in many chronic conditions like neurodegeneration, cancer and metabolic diseases [2,8,9]. Tumor cells have increased unfolded/misfolded proteins due to inadequate supply of glucose and subsequent reduction in glycosylation of proteins and ATP, which results in ER stress. The induction of autophagy during the ER stress plays critical role in tumor cell survival, thus contributing significantly to tumorigenesis. The regulators of cross talk between autophagy and cell death during ER stress are not well understood.

Increasing evidences suggest that ubiquitin mediated post-translational modification is the central mechanism for regulation of crosstalk between autophagy, cell death and survival [10,11]. Ubiquitination of target protein involves sequential action of three enzymes: E1, E2 and E3, for transferring the ubiquitin to the target protein [12]. The terminal enzyme E3, transfers Ub from the E2 to a lysine residue on a substrate protein, resulting in an isopeptide bond formation between the substrate lysine and the C-terminus glycine of Ub. E3 ligases provide specificity to the pathway as they recognize the substrate, interact with definite E2 and determine the topology of ubiquitination. Several ubiquitin E3 ligases have been identified which determine the critical pattern of substrate ubiquitination leading to unique outcome, either degradation of proteins through UPS or regulation of their activity [13,14]. The role of ubiquitin ligases regulating crosstalk of cell death and autophagy during ER has not been investigated in detail.

Ubiquitin E3 ligases have been broadly classified in three major families called as RING, HECT and U Box. The majority of the ubiquitin ligases belong to RING family which are characterized by the presence of RING domain [15]. The role of RING E3 ligases have not been well studied in the context of many different cellular functions. TRIM family proteins (>70), member of RING type ubiquitin E3 ligases, are characterized by the presence of N-terminal RING, B-Box, Coiled Coil (CC) domain and variable C-terminal domain [16]. The role of TRIM family proteins are emerging in several processes like innate immune response, regulation of

* Corresponding author at: Department of Cell Biology, School of Biological Sciences and Biotechnology, Indian Institute of Advanced Research, Koba Institutional Area, Gandhinagar 382007, Gujarat, India. Tel.: +91 79 30514240; fax: +91 79 30514110.
E-mail address: rsingh@iiar.res.in (R. Singh).

TBK1 regulates p62/sqstm1 mediated autophagic clearance of intracellular ubiquitinated *Staphylococcus aureus* in human epithelial cells

Arun Kumar Singh[2], Pooja Patel[1], Dhanendra Tomar[2], Rochika Singh[2], Lakshmi Sripada[1], Paresh Prajapati[1], Kritarth Singh[1], Rajesh Singh[2]

[1]*Department of Cell Biology, School of Biological Sciences and Biotechnology, Indian Institute of Advanced Research, Gandhinagar, Gujarat 382007, India.*
[2]*Department of Bio-Chemistry, Faculty of Science, The M.S. University of Baroda, Vadodara, Gujarat 390002, India.*

Correspondence to: Dr. Rajesh Singh, Department of Bio-Chemistry, Faculty of Science, The M.S. University of Baroda, Vadodara, Gujarat 390002, India. E-mail: singhraj1975@gmail.com

ABSTRACT

Aim: *Staphylococcus aureus* (*S. aureus*), previously considered an extracellular pathogen, can also survive in the intracellular environment of the host cell. It is now evident that autophagy controls intracellular survival of bacteria, however, the role of autophagy in controlling *S. aureus* survival in epithelial cells is not well understood. The objective of current work was to study the role of ubiquitin in regulating selective autophagy of *S. aureus*. **Methods:** Intracellular survival of *S. aureus* in epithelial cells was studied by gentamycin protection assay. Autophagy was monitored by microtubule-associated protein 1A/1B-light chain 3 (LC3) western blotting and fluorescence microscopy. The co-localization of red fluorescent protein-Ub, green fluorescent protein (GFP)-p62 and GFP-LC3 with GFP- or CFP-*S. aureus* was monitored by confocal microscopy. **Results:** The authors observed that *S. aureus* survives in epithelial cell by modifying the autophagy pathway. Intracellular *S. aureus* is ubiquitinated and recruits autophagy adaptor proteins p62 and LC3. TANK-binding kinase 1 (TBK1) regulates the integrity of the autophagosomal during *S. aureus* infection and its knockdown enhanced survival of *S. aureus*. Aspirin treatment reduces intracellular survival of *S. aureus*. **Conclusion:** The results of the current study strongly suggests that intracellular *S. aureus* is ubiquitinated and recruits p62 that targets it for lysosomal degradation. TBK1 regulates autophagosomal integrity during *S. aureus* infection and hence intracellular survival. Aspirin enhances autophagy flux and decreases *S. aureus* survival.

Quick Response Code: